UNIVERSITY OF WARMIA AND MAZURY IN OLSZTYN

FACULTY OF TECHNICAL SCIENCES

POLISH SOCIETY OF THEORETICAL AND APPLIED MECHANICS

1st Workshop on Porous Media

BOOK OF ABSTRACTS

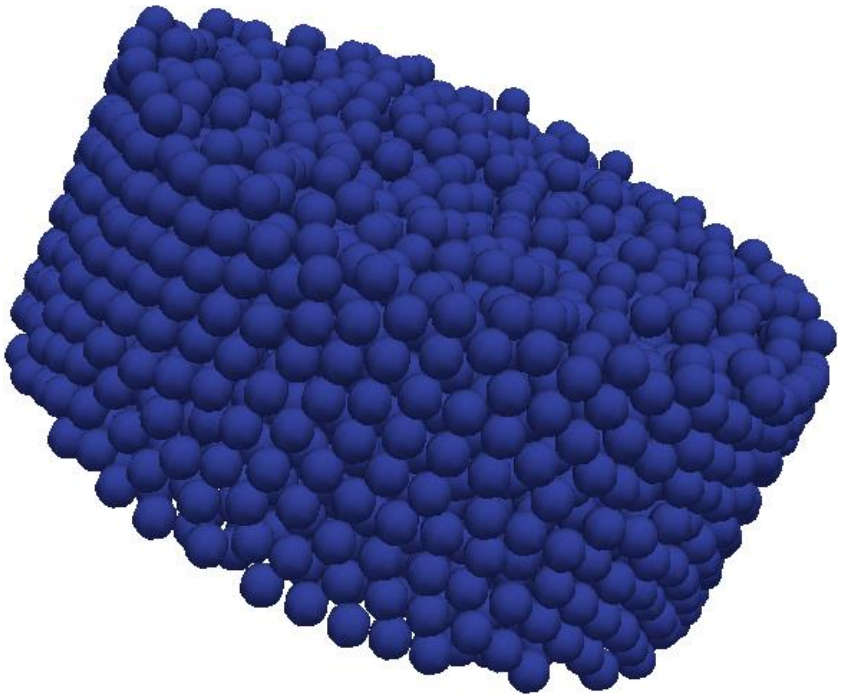

OLSZTYN - POLAND

1-3 JULY 2016

SCIENTIFIC COMMITEE

- Wojciech Sobieski (chair of committee)
- Janusz Badur
- Mariusz Kaczmarek
- Adam Lipiński
- Teodor Skiepko
- Mieczysław Cieszko
- Piotr Srokosz
- Adam Szymkiewicz
- Anna Trykozko
- Maciej Marek
- Maciej Matyka
- Joanna Wiącek

ORGANIZING COMMITEE

- Wojciech Sobieski (chair of committee)
- Seweryn Lipiński
- Dariusz Grygo
- Tomasz Tabaka
- Aneta Molenda

ISBN 978-83-950921-0-7

9 788395 092107

Book of abstracts published from materials provided by Authors
Edited by Seweryn Lipiński

CONTENTS

Numerical modeling of cucumber fruits with the use of reverse engineering

Andrzej Anders, Zdzisław Kaliniewicz, Piotr Markowski
Department of Heavy Duty Machines and Research Methodology
University of Warmia and Mazury in Olsztyn
ul. Oczapowskiego 11, 10-736 Olsztyn, Poland
anders@uwm.edu.pl

Keywords: reverse engineering, 3D scanner, modeling, fruit, cucumber

The introduction of new products and technologies to the market, and an improvement in their quality, increasingly often require modern measurement techniques and software allowing to perform advanced computer simulations of selected technological processes. Modeling of agri-food raw materials should be linked with the designed technological process and should aim to realistically reproduce their shapes [1]. The starting point for the design could be a 3D model of raw material with precisely determined geometrical and physical properties. According to the conventional approach, modeling is based on homogeneity and isotropy and assigning regular shapes (e.g. cylinder, sphere, cone, etc.) to the analyzed agri-food raw materials. Computer simulations of complex processes that occur during the processing of agricultural and food products can be performed with the use of Computer Aided Design (CAD) and Computational Fluid Dynamics (CFD) software [4], [5]. The key problem with the design of food processing machinery and equipment is to develop a model that would reproduce all individual characteristics and imperfections of a given raw material and could be used for computer simulations. The aim of this study was to create, with the use of a 3D laser scanner, numerical models of the fruits of cucumber cv. *Śremski* and to use those models for analyzing selected geometrical attributes.

The experimental materials comprised the fruits of cucumber cv. Śremski, which were stored indoors at a constant temperature of 18±1°C and air humidity of 60%. The cucumbers used in the experiment were purchased at the Production and Agricultural Experiment Station "Pozorty" in Olsztyn. A total of 50 fruits of field-grown cucumbers, with no visible damage, were randomly selected for the study. The cucumbers were mounted on a rotation table and were scanned with the NextEngine 3D laser scanner with capture density of 15 points per mm^2. To obtain numerical models of cucumbers, the scans were combined using NextEngine ScanStudio HD PRO software [3]. The models were used to determine the surface area, volume, length, width and thickness of cucumbers (Fig.1) in the MeshLab processing system [2]. The measurements were performed within an accuracy of d = 0.01 mm.

Fig. 1. A textured model of a field-grown cucumber from a 3D laser scanner: *L* – length, *W* – width, *T* – thickness.

Fig. 2. A 3D model of a field-grown cucumber in the form of a triangle mesh.

The mass of the smallest and the largest cucumber fruits was 43.05 g and 123.70 g, respectively. An analysis of 3D laser scanner data indicated that the external surface area of the examined cucumber fruits ranged from 74.84 cm^2 to 145.38 cm^2 (111.25 cm^2 on average). The volume of cucumber fruits, determined with a 3D laser scanner, ranged from 46.65 cm^3 to 127.38 cm^3 (77.26 cm^3 on average). Physical properties such as mass and density were assigned to the numerical models of cucumber fruits, so that the models could be used in further research and engineering projects.

References:

[1] Datta A.K., Halder A., 2008. Status of food process modeling and where do we go from here (synthesis of the outcome from brainstorming). Comprehensive Reviews in Food Science and Food Safety 7, 117–120.

[2] MeshLab Visual Computing Lab – ISTI – CNR, 2013. http://meshlab.sourceforge.net.

[3] NextEngine User Manual, 2010. http://www.nextengine.com.

[4] Rahmi U., Ferruh E. (2009): Potential use of 3-dimensional scanners for food process modeling. Journal of Food Engineering, 93, 337-343.

[5] Verboven P., De Baerdemaeker J., Nicolai B.M., 2004. Using computational fluid dynamics to optimize thermal processes. In: Richardson, P. (Ed.), Improving the Thermal Processing of Foods. CRC Press, Boca Raton, FL, pp. 82–102.

Modelling liquid spreading in trickle-bed reactors

Dariusz Asendrych, Paweł Niegodajew
Institute of Thermal Machinery, Częstochowa University of Technology
darek@imc.pcz.czest.pl

Keywords: packed bed, two-phase flow, trickling flow, VOF, Eulerian approach

Modelling two-phase flow in an unstructured packed beds, even for isothermal and non-reacting conditions, seems to be one of the most challenging fluid mechanics problems. Complex geometry, locally unpredictable flow patterns, mutual interactions between all (solid, gas and liquid) phases make the flow description extremely difficult. Various concepts have been proposed in the source literature to provide reasonable solutions. In their review paper Wang et al. [1] discussed different approaches to the subject including those with limited applications (e.g. packed beds composed of spheres) up to methods allowing to accurately predict pressure drop, liquid holdup and even liquid spreading intensity for various packing element types. In principle the specific characteristics of the packed bed are introduced into the flow governing equations by the source terms in momentum equation, which may take different forms and depend on numerous parameters. In a recent paper of Solomenko et al. [2] the very good agreement between experimental measurements (γ-ray tomography) and the simulation results was obtained with the use of an Euler-Euler 2-fluid model taking into account the capillary and mechanical mechanisms with adequately chosen model constants. However, all the Eulerian-type models allow to predict the flow statistics only, losing its local nonuniformities resulting from realistic geometry of packed bed manifested by spatial variations of bed porosity. That in turn may lead to significant variations of flow velocities and liquid holdup and thus influence all the processes (heat and mass transfer) built on flow hydrodynamics. This drawback of Euler-Euler approach can be overcome by Volume of Fluid (VOF), being a surface tracking technique. However, its application requires the precise definition of flow boundaries (i.e. packed bed geometry) which makes it very expensive computationally and restricts its applicability to small segments or periodic regions [1].

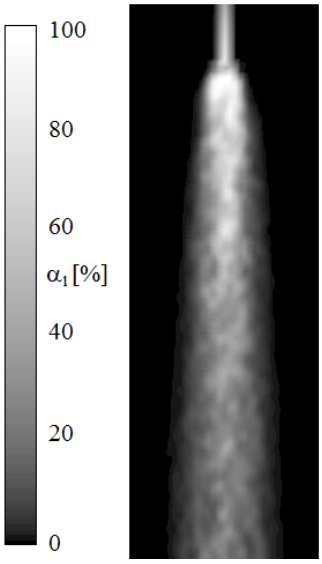

Fig.1. Instantaneous liquid volume fraction α_l distribution in a packed bed. White colour corresponds to liquid while black one to gas phase.

In the present paper a combined VOF-Eulerian two-fluid simulation strategy was applied to the two-phase countercurrent flow in a random packed bed composed of Raschig rings. The realistic packed bed geometry was generated numerically using the in-house code [3], which then could serve as geometrical constraints for the liquid flow simulation with the use of VOF model. As an outcome the probability distribution function (PDF) of velocity vector orientation angle was determined, which then could be implemented into a 2-fluid Euler-Euler multiphase model of packing column [4] developed in Ansys Fluent environment. The velocity vectors were generated in random way, however, satisfying both the PDF of vector orientation as well as the cross section averaged liquid loads. Using this procedure the flow structure could be recovered in a way reflecting the realistic geometrical constraints, i.e. local nonuniformities of the flow velocity and volume fraction fields. In Fig. 1 the sample distribution of the liquid volume fraction is presented for the case when water is injected from centred fine-diameter distributor. One can easily notice the irregular flow structure manifested by varying greyscale intensity reflecting liquid accumulations and zones with significantly reduced water content. The variations of liquid volume fraction around the expected (Eulerian) level influence a gas velocity field which in turn may lead to increased pressure drop. Taking the reacting flow conditions into account the solution of the flowfield in such a form allows for more precise calculations of local heat and mass transfer being actually related (in nonlinear manner) to volume fractions and compositions of counterflowing phases.

The presented VOF-Euler simulation strategy has been shown to provide the adequate description of the trickling flow and the liquid spreading in an unstructured packed bed in reasonable time. The speeding up of the procedure was achieved by implementation of velocity vector distribution instead of detailed flow modelling in a realistic packed bed geometry. The model is intended to be applied for the simulation of reacting flows, in particular to simulate the carbon dioxide capture by chemical absorption, i.e. one of the most common post-combustion carbon capture and storage (CCS) technologies.

References:

[1] Wang Y., Chen J., Larachi F.: *Modelling and Simulation of Trickle-Bed Reactors Using Computational Fluid Dynamics: a State-of-The-Art Review*, The Canadian Journal of Chemical Engineering 91: 136-180, 2013
[2] Solomenko Z., Haroun Y., Fourati M., Larachi F., Boyer C., Augier F.: Liquid spreading in trickle-bed reactors: *Experiments and numerical simulations using Eulerian–Eulerian two-fluid approach*, Chemical Engineering Science 126: 698-710, 2015
[3] Marek M.: *Numerical generation of a fixed bed structure*, Chem. Process Eng. 34: 347-59, 2013
[4] Niegodajew P., Asendrych D., Marek M., Drobniak S.: *Modelling liquid redistribution in a packed bed*, J. Phys. Conf. Ser. 530: 1-8, 2014

On the effective stress principle within a generalized porous media

Janusz Badur[1], Paweł Ziółkowski[1], Tomasz Kowalczyk[1,2]
[1]Energy Conversion Department, Institute of Fluid Flow Machinery PAS-ci, Gdańsk
[2] Conjoint Doctoral School at the Faculty of Mechanical Engineering, Gdańsk University of Technology
pziolkowski@imp.gda.pl

Keywords: effective stress, poro-mechanics, poro-thermo-chemo-mechanical interactions, Biot's poro-thermo-elasticity, continua with microstructure

From the Rational Thermodynamics point of view, the science of poro-mechanics, which has been developed by pioneers and veterans for more than 70 years, formally needs to introduce additional law of thermodynamics. According to Truesdell's suggestion, the Therzaghi principle of effective stress should play a role of exceptional law among of whole laws of the classical field theory. Therefore, having a line of reasoning directed towards this principle, numerous concepts of poro-thermo-elasticity have been recently developed by Capritz [1], Sciarra et al [2], Wilmański [3], Kubik, Cieszko and Kaczmarek [4]. Among them, taking the effective stress principle as a starting point, there are few models that take into account more complex microstructure of the porosity.

Simultaneously, from the rational mechanics point of view, modelling of complex phenomena within the poro-thermo-chemo-mechanical interactions only by a simple media model is not sufficient and under some circumstances even wrong. Therefore, having not yet explored Biot's ideas [5] in mind, a novel concept of generalized poro-mechanical model has been recently recognized and developed by the authors [6].

In the present work, we have developed the principle of effective stress onto a new situation where the exchange of momentum and thermal energy in porous continua undergo a more complex state. Basing on the exergy destruction procedure [6]: we are able to find more consistent definitions of: entropy, porotic and momentum effective fluxes. Next, with these correct definitions at hands, more consistent constitutive equations could be defined.

Finally, three specific examples of effective stresses definitions have been worked out, e.i. for the coke production, the CO_2 sequestration and the early age concrete.

References:

[1] Capriz G.: *Continua with Microstructure*, Springer Tracts in Natural Philosophy, no 35, ed. C. Truesdell, Springer Verlag, New York, 1998.
[2] Sciarra G., dell'Isola F., Coussy O.: *Second gradnient poromechanics*, Int. J. Solid and Struc. 44: 6607-6629, 2007.
[3] Wilmański K.: *Thermodynamical admisibility of Biot's model of poroelastic saturated materials*, Arch. Mech. 54: 709-736, 2002.
[4] Kubik J., Cieszko M., Kaczmarek M.: *Podstawy dynamiki nasyconych ośrodków porowatych,* Wyd. IPPT PAN, Warszawa 2000.
[5] Biot M.: *Variational-Lagrangean irreversible thermodynamics of initially-stressed solids with thermo-molecular diffusion and chemical reactions*, J. Mech. Phys. Solids, 25: 289-307, 1977.
[6] Badur J., Ziółkowski P., Kowalczyk T.: *A thermo-dynamical justification of the effective stress principle,* submitted, Arch. Hydro-Eng. Environ. Mech., 2016.

Laminar flow past the bottom with obstacles: suspension and porous medium approximations

Włodzimierz Bielski[1], Ryszard Wojnar[2]
[1]Institute of Geophysics, Polish Academy of Sciences
[2]Institute of Fundamental Technological Research PAS
wbielski@igf.edu.pl; rwojnar@ippt.gov.pl

Keywords: rough bottom, plants, Stokes'-Brinkman's flow interface

We study flow of viscous fluid in a wide channel, when the influence of the channel banks can be neglected and the two-dimensional problem can be considered only. We admit that the channel bottom is naturally uneven, covered by small obstacles or sub-water plants. Such problem we solve on two ways: (i) we treat the obstacles as a suspension, cf. [1], and (ii) we regard its as a porous medium.

The two-layer (A and B) flow of the same viscous fluid on the bottom plane slightly inclined to the horizontal plane under the gravity force component is considered. The fluid A flows past the fluid B. The upper surface of the fluid A is free and suffers only the air pressure, and the flow in both cases, (i) and (ii) is laminar, described by Stokes' equation. In the case (i) the lower fluid B bears a suspension, and in the case (ii) the lower fluid B flows through a porous medium. In both cases the continuity of the velocities and the shear stresses on the A--B interface is postulated and achieved. Brinkman's suspension relation, cf. [2], (a generalization of Einstein's formula) is used in the case (i), and Brinkman's equation, cf. [3], gives satisfactory description of the problem (ii).

References:

[1] R. Wojnar and W. Bielski, *Laminar flow past the bottom with obstacles - a suspension approximation*, Bulletin of the Polish Academy of Sciences, techn. ser., 63(3) 685-695 (2015).
[2] H.C. Brinkman, *The viscosity of concentrated suspensions and solutions*, J. Chemical Physics 20, 571-571 (1952).
[3] H.C. Brinkman, *A calculation of the viscous force exerted by a flowing fluid on a dense swarm of particles*, Applied Scientific Research 1(1), 27-34 (1949).

Acknowledgements:
The publication has been partially financed from the funds of the Leading National Research Centre (KNOW) received by the Centre for Polar Studies for the period 2014-2018.

Influence of granular bed parameters on emulsion flow and elution process of oil in water emulsion

Mariola Błaszczyk, Łukasz Przybysz, Jerzy Sęk
Lodz University of Technology, Faculty of Process and Environmental Engineering
mar.blaszczyk@o2.pl

Keywords: porous medium, emulsion, elution

Issues related to the flow and elution of emulsions from porous bed have the immense importance while conducting processes such as soil remediation from various kinds of multi-phase organic substances, and secondary methods of extracting oil from underground reservoirs. Expanding knowledge on emulsion systems migration in granular structures can also contribute to the development of new techniques for obtaining oil from oil sands and oil shales [1]. Knowledge of processes of emulsion flow in porous media is also useful in the treatment of waste water from various organic substances. Filtration of oily fluid, by passing them through coalesces composed of porous fibrous media, is used here [2].

Emulsions flow in porous media differ from the independent movement of the individual phases, and therefore must be considered separately. To describe the nature of such flows, permeability reduction mechanisms and changes in concentration of internal phase must be taken into account. This will enable to understand and to predict the way in which emulsion systems behave during transport in porous media. This knowledge is extremely useful to obtain a comprehensive picture of multiphase flow in porous media.

Due to the existing retention mechanisms of fluid in porous structure, caused by capillary forces, oil droplets can be trapped in it [1]. During the process of elution by washing liquid, these droplets can move as emulsion systems. Often to the washing media surfactants are added, in order to reduce surface tension, and thereby increase the degree of elution. This is an additional factor causing the formation of the emulsion during the elution process [3]. The emulsions may also be formed in the bed by itself. Many petroleum substances in their composition contain an amount of naphthalene acid, which exhibit the properties of natural surfactant to facilitate the formation of the emulsion structures. Moreover, the presence of variety of alkali in these liquids, causes stabilization of formed systems. Evaluation of how the emulsion systems will move in the granular bed while conducting soil treatment techniques from oil-derived substances may help to increase process efficiency and reduce the associated financial expenditure [4].

When describing the process flow of O/W emulsion in a porous medium it is important whether it can be treated as a homogeneous liquid. If the emulsion droplets are very small, compared to the size of the flow channels, it can be considered that the fluid is an one phase continuous medium and totally ignore the microscopic droplets of the emulsion [5]. However, in most practical cases, the sizes of the emulsion droplets are not much smaller than the pore size, or even from larger them, which means that their presence in the bed cannot be ignored. In this case, it is necessary to examine how the various properties of the emulsion affect the flow through a porous medium [6].

The flow of the emulsion through the porous medium is dependent on the properties of both the porous medium and the emulsion itself. Taking into account the properties of the emulsion, such factors as: emulsion stability, concentration, droplets size and interfacial interactions, play here particular role. As regards to the parameters characterizing granular bed, wettability, pore average size and pore size distribution are the most relevant here. Wettability of the porous medium controls the flow, location and distribution of the fluid in the porous bed. This parameter affects the capillary pressure, relative permeability, water and oil saturation, and other properties [1]. Pore sizes and their distribution are directly related to the capture and retention of oil drops. The pore diameter size distribution affects the reduction of permeability [7].

Study on the effect of particle size fractions on the processes of emulsion flow and elution from the porous bed have been performed. For this purpose, experiments with the use of glass microspheres, with three different ranges of particle size diameters were carried out. Due to the fact that the particle size directly affects the intergranular space, the flow of emulsion through the bed depends on the size of its grain-size fraction. In the case of deposits with larger grain size, flow resistances of the emulsion were small. Significant decrease in the concentration of the emulsion flowing from a deposit in the initial flow phase also was not present here. In the case of deposits with smaller grains, the situation was reversed. Flow resistance and the occurrence of straining phenomena were more noticeable. For deposits with a larger particle size fraction achievement of steady state also occurred faster, both for the flow and elution of emulsion with water. This was due to the fact that in the case of deposits with large grain size, there were fewer pores, which size was similar to the droplet size of the emulsion oil phase, that is, which may have become blocked. As a consequence, the resulting permeability of the bed was higher than in the case of smaller grain-size fraction.

References:

[1] Dullien F. A. L., *Porous Media Fluid Transport and Pore Structure*, Academic Press Inc, San Diego, California, 1992
[2] Allan F.M., Kamel M.T., Mughrabi T.A., Hamdan M.H., *Infiltration of oil into porous sediments*, App. Math. and Comp., 177, 659–664, 2006
[3] Li J., Gu Y., *Coalescence of oil-in-water emulsions in fibrous and granular beds*, Sep. and Pur. Techn., 42, 1–13, 2005
[4] Cobos S., Carvalho M.S., Alvarado V., *Flow of oil–water emulsions through a constricted capillary*, Int. J. of Multi. Flow, 35, 507–515, 2009
[5] Cortis A., Ghezzehei T. A., *On the transport of emulsions in porous media*, J. of Coll. and Int. Sci., 313, 1–4, 2007
[6] Wang J., Dong M., *Trapping of the non-wetting phase in an interacting triangular tube bundle model*, Chem. Eng. Sci., 66, 250–259, 2011
[7] Heinemann Z. E., Fluid flow in Porous media, Textbook Series, 1, Leoben, 2005

Characteristics of porous beds based on fractal parameters

Mirosław Bramowicz[1], Sławomir Kulesza[2], Wojciech Sobieski[1]
[1] University of Warmia and Mazury, Faculty of Technical Sciences, Olsztyn, Poland
[2] University of Warmia and Mazury, Faculty of Mathematics and Computer Science, Olsztyn, Poland
miroslaw.bramowicz@ uwm.edu.pl

Keywords: granular beds, porosity, fractal analysis, numerical modelling

This paper presents the results of fractal analysis of a set of virtual porous beds with a porosity ranging from 0.4 to 0.95 (Fig. 1). These beds were generated by the so-called growing particle method with the use of the Discrete Element Method, in a space of dimensions $l \cdot l \cdot 2l$, where l is the characteristic dimension of the computational space [m]. In this method, an initial cloud of particles (without any contacts) is generated, and then all particles increase in size until the target porosity is reached. The number of contacts between particles increases during calculations and is fixed at a constant level after some time. This process takes place in an iteration loop and all interactions between particles related to the friction are taken into account. Other external forces, e.g. gravity forces are excluded. It is very important that in the calculation process, the friction angle of sphere material decreases in time (it is defined by appropriate function of the model). Thus, the porosity decreases with time, too. Results presented in the paper are a part of research conducted within the framework of the so-called PathFinder project [1].

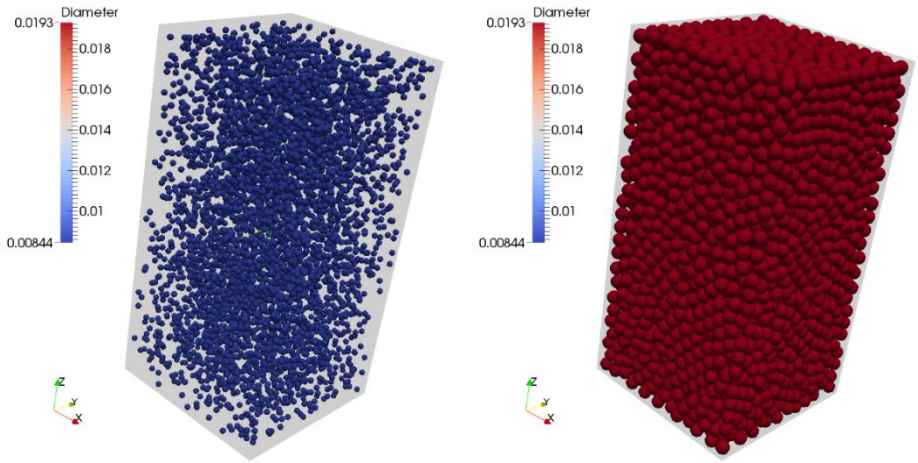

Fig.1. Visualization of beds with the largest (left) and the lowest porosity (right).

Presented analysis concerns fractal results obtained using the multi-step algorithm described in [2] that involved: (1) computation of a 2-dimensional autocorrelation function, (2) computation of an angle-averaged profile structure function (SF), (3) numerical fit of a log-log plot of the SF with power-law dependence parametrized by fractal dimension D, topothesy Λ, and corner frequency τ_c. As seen in Fig. 2 and in accordance with [3], porous beds can be characterized using fractal dimension D, which is associated with the shape and size of elemental particles. On the other hand, fractal dimension is found almost independent of the porosity, and in case the bed is composed of perfect spheres D = 2,52±0,01. Unlike that, however, the two remaining fractal parameters, namely: topothesy and corner frequency, appear to be much more sensitive to the porosity.

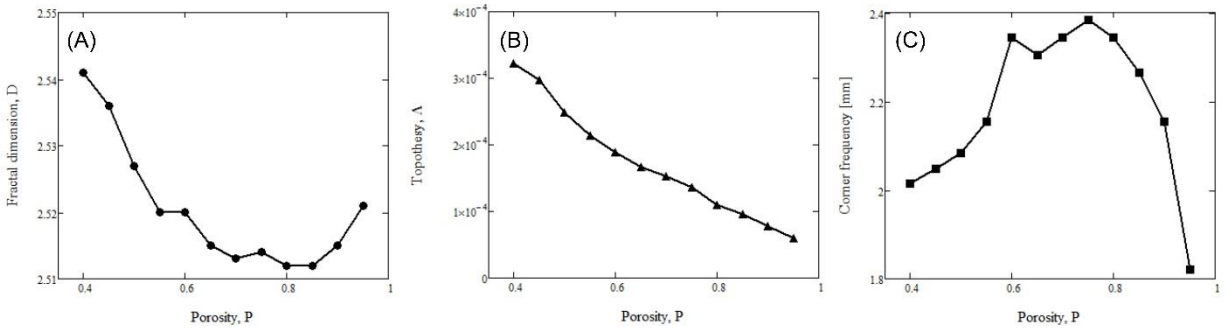

Fig.2. Plots of fractal parameters vs bed porosity: (A) – fractal dimension, (B) – topothesy, (C) – corner frequency.

References:

[1] PathFinder Project [on-line]. URL: http://www.uwm.edu.pl/pathfinder/index.php (Available at February 1, 2016). University of Warmia and Mazury in Olsztyn (Poland).
[2] Kulesza S., Bramowicz M. *A comparative study of correlation methods for determination of fractal parameters in surface characterization.* Applied Surface Science, Vol. 293 pp.196-201 (2014), http://dx.doi.org/10.1016/j.apsusc.2013.12.132.
[3] Sun H., Koch M. *Numerical generation of porous structure with fractal properties*. Computational Methods in Water Resources XII, Vol. 2, pp. 149-157 (1998).

Back analysis of the results of cyclic torsional shear of cohesive soils

Marcin Bujko
University of Warmia and Mazury in Olsztyn, Faculty of Geodesy, Geospatial and Civil Engineering
marcin.bujko@uwm.edu.pl

Keywords: soil mechanics, small strains, torsional shear

Proper procedure of geotechnical research, leading to measure mechanical parameters of the soil, should consist on: 1) "in situ" field test in natural conditions, and then 2) laboratory test with sample taken from the field and isolated from the environment. All the research methods lead to load the soil and check the arising value of strain. The soil deforms plastically since the beginning of loading process. Elastic strains are only the very small part of total strains – elastic work of the grains of the soil and grain-bound water. Plastic strains connected with structural changes of the soil are caused by the mutual displacement of the soil grains or the destruction of weak ones. Cyclic loading and unloading results in different strain values. Typical feature of the soil is the variability of the strain modulus. It seems quite unusual in comparison with linear-elastic materials – common in civil engineering. Complex nature of the soil determines the necessity of executing more complex laws and techniques to understand and use mechanical features of the soil in engineering.

Cyclic Torsional Shearing Apparatus allows to measure and analyse parameters in range between 0,01% and 0,1%, what makes this method much more accurate than Triaxal Compression Apparatus. Moreover, there is widely published statistics which stands that geotechnical structures load the soil causing shear strains at the level of 0,01% - small strain range. Furthermore, in comparison with Bender tests, which theoretically lets to get the initial shear modulus, cyclic torsional shear test brings much more certain results – smaller number of measurement uncertainties. There is plenty of reasons to take Cyclic Torsional Shearing test as the authoritative method of the soil measurement. As many other methods based on propagation of the elastic waves, Cyclic Torsional Shearing has been designed for seismological usage. Since 60's it has started to be used by geotechnical engineers (see [1,2]) and still it's getting more appreciated and popular [3]. The main idea is based on the measurement of the elastic features of the material. Measurement bases on the reaction on forced shearing. According to this method it is possible to measure damping coefficient as well as shear strain modulus of the soil.

In Torsional Shearing (TS) mode the shear modulus is calculated directly basing on the relation of shear stress **τ** and shear strains **γ** during cyclic shear of the free ending of the sample by shear moment **T** with frequency lower than 1Hz. It is possible to make an interpretation of measured physical quantities using back analysis algorithm based on theoretical model describing visco-elastic behaviour of sheared material (see [4]). A typical example of the results of such kind of analysis is presented in Fig.1.

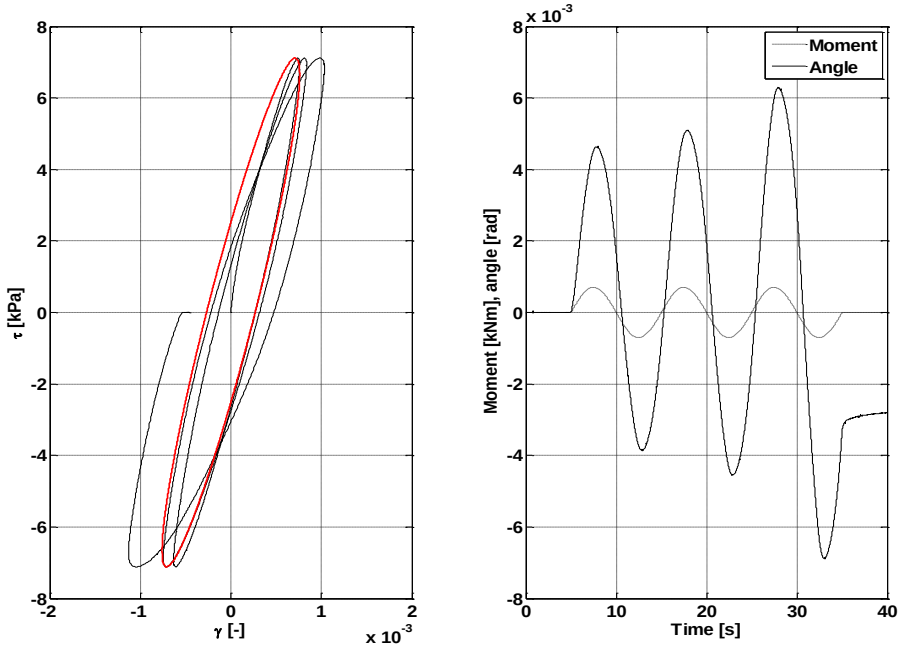

Fig.1 Example of the back analysed hysteresis loop $\tau(\gamma_{max})$.

The Author experienced that this new approach might develop basic method of interpretation of results as well as seems to be helpful in getting more accurate outcomes what brings hope for more insightful engineering practice.

References:

[1] Drnevich V.P.: *Effects of strain history on the dynamic properties of sand*, PhD thesis, University of Michigan, 1967
[2] Hardin B.O., Richart F.E.Jr.: *Elastic wave velocities in granular soils*, Journal of Soil Mechanics and Foundations Divisions. Proc. of ASCE, vol. 89, No. SM1, 33-65, 1963
[3] Srokosz P.E., Bujko M., Górska-Pawliczuk A., *Zastosowanie systemu klasyfikacyjnego do interpretacji wyników badań skrętnego ścinania gruntów*, Inżynieria Morska i Geotechnika, 5, 686-692 ,2015
[4] Dyka I., Srokosz P.E.., *Badania gruntu w aparacie skrętnego ścinania*, Inżynieria Morska i Geotechnika, 6, 700-707, 2012

Vertical mixing caused by gravity waves

Włodzimierz Chybicki[1], Piotr, E.,Srokosz[2],Andrzej Wróblewski[2]
[1]The State University of Applied Sciences in Elbląg
[2]University of Warmia and Mazury in Olsztyn
andrzej.wroblewski@uwm.edu.pl

Keywords: vertical mixing

The processes of heat transfer and mixing of ocean waters play a very important role in predicting the processes related to the circulation of water in the oceans, weather, climate change on the earth and under the above mentioned causes biological implications. The problem of climate change is becoming clearer. Among the last few months the turn of 2015 and 2016 year, three months was a record in terms of recorded average monthly temperatures.

Considering climate change on earth cannot ignore the influence of the surface water of the ocean to the processes associated with these changes - just to mention that the amount of heat required to heat the whole atmosphere of the earth by one degree is the same that is needed to heat the only three-meter surface water in the oceans of one degree. Example of the close relationship of climate to the temperature of the surface water of the oceans are the phenomenon of El Niña or El Niño - the flow of cold water on the ocean's surface off the western shores of South America, or the lack of such a flow, it changes the average annual temperature of the whole earth.

In winter, when the water at the ocean surface is colder and denser than the lower layers, then by convection it will begin to move down while the warmer water move up. In this way, the heat accumulated by the water will be given to the atmosphere. In the summer, when the warm water is at the very top heat conducting processes from the surface to deeper layers are more complicated. In this case, heat conducting is primarily connected with the turbulent heat transfer coefficient. The effect of induced turbulence may be the result of break of the surface waves or stream surface caused by the wind. Studies in nature suggests that there must be additional mechanisms associated with a surface waving explaining what is happening there, but the way they generate a turbulent motion is not fully understood. One reason may be a effect closely associated with the movement of the wave which is the Stokes drift or Langmuir circulation.

It is assumed that the velocity field in the ocean is not a potential field. The impact on the appearance of vorticity are boundary layers and processes that take place there: the brake of the wave and the friction between the water and wind or water and bottom. Thus vorticity field generated affects the mixing of water vertically in the surface watr of the ocean. As noted Saffman, vorticity field is important because it inevitably leads to turbulence. In order to take into account of the mixing process of the surface waters of the ocean surface waves associated with the most commonly used turbulent diffusion coefficient K .

The work is devoted to study different mechanism causing the velocity field is not a potential field. If the density of the liquid is variable and depends on the depth, the velocity field as there is the potential - is induced pressurized vorticity. Vorticity may explain the observed effect in which the mixing of liquid in a limited area where the density gradient fluid is large, is larger.

Macroscopic Description of Capillary Transport of Liquid and Gas in Unsaturated Porous Materials

Mieczysław Cieszko
Institute of Mechanics and Applied Computer Science
Kazimierz Wielki University, Bydgoszcz
cieszko@ukw.edu.pl

Keywords: unsaturated porous materials; macroscopic description; capillary transport

A new macroscopic description is proposed for the capillary transport of liquid and gas in porous materials of the homogeneous and isotropic pore space structure, [1]. Theoretical considerations are conducted within the framework of the multiphase continuum mechanics and are based on three key model assumptions. This concern:

- division of liquid in the pore space into two macroscopic constituents called mobile liquid and capillary liquid (Fig.1),
- description of menisci motion by an additional macroscopic velocity field,
- parametrization of saturation changes by a macroscopic pressure-like quantity that for quasi static and stationary processes is equal to the capillary pressure.

The division of liquid into two continua is justified both kinematically and energetically. The capillary liquid forms a film on its contact surface with the skeleton. This liquid is immobile and contains the whole interfacial (capillary) energy of liquid in the pore space. The remaining part of the liquid surrounded by the layer of capillary liquid and menisci forms the mobile liquid. Both liquids exchange mass, linear momentum and energy in the vicinity of menisci surfaces and this occurs only during menisci motion in the pore space.

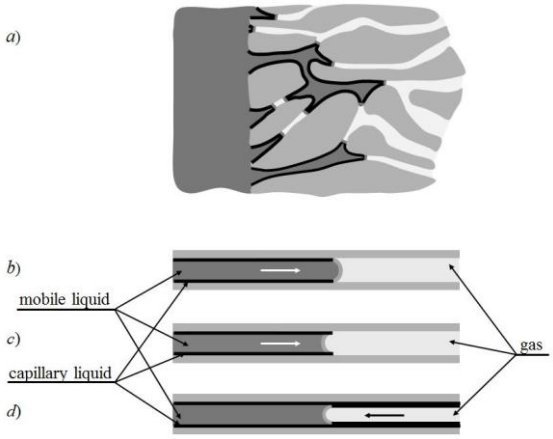

Fig.1. Schematic illustration of non-wetting liquid intrusion into a sample of porous material (*a*) and of three typical compositions of constituents in the medium: *b*) non-wetting liquid intrusion, *c*) wetting liquid inflow, *d*) wetting liquid extrusion.

The additional velocity field describing menisci motion reflects the complexity of kinematics in unsaturated porous materials and enables the modeling of mechanisms of menisci motion in the pore space.

Parametrization of saturation extends the dimensionality of the description of processes taking place in an unsaturated porous material enabling, among others, the description of liquid distribution in quasi-static processes and in the stationary flow.

For all constituents of the porous medium, balance equations of mass, linear momentum and energy are formulated and constitutive relations for mechanical processes are derived. The approach is used based on the analysis of dissipation inequality of mechanical energy formulated for the whole system. A new approach is proposed, similar to that used in the rational thermodynamics, based on entropy inequality analysis and the Lagrange multipliers method. The velocity field of the menisci motion in the pore space induced by changes of the capillary pressure is defined by an additional constitutive relation, similar to Fick's first law of diffusion.

It is shown that the equations obtained describe both quasi-static and quasi-stationary processes of capillary transport of liquid and gas in unsaturated porous materials as special cases of the new mathematical model. This concern, among others, the description of quasi-static intrusion of mercury into porous materials and description of liquid or gas flow through unsaturated porous material. In the first case, the equations have a form of non-stationary diffusion in which, instead of time as the independent variable, the mercury pressure is present. In the second case, for example, even the geometrically very simple problem of liquid flow through a layer of unsaturated porous material is described by a system of three coupled, nonlinear equations for distributions of saturation, the fluid pressure and its flow velocity in the layer. In this case the fluid flow through the layer of unsaturated porous material is similar to flow through an elastic tube the cross-section of which is being changed depending on the local pressure in fluid.

References:

[1] Cieszko M.: *Macroscopic Description of Capillary Transport of Liquid and Gas in Unsaturated Porous Materials*, Meccanica 22: 1-22, 2016

Extended macroscopic description of a non-wetting liquid intrusion into a ball of porous material

Tomasz Czerwiński[1], Mieczysław Cieszko[2], Eugeniusz Czapla
Institute of Mechanics and Applied Computer Science
Kazimierz Wielki University, Bydgoszcz
thhomekcz@gmail.com[2], cieszko@ukw.edu.pl[2]

Keywords: non-wetting liquid, porous ball, liquid intrusion into a ball, macroscopic description

The problem of macroscopic description of quasi static intrusion of non-wetting liquid (mercury) into a ball of porous material is considered. Modelling of these processes is of great importance for interpretation of the mercury intrusion curves used for determination of the pore size distribution and other pore structure parameters of porous materials. For interpretation of such curves the simplified microscopic models of the pore space structure are applied that do not take into account the shape and size of the investigated sample and therefore lead to significant faults. Application of the macroscopic description of mercury intrusion is a new approach to this problem allowing avoiding these faults in interpretation of the experimental data.

A new macroscopic description is proposed for quasi static process of non-wetting liquid intrusion into a ball of porous material. The analysed problem is an extension of the description presented in the paper [1]. Considerations are based on the continuum model of the capillary transport of liquid and gas in unsaturated porous materials, proposed by one of authors of the present paper [2]. The key assumptions of this model are: division of liquid in the pore space into two macroscopic constituents called mobile liquid and capillary liquid; description of menisci motion by an additional macroscopic velocity field; parametrization of saturation changes by a macroscopic pressure-like quantity that for quasi static and stationary processes is equal to the capillary pressure. The capillary liquid forms a film on its contact surface with the skeleton. This liquid is immobile and contains the whole interfacial (capillary) energy of liquid in the pore space. The remaining part of the liquid surrounded by the layer of capillary liquid and menisci forms the mobile liquid. Both liquids exchange mass, linear momentum and energy in the vicinity of menisci surfaces and this occurs only during menisci motion in the pore space. The additional velocity field describing menisci motion reflects the complexity of kinematics in unsaturated porous materials and enables the modeling of mechanisms of menisci motion in the pore space. For all constituents of the porous medium, balance equations of mass, linear momentum and energy are formulated and constitutive relations for mechanical processes are derived. Based on equations of this theory, equations for the quasi static process of non-wetting (mercury) liquid intrusion into porous materials were derived.

We assume that at the beginning of the intrusion process pressure of mercury surrounding the ball is equal to zero and the ball pore space is empty (vacuum) (Fig. 1). The increase of pressure in mercury causes penetration of mercury into pores of the ball and its spatial distribution that evolve during the process of mercury intrusion. This process is stopped when all pores of the ball are fulfilled with mercury.

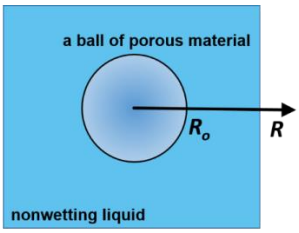

Fig.2. Scheme of quasi static intrusion of a non-wetting liquid into a ball of porous material.

The quasi static processes of mobile liquid intrusion into a ball porous material is the special case of the model presented in the paper [2]. This process is described by evolution equation for saturation distribution with the mobile liquid. In the spherical coordinate system this equation takes the form

$$\frac{\partial s_m}{\partial p}\left(1+\frac{ds_c}{ds_m}\right)-C_m(s_m,p)\left(\frac{\partial s_m}{\partial r}\right)^2=C_s(s_m,p), \tag{1}$$

where by s_m, s_c saturation of the ball with the mobile and capillary liquid are denoted, respectively, and p stand for the pressure in the mobile liquid that is homogeneous. Quantities $C_m(s_m,p)$, $C_s(s_m,p)$ are coefficients characterizing the internal pore space structure of the porous material.

During the process of mercury intrusion it penetrate only the pores the diameters of which are greater than the critical diameter defined by Washburn formula $D^*=-4\sigma\cos(\theta)/p$. Therefore, the boundary condition on the ball surface $(r=r_o)$ depends on the mercury pressure. Equation (1) is strongly nonlinear and is solved using the method of characteristics and the analysis of the process is performed numerically.

References:

[1] Cieszko M., Czapla E., Kempiński M.: *Continuum Description of Quasi-Static Intrusion of Non-Wetting Liquid into a Porous Body*, Continuum Mechanics and Thermodynamics 27(1): 133-144, 2015
[2] Cieszko M.: *Macroscopic Description of Capillary Transport of Liquid and Gas in Unsaturated Porous Materials*, Meccanica 22: 1-22, 2016

Preparation of macroporous $SrTiO_3$ materials using polimethyl metacrylate template

Zuzanna Czwarkiel, Ewa Drożdż
AGH University of Science and Technology, Kraków

Keywords: polimethyl metacrylate, strontium titanate, 3DOM

Strontium titanate ($SrTiO_3$) with a perovskite-type structure is interesting material because of being thermally stable solid electrolyte in wide temperature ranges in both –reducing and oxidizing atmosphere. Perovskite-type materials, with general chemical formula ABO_3, have usually cubic or tetragonal structure (also orthorhombic or trigonal structures occur). Idealized cubic cell has type 'A' atoms at cube corner positions, type 'B' atoms at body centre positions and oxygen atoms at face centered positions. The stability of $SrTiO_3$ structure allows partial substitution of A or B site cations by other metals with different oxidation state, resulting in creation of point defects such as anionic or cationic vacancies that could enhance conductivity of $SrTiO_3$. This kind of substitution provides materials with high mobility of ions. Using an appropriate dopant can maximize the number of free electrons, thus it is possible to create in this way a mix-conductor[1]. This is the a reason why perovskite materials may be used in electrical appliances.

In this paper features of macroporous Nb-doped $SrTiO_3$ were investigated. Nb^{5+}, as a donor dopant, has a higher cationic charge than the host, Ti^{4+} which is replaced. Thus, to keep electroneutrality, free electron has to be released in conduction band. In [2], it was reported that mixed ionic-electron conductivity of donor-doped $SrTiO_3$ can be obtained. Macroporous systems are being used in solid oxide fuel cells (SOFC) in order to increase the number of triple phase boundary (TPB). TPB is a region where three phases are in contact: electrolyte, electrode and gaseous fuel. Only there, owing to electronic conductivity of electrolyte, electrode reactions (with the interchange of electron) can take place. Nb-dopped $SrTiO_3$ can simultaneously serve as the electrode and electrolyte, so it is important to increase the surface area of perovskite powder.

Usually, similar materials are prepared by the reaction of solid state, but this method results in a material of low porosity. In order to increase porosity, foam-forming agents, as amylum, cellulose, gelatine, carbon or ammonium carbonate can be used. Unfortunately, this method causes the traces of the carbon, which locates in grain boundaries, thereby reducing conductivity. The wet synthesis method with using of templates allows one to obtain structures with high, regular porosity and high phase purity. Polimethyl metacrylate (PMMA), SiO_2 colloidal spheres and monodispersed polystyrene (PS) are used as templates [3].

Synthesis is based on sol-gel method with application of colloidal crystal template method. An aqueous solution of strontium nitrate, titanium isopropoxide and a solution of niobium ethoxide in ethanol were used as precursors of Nb-dopped $SrTiO_3$. The precursors were dissolved in methanol solution of citric acid and applied to spheres. The amount of incorporated Nb in prepared powders were: 0,5mol%, 1mol%, 2mol% and 3mol%.

As a result a three-dimensionally ordered macroporous materials (3DOM) with high purity were obtained. Average pore diameter was 120nm as shown in picture below. Figure 1 (a) shows SEM picture of 1mol% Nb-dopped $SrTiO_3$ 3DOM prepared using described synthesis technique, when Figure 1 (b) shows the starting polymeric spheres of PMMA, whose diameters are around 400nm. It seems that the pore diameters are smaller than the diameters of the spheres used.

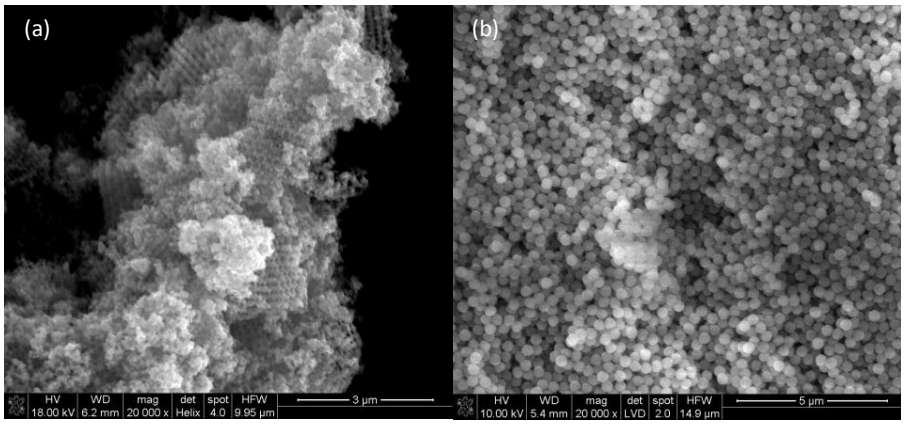

Fig.1. SEM pictures of obtained $SrTiO_3$ material (a) and PMMA template (b).

In order to investigate features of received powders, XRD and SEM measurements have been performed. XRD patterns correspond to a single-phase $SrTiO_3$.

Acknowledgment
This work was financially supported by the National Science Centre of the Republic of Poland, Grant No 2014/14/EST5/00763.

References:

[1] Ruiz-Morales J.C., Canalez-Vazquez J., Savaniu C., Marrero-Lopez D., Zhou W.Z., Irvine J.T.S.: *Disruption of extended defects in solid oxide fuel cell anodes for methane oxidation*, Nature, 439 (2006) 568
[2] JunFei F., YiMin X., Qiang L.: *Preparation of three-dimensionally ordered macroporous perovskite materials*, Chinese Science Bulletin, July 2011

Experimental investigation of fluid flow through granular beds

Waldemar Dudda, Wojciech Sobieski
University of Warmia and Mazury in Olsztyn
dudda@uwm.edu.pl

Keywords: porous bed, pressure drop, Forchheimer equation

The work concerns the experimental investigations of water flow through three porous beds, consisting of glass marbles with average diameters of 3.932 [mm], 6.072 [mm], 7.916 [mm] and the porosity 0.407, 0.413, 0.411, respectively.

Fig. 1.a) shows the main idea of the measurement methodology used for determining the resistance of fluid flow through the porous medium. The system consists of a column of A cross-section, filled with porous material in the L section, and a set of measuring spigots (minimum of two).

The measuring stand used in the experiment is shown in Fig. 1b). The piezometric heads (dh_{4-1}) in 4 points were measured for 17 different filtration velocities ($\vec{v}_f$). Every measurement was repeated 10 times and the results were then averaged. In the next step, the piezometric heads were recalculated to the pressure drops (dp_{4-1}). To eliminate the impact of the temperature variations on the results [1], in all measurements the temperature was approximately constant and equal to 33±2 [°C].

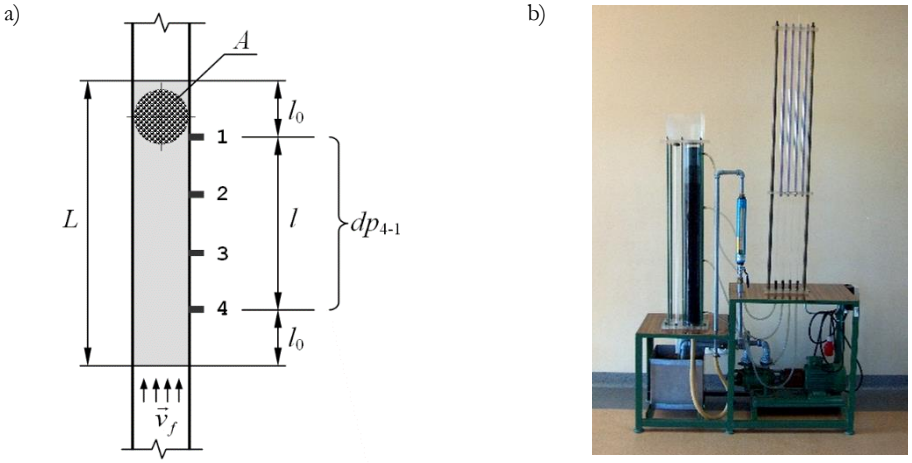

Fig. 1. Scheme of a typical measuring system (a) and the stand used in the experiment (b).

Based on the measurements data, the Forchheimer Plot Method was applied [2,3], in which a reverse problem is solved. An own software was used on this stage [4]. As the result the $1/\kappa$ and β coefficients of Forchheimer equation [1,2,3] were obtained. The final values of these coefficients were as follows: 0.9948280000E+08 and 0.864587E+04 for the smallest; 0.3914000000E+08 and 0.545758E+04 for the medium; 0.1835540000E+08 and 0.295523E+04 for the biggest granulate.

In Fig. 2 the pressure drops in relation to the filtration velocity are visible, those obtained in the experiment, as well as in the analytical model. The relative errors were below 3% in most cases.

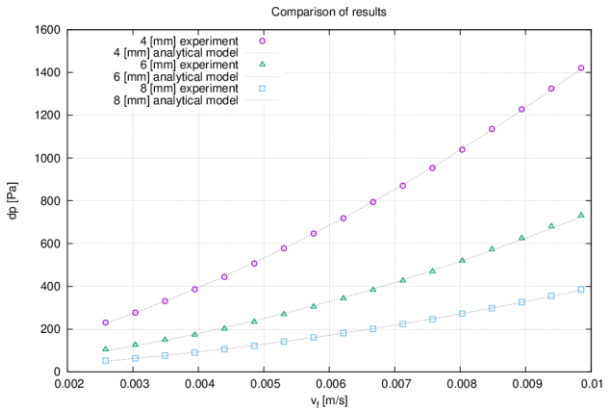

Fig. 2. Comparison between the experiment and calculations based on the Forchheimer equation.

References:

[1] Sobieski W., Trykozko A.: Sensitivity aspects of Forchheimer's approximation. Transp Porous Media 2011, 89(2), 155-164.
[2] Sobieski W., Trykozko A.: Darcy's and Forchheimer's laws in practice - Part 1: The experiment. Tech Sci 2014, 17(4), 221-335.
[3] Sobieski W., Trykozko A.: Darcy's and Forchheimer's laws in practice - Part 2: The numerical model. Tech Sci 2014, 17(4), 337-350.
[4] The PathFinder Project [on-line]. URL: http://www.uwm.edu.pl/pathfinder/ (Available at June 1, 2016).

Computer simulation of slurry swelling process in aerated concrete production

Paweł Gadzała, Mieczysław Cieszko
Institute of Mechanics and Applied Computer Science
Kazimierz Wielki University, Bydgoszcz
pgadzala@ukw.edu.pl

Keywords: autoclaved aerated concrete, slurry swelling, computer simulation, porous materials

Computer simulation of slurry swelling process is presented in the paper occurring in production of the autoclaved aerated concretes (AAC). Simulation consists of two stages and is realized in the environment of the Blender software. First, the growth process of one gas babble immersed in a dense liquid is modelled. Next, this model is multiplied to model the growth of thousands of babbles of random diameters in the slurry.

Autoclaved aerated concrete is a building material, which found a reasonable compromise between lightness and strength with good thermal insulation. In Poland, AAC began to be produced in the fifties under license of Swedish companies Ytong and Siporex, [1]. AAC is made of easily accessible and abundant components of natural occurrence, such as: cement and lime, quartz sand or fly ash, water and optional additives that improve the cement properties. One of the stages of AAC production is a growth process of slurry caused by proliferation of hydrogen bubbles emitted in chemical reaction. Foaming agent is aluminum powder or paste, which reacts with calcium hydroxide, resulting in the formation of hydrogen bubbles dispersed in the whole volume of the slurry. From 1 kg of aluminum powder approximately 1.25 m^3 of hydrogen is obtained. Slurry grows like yeast cake. For example, 1 m^3 of slurry in the process of growth gives 2.5 m^3 of the aerated concrete.

Blender is the free and open source software designed for three dimensional modelling and animation, used by many of visual effects specialists, animators and groups of scientists, [3-6]. The software is available on many platforms (Linux, Windows, OSX) and can be downloaded from official website, [2]. In addition to the rendering of images from three dimensional models, Blender provides a game engine for interactive graphics along with support for animating two and three dimensional characters, Bullet physics engine integration. Many other tools are present in Blender including methods for rendering complex surfaces and volumes. Advanced users employ Blender's API for Python scripting to customize the application and write specialized tools. In addition, Blender includes simulation tools for modeling physical phenomena, including fluids using the Lattice Boltzmann Method, smoke as particles and rigid body mechanics using Newtonian physics.

In the paper, the process of slurry swelling is modelled as growth of gas bubbles in a viscose liquid contained in a cylindrical chamber. For the purposes of simulation we assume that liquid forms cloud of small interacting balls. At the beginning of the simulated process all objects have the same size. Some part of the balls dispersed in the fluid increase their diameters interacting with the balls representing the fluid surrounding the bubble. This results in swelling of the slurry. Changing of the ball dimensions is determined by laws of the kinetics of chemical reaction of the alumina particles and by conditions of mechanical equilibrium of pressures in the gas of bubbles and fluid. We assume that external pressure is exerted on the liquid affecting the dynamics of changes in the system under study.

References:

[1] Jatymowicz H., Siejko J., Zapotoczna-Sytek G., *Technologia autoklawizowanego betonu komórkowego*, Arkady, Warszawa 1980.
[2] Blender official website: www.blender.org
[3] Kent B.R., *3D Scientific Visualization with Blender*, Morgan & Claypool Publishers 2015. Doi:9781627056120.
[4] Kent B. R., *Visualizing Astronomical Data with Blender*, PASP 125, 731–748, 2013.
[5] Naiman J. P., *AstroBlend: An Astrophysical Visualization Package for Blender*, Astronomy and Computing, 2016, http://dx.doi.org/10.1016/j.ascom.2016.02.002.
[6] Monaghan J. J., *Smoothed particle hydrodynamics*, ARA&A 30 543–574, 2016, doi:10.1146/annurev.aa.30.090192.002551.

Effect of particle shape anisotropy on the results of the granulometric analysis of clays by laser diffraction method

Aleksandra Gorączko[1], Szymon Topoliński[2]

[1]Department of Geomatics, Geotechnics and Spatial Economy, Faculty of Civil and Environmental Engineering and Architecture

[2] Department of Geomatics, Geotechnics and Spatial Economy, Faculty of Civil and Environmental Engineering and Architecture

aleksandra.goraczko@utp.edu.pl

Keywords: granulometric analysis, laser diffraction method, shape anisotropy, clay

Laser diffraction method (LDM) is increasingly used to determine grain size distributions. Grain size measurements based on LDM is assumed as high-repeatable and high-accurate [1]. However, there is no standardized test procedures, although the methodology of research should be precisely adjusted to the type of particles [2], [3], [4].

Measurements of particle with high shape anisotropy based on LDM may produce different results than traditional sedimentation techniques of grain size analysis [5], [6]. This causes the optical particle diameter measured by the laser is much larger than that determined as equivalent spherical diameter in traditional techniques based on Stoke's law. Therefore, the interpretation of the results must take into consideration the type of measured particles [7], [8].

For this reason, clay minerals, which are significantly plate-shaped and elongated, are particularly difficult to granulometric measurements [9], [10]. Moreover, the flocculation and the swelling of the clay particles can cause unexpected effects during the ultrasound pretreatment in LDM [11].

The article presents the results of grain size analysis of natural montmorillonite clay soils. The research was conducted for the Neogene clays from Bydgoszcz, characterized by significant lithological differentiation in regard to participation the clay fraction particles. Methodological aspects, like obscuration level and dispersion process were discussed. A significant difference in clay fraction particles determination were found in relation to applied methods of grain size analysis. A set of equations to transform LDM results to hydrometric results was proposed for investigated soils.

References:

[1] Goossens D.: *Techniques to measure grain-size distributions of loamy sediments: a comparative study of ten instruments for wet analysis*, Sedimentology 55: 65-96. 2008

[2] ISO 13320-1, 1999. Particle size analysis – Laser diffraction methods, Part 1: General Principies.

[3] Keck C.M., Muller R.H.: *Size analysis of submicron particles by laser diffractometry – 90% of the published measurements are false*. Int. J. Of Pharmaceutis 355: 150-163, 2008

[4] Ryżak M., Bieganowski A.: *Metodological aspects of determining soil particle-size distribution using laser diffraction method*, J. Plant Nutr. Soil Sci. 174: 624-633, 2011

[5] Beuselinck L., Govers G., Poesen J., Degraer G., Froyen L.: *Grain-size analysis by laser diffractometry: comparison with the sieve-pipette method*, Catena 32: 193-208, 1998

[6] Di Stefano C., Ferro V., Mirabile S.: *Comparison between grain-size analyses using laser diffraction and sedimentation methods*, Biosystem engineering 106: 205-215, 2010

[7] Buurman p., Pape Th., Muggler C.C.: *Laser grain-size determination in soil genetic studies. 1. Practical problems*. Soil Science. Vol. 162. No3.: 211-218, 1997

[8] Jonkers L., Prins M.A., Brummer GJ.A., Konert M., Lougheed B.C.: *Experimental insight into laser diffraction particle sizing of fine-grained sediments for use in paleoceanography*, Sedimentology. 56: 2192-2206, 2009

[9] Scott-Jackson J.E., Walkington H.: *Methodological issues raised by laser particle size analysis of deposits mapped as Clay-with-flints from the palaeolithic site of Dickett`s Field, Yarnhams Farm, Hampshire, UK*, J. of Archeological Science 32: 969-980, 2005

[10] Konert M., Vandenberghe J.: *Comparison of laser grain size analysis with pippette and sieve analysis: a solutions for the underestimation of clay fraction*, Sedimentology 44: 523-535, 1997

[11] Lapides I., Yariv S.: *The effect of ultrasonic threatment on the particle – size of Wyoming bentonite in aqueous suspensions*, Journal of material science 39: 5209-5212, 2003

Application of the global radial basis function collocation method for analysis of fluid flow through the porous medium

Jakub Krzysztof Grabski[1], Magdalena Mierzwiczak[1], Jan Adam Kołodziej[1]
[1]Institute of Applied Mechanics, Poznan University of Technology, ul. Jana Pawła II 24, 60-965 Poznań
jakub.grabski@put.poznan.pl

Keywords: global radial basis function collocation method, meshless method, porous medium, permeability

Usually the finite difference method (FDM), the finite element method (FEM) or the finite volume method (FVM) are used in solving different engineering problems. The global radial basis function collocation method (GRBFCM) belongs to so called meshless method which are a kind of alternative to commonly used methods (FDM, FEM or FVM). The GRBFCM was proposed in 1990 by Edward Kansa [1].

In the GRBFCM method the approximate solution is assumed as a linear combination of radial basis functions (RBF) [2]:

$$u(x) = \sum_{j=1}^{M} c_j \, \varphi(r) \tag{1}$$

where c_j (j = 1,2,…,M) are unknown coefficients, M is the number of nodes and $\varphi(r)$ is the form of the RBF. The unknown coefficients are calculated by direct collocation of the governing equation and the boundary conditions.

Over the years different modifications of the method was proposed. One of the most import modification of the GRBFCM is based on the Hermite interpolation approach [3]. It is sometimes called symmetric Hermite RBF collocation because the matrix of linear equations is symmetrical in the method. That ensures in collocation method well-posedness and solvability of the problem.

The GRBFCM was successfully applied for solving many problems in applied mechanics, e.g. biphasic or triphasic mixture models in tissue engineering problems [4,5], nonlinear Burger's equation [6], heat transfer [7] and many others. Recent developments of the GRBFCM was summarized in [8].

In the present paper the GRBFCM is applied for analysis of fluid flow through the porous medium which is modelled as a regular bundle of cylindrical fibres (arranged in a triangular, square or hexagonal array). The microstructural flow between the fibres is considered using the GRBFCM and then the filtration velocity can be calculated. Using this in the Darcy equation the permeability is easily determined. The forms of the RBF used in the paper are presented in Tab. 1.

Table 1. Forms of the RBF.

Name of the RBF	**Abbreviation**	**Form of the RBF**
Gaussian Function	GF	$\exp\left(-\beta r^2\right)$
Inverse Quadric Function	IQ	$\dfrac{1}{r^2 + c^2}$
Multiquadric Function	MQ	$\sqrt{r^2 + c^2}$
Inverse Multiquadric Function	IMQ	$\dfrac{1}{\sqrt{r^2 + c^2}}$

References:

[1] Kansa E.J., *Multiquadrics–a scattered data approximation scheme with applications to computational fluid-dynamics–II. Solutions to parabolic, hyperbolic and elliptic partial differential equations*, Computers and Mathematics with Applications 19: 147-161, 1990
[2] Buhmann M.D., *Radial basis functions*, Acta Numerica 9: 1-38, 2000
[3] Franke C., Schaback R., *Solving partial differential equations by collocation using radial basis functions*, Applied Mathematics and Computation 93: 73-82, 1998
[4] Hon Y.C., Lu M.W., Xue W.M., Zhu Y.M., *Multiquadric method for the numerical solution of biphasic mixture model*, Applied Mathematics and Computation 88: 153-175, 1997
[5] Hon Y.C., Lu M.W., Xue W.M., Zhu X., *A new formulation and computation of the triphasic model for mechanoelectrochemical mixtures*, Computational Mechanics 24: 155-165, 1999
[6] Hon Y.C., Mao X.Z., *An efficient numerical scheme for Burgers' equation*, Applied Mathematics and Computation 95: 37-50, 1998
[7] Zerroukat M., Power H., Chen C.S., *A numerical method for heat transfer problems using collocation and radial basis functions*, International Journal for Numerical Methods in Engineering 42: 1263-1278, 1998
[8] Chen W., Fu Z.-J., Chen C.S., *Recent advances in radial basis function collocation methods*, Springer, 2014

Determination of force thrust on the head of impulse valve of water ram

Dariusz Grygo
Department of Mechanics and Machine Design, University of Warmia and Mazury in Olsztyn, ul. Oczapowskiego 11, 10-719 Olsztyn
dariusz.grygo@gmail.com

Keywords: ram water, force thrust, pressure, impulse valve

The water ram is a type of water pump that its operation is based on the use of the kinetic energy of water flowing through this device [1; 2; 3]. The water ram can have provided the water for various purposes, among others: the provision of drinking water for people and animals in difficult areas where is not a water supply system, irrigation of green areas, provided water for technological purposes, may serve as tourist/technical attraction, can fill a water tanks for example temporary lake.

The main aim of this presentation will be to determine the thrust of water flowing on the head of impulse valve using the fluent program (Fig. 1 and 2).

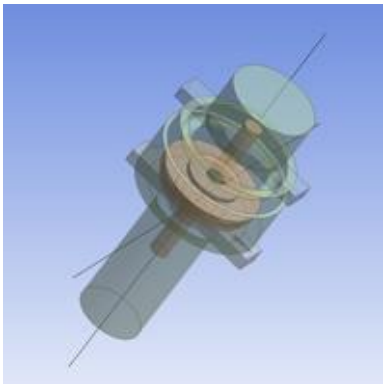

Fig. 1. Interior of impulse valve of water ram.

The first part of the presentation will concern general information about the water ram among others start-up and operation of water ram, description of the phenomena occurring at the work of water ram, place of its use and trivia. In second part of the presentation will be describe modeling process impulse valve and results. In conclusion will be interpreted the results.

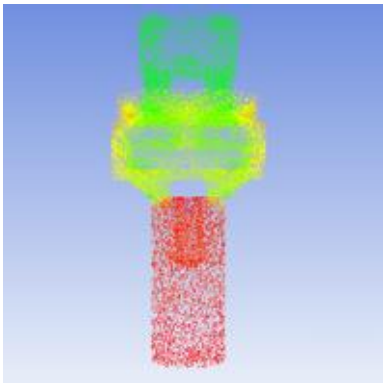

Fig. 2. Interior pressure in impulse valve of water ram.

The motivation to take the subject arose from the interest in machines and devices that work using renewable energy. Devices that can be used in households to improve their energy balance.

References:

[1] Furze, J.: *Compendium in hydraulic ram*, University of Aarhus. Faculty of Political Science. Retrieved from http://www.slideshare.net/Fatin62c/compendium-in-hydraulic-rampumps, 2012, August 2014.
[2] Lansford, W. L., Dugan, W. G.: *An analytical and experimental study of the hydraulic ram*., 1941, University of Illinois, Urbana.
[3] Watt, S. B. (1975). *A manual on the hydraulic ram for pumping water*, 1975, Retrieved from http://www.watersanitationhygiene.org/References/EH_KEY_REFERENCES/WATER/Water%20Pumping/Ram%20Pumps/Hydraulic%20Ram%20Pump%20Manual%20(ITDG).pdf, August 2014.

Performance characteristics of ram water

Dariusz Grygo
Department of Mechanics and Machine Design, University of Warmia and Mazury in Olsztyn, ul. Oczapowskiego 11, 10-719 Olsztyn
dariusz.grygo@gmail.com

Keywords: ram water, test stand, equations of performance

The water ram (Fig. 1) is a type of water ram that its operation is based on the use of the kinetic energy of water flowing through this device. The supply water sources can be any flow for example: river, stream, lake, etc., it is important only the flow must provide adequate water flow which will create an appropriate water hammer necessary to further correct its work [1; 2; 3].

The main aim of presentation was to determine the performance characteristics of water ram (q_c) taking into account the relationship between the volumes of air chamber (v), the level height of supply water source (h_s) and the level height of the delivery water (h_c) (Fig. 1).

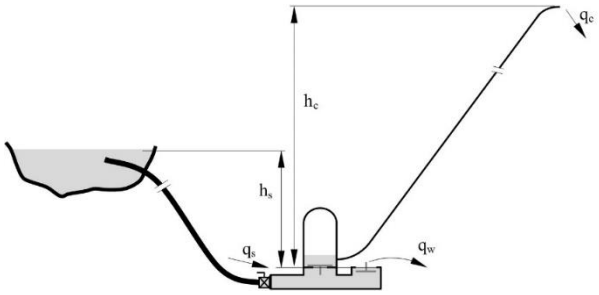

Fig. 1. Diagram of the water ram.

The first part of the presentation applies to a test stand especially built to the study physics phenomena in water ram and the mass measurement system of performance. The presentation presents also the measurements results and developed performance equations of water ram for two variants in which the first include the volume of air chamber (V) (equation 1) and other not (equation 2).

$$q_c=-0.8467+4.8672\cdot h_s-0.6626\cdot h_c-0.9106\cdot V-0.5098\cdot h_s^2+0.0171\cdot h_c^2-0.0158\cdot V^2-0.0881\cdot h_s\cdot h_c+0.2094\cdot h_s\cdot V+0.0346\cdot h_c\cdot V \quad (1)$$

$$q_c=5.4211+0.5363\cdot h_s-0.5240\cdot h_c \quad (2)$$

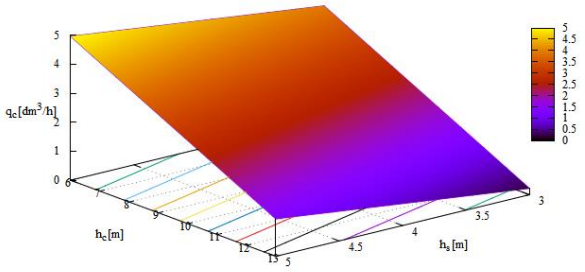

Fig. 2. The regression equation (2) graph.

In conclusion of the presentation made the interpretation of developed mathematical relations.

The motivation to deal these issues arose from the impact of setting appropriate parameters (v, h_c, h_s) on the performance of the water ram (q_c). Knowing the parameters settings (v, h_c, h_s) can obtain optimum its performance. The water ram can be used in many areas among others: supplying the water to the buildings, for the animals, for technological purposes, for fields irrigation.

References:

[1] Clarke, J. W.: *Hydraulic rams their principle and construction*, 1900, Retrieved from https://archive.org/details/hydraulicramsth03clargoog, August 2014.
[2] Furze, J.: *Compendium in hydraulic ram*, University of Aarhus. Faculty of Political Science. Retrieved from http://www.slideshare.net/Fatin62c/compendium-in-hydraulic-rampumps, 2012, August 2014.
[3] Watt, S. B. (1975). *A manual on the hydraulic ram for pumping water*, 1975, Retrieved from http://www.watersanitationhygiene.org/References/EH_KEY_REFERENCES/WATER/Water%20Pumping/Ram%20Pumps/Hydraulic%20Ram%20Pump%20Manual%20(ITDG).pdf, August 2014.

Characterization of porosity of oxide layers formed on steel used in the power industry

Monika Gwoździk
Czestochowa University of Technology, Faculty of Production Engineering
and Materials Technology, Institute of Materials Engineering,
19 Armii Krajowej Av., 42-200 Czestochowa, Poland
gwozdzik@wip.pcz.pl

Keywords: 13CrMo4-5 steel, oxide layer, porosity

Steels for use at elevated temperatures find wide application in conventional and nuclear energy generation. Oxide layers formed on long-term operated steels fulfil as important role as the creep limit or the creep strength [1], [2]. In most cases the growth of the oxides/deposits layer is accompanied by the formation of pores and fissures. These defects are the dominating factor causing spalling and scaling of the protective oxides layer. From this point of view it is important to reduce the quantity and the size of pores and fissures in oxides [3].

The paper contains results of studies on the formation of oxide layers on 13CrMo4-5 steel (Table 1) long-term operated at an elevated temperature. The material studied comprised specimens of 13CrMo4-5 steel operated at the temperature of 455°C during 130,000 hours (steel 1) and 540°C during 120,000 hours (steel 2). The oxide layer was studied on a surface and a cross-section at the outer surface of the tube wall (Fig. 1). The paper contains results of studies of quantitative analysis of porosity in the oxide layer. The oxide layer formed on the studied steel 1 is ~146 µm thick, while on the steel 2 ~248 µm (Fig. 2). It has been found that steel 2 has higher porosity.

Table 1 Chemical composition of examined steel, wt %

Acc.	Chemical composition, wt %						
	C	Si	Mn	P	S	Cr	Mo
Analysis (steel 1)	0.16	0.30	0.57	0.019	0.009	0.90	0.54
Analysis (steel 2)	0.09	0.31	0.47	0.014	0.007	0.91	0.52
PN-EN 10028-2 [4]	0.08-0.18	max. 0.35	0.40-1.00	max. 0.025	max. 0.010	0.70-1.15	0.40-0.60

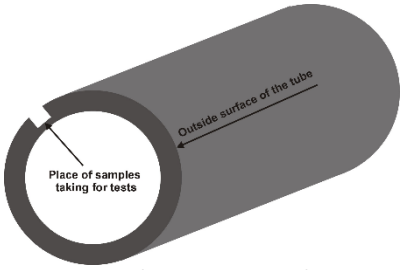

Fig. 1. Place of samples taking for tests.

a) b)

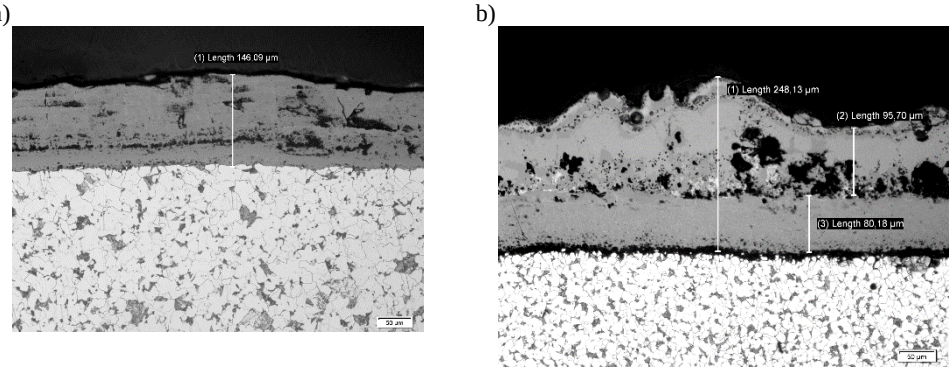

Fig. 2. The thickness of oxides layer formed on the steel examined: (a) steel 1 – LM, (b) steel 2 – LM.

References:

[1] Gwoździk M.: *Mechanizm degradacji warstw tlenkowych na stalach długotrwale eksploatowanych w energetyce,* Monografia nr 291, Wydawnictwo Politechniki Częstochowskiej, Częstochowa 2014, ISBN 978-83-7193-616-6, ISSN 0860-5017

[2] Gwoździk M., Nitkiewicz Z.: *Studies on the adhesion of oxide layer formed on X10CrMoVNb9-1 steel*, Archives of Civil and Mechanical Engineering, 3 (14): 335-341, 2014

[3] Gwoździk M.: *Characterization of oxide layers formed on 13CrMo4-5 steel operated for a long time at an elevated temperature*, Archives of Metallurgy and Materials, 3 (60): 1783-1788, 2015

[4] PN-EN 10028:2010, Wyroby płaskie ze stali na urządzenia ciśnieniowe. Część 2: Stale niestopowe i stopowe o określonych własnościach w podwyższonych temperaturach.

Modelling of the hydrodynamics of cocurrent gas and liquid flow through packed bed

Daniel Janecki[1], Grażyna Bartelmus[2], Andrzej Burghardt[2]
[1] Department of Process Engineering, University of Opole, ul. Dmowskiego 7-9, 45-365 Opole, Poland
[2] Institute of Chemical Engineering, Polish Academy of Sciences, ul Bałtycka 5, 44-100 Gliwice, Poland
zecjan@uni.opole.pl

Keywords: trickle-bed reactors; CFD; hydrodynamics

Three-phase reactors in which the gas and liquid phases flow down a fixed catalytic bed are termed "trickle bed reactor" (TBR). Depending on the flow rates of the two phases and their physicochemical properties various flow patterns can be observed of which two are of considerable industrial importance: the gas continuous flow regime (GCF) and the pulsing flow regime (PF).

The aim of the present study is to simulate cocurrent gas and liquid flow through packed bed in GCF regime using computational fluid dynamics (CFD). The mechanism of the cocurrent gas and liquid flow through fixed bed of small particles is more complex than in counter-current and is determined as the result of changes in flow velocity of both phases, their physicochemical properties, shape and dimension of packing etc.

The proper description of the bed structure in a column should contain the following elements: overall mean porosity, axially averaged radial porosity distribution, and variance of the porosity distribution in axial direction (Jiang et al., 2002). In the present work the overall mean porosity was determined experimentally ($\varepsilon = 0.38$). The most commonly used in literature correlation, suggested by Martin (1978), was applied to describe radial porosity distribution. Statistic properties of a packed bed was used to describe porosity changes in axial direction. The generating random numbers algorithm of normal distribution, a given mean value and standard deviation were used to determine this parameter.

The above dependences were introduced into the Fluent programme by means of user definition function (UDF). A structural grid was generated to reconstruct the area occupied by the bed and the fluids flowing through it. The grid was created by means of GAMBIT preprocessor. There are 6050 cells in the grid (22 elements in radial direction and 275 elements in axial direction) 4400 of which are 3 mm by 5 mm and 1650 elements forming the wall-layer are 1.5 mm by 5 mm. Fig.1 shows volume fraction distribution of a solid taking into account the porosity change along the radius and axis of the column.

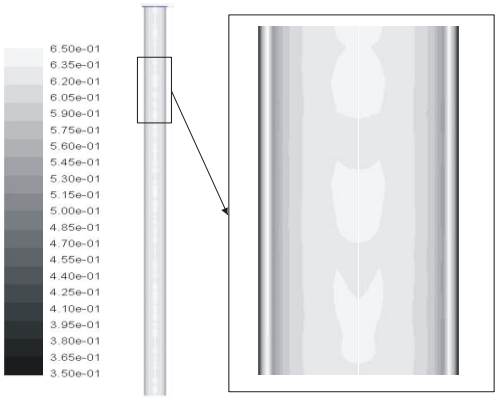

Fig.1. Volume fraction distribution of a solid taking into account the changes in porosity along the radius and axis of the column (particle diameter – 0.003m).

The following boundary conditions were used in the generated grid: symmetry in the axis, no slip of the fluid in the wall region, flat velocity profile at the inlet, zero velocity gradient at the outlet.

The Euler model (Euler-Euler) including mass and momentum balance for each phase was used to simulate fluids flow in a TBR. This model treats every phase as continuous fluids having various velocities, volume fractions and physicochemical properties. The application of multiple gas-liquid-solid model requires the knowledge of relationships determining interactions between phases. It is a very significant element of uncertainty in the modeling of the processes. These forces are considerable and dominate the momentum balance equations. The exchange coefficients of these forces were defined by means of equations suggested by Attou et.al (1999).

As a result of the computational simulation the following data were obtained: gas pressure drop in the bed, volume fraction distribution of a given phase (liquid and gas holdups) along the packing and its mean value in the reactor. The comparison of the values of liquid holdup and gas pressure drop in the bed, both calculated and experimentally obtained, indicates that the CFD model used in this work can be applied to model the hydrodynamics of cocurrent gas and liquid flows through a packed bed because a good compatibility of the compared hydrodynamic parameters was obtained.

References:

[1] Jiang Y., M.R. Khadilkar, M.H. Al-Dahhan, M.P. Dudukovic,: *CFD of multiphase flow in packed-bed reactors: I. K-fluid modelling issues*, AIChE J. 48: 701-715, 2002.
[2] Martin H.: *Low Peclet number particle to fluid heat and mass transfer in packed beds*, Chem. Eng. Sci. 33: 913-919, 1978
[3] Attou A., Boyer C., Ferschneider G.: *Modeling of the hydrodynamics of the cocurrent gas-liquid trickle flow through a trickle-bed reactor*, Chem. Eng. Sci. 54: 785-802, 1999

Chemo-mechanical and thermal behaviour of PVA hydrogels

Katarzyna Kazimierska-Drobny, Mariusz Kaczmarek, Joanna Nowak
Institute of Mechanics and Applied Computer Science, Bydgoszcz Kazimierz Wielki University, Kopernika 1 street, 85-074 Bydgoszcz, Poland e-mail: kkd@ukw.edu.pl
kkd@ukw.edu.pl

Keywords: chemo-deformation, thermo-consolidation, PVA hydrogels

The reactivity of hydrogels causes that the effective specification of structural and physical properties demand the incorporation of complex experimental studies and the application of an adequate mathematical model describing the realistic behaviour of the material. The available results of experimental studies regarding selected material parameters show considerable spread and in some cases discrepancy [1]. There is no standards for studies of hydrogels, including determination of deformation and the conditions which must be fulfilled (e.g. temperature) throughout the test. This paper presents the identification procedures of transport, mechanical, and coupled chemo-mechanical parameters of porous hydrogels based on poli(vinyl alcohol) PVA. Thermal behaviour of hydrogels is also recognized in experimental studies.

The macroscopis models of chemo-mechanical deformation and reactive transport corresponding to the proposed experimental test are considered. The system of equations useful for solving problems of identification for chemo-mechanical model is as follows:

$$\begin{aligned}&(1+a\alpha^2M)\frac{\partial p}{\partial t}-(\gamma+a\alpha dM)\frac{\partial c}{\partial t}-\frac{n_0^2M}{b}\frac{\partial^2 p}{\partial x^2}+\frac{n_0Mb_1}{b}\frac{\partial^2 c}{\partial x^2}=0\\&R\frac{\partial}{\partial t}c-K_2\frac{\partial}{\partial t}p+\upsilon_0^f\frac{\partial}{\partial x}c-D\frac{\partial^2}{\partial x^2}c+D_1\frac{\partial^2 p}{\partial x^2}=0\end{aligned}\qquad(1)$$

where c is concentration of solution and p is pore pressure. The description of the model, parameter and solution of 1-D initial – boundary value problems using Matlab and Comsol environments are given in [2].The theory used to identify mechanical properties from the creep test is based on Biot's poroelasticity.

The studies of mechanical, chemo-mechanical and transport processes were carried out with specially designed experimental set-up. The chemo-mechanical experiment (Fig.1) is based on modified classical reservoir test.

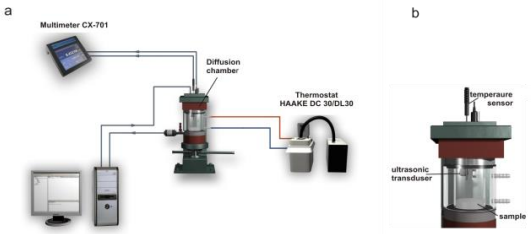

Fig.1: The experimental system for studies transport properties and chemical deformation (a) and diffusion chamber (b).

The method based on unconfined one dimensional compression shown in Fig. 2 is applied to determine mechanical and rheological and thermal parameters.

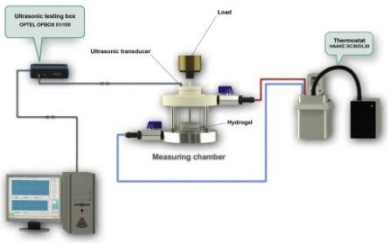

Fig. 2: The experimental system for studies of mechanical properties.

The chemical, mechanical and thermal deformation of sample were continuously recorded by time of flight method using Optel ultrasonic testing system and pulse signal. The tested material are poly (vinyl alcohol) (PVA) hydrogels.

The procedure of identification was carried out with help of the optimization methods, implemented in the Matlab environment. The identification of set of parameters is based on the previously developed solutions of inverse problem using the obtained experimental data and the solution of the macroscopic models. The results of identification (given in Table 1), where transport parameter are: diffusion coefficient (D) and retardation factor (R); mechanical parameters: drained Young modulus (Es) and Poisson's Ratio (vs); hydraulic permeability (K); chemo-mechanical couplings parameters (d, γ) and also chemo-osmotic parameters (kc) and (D1). The obtain results have a crucial role for the recognition of the associated phenomena: mechanical, chemo-mechanical, chemo-osmotic and transport behaviour of organic hydrogels and may form the basis for the broadening of the works towards other chemically sensitive materials like gels and soils.

References:

[1] Patachia, S. and Valente A.J.M., *Effect of non-associated electrolyte solutions on the bahaviour of poly(vinyl alcohol)-based hydrogels*, European Polymer Journal 43: 460–467, 2007

[3] Kazimierska-Drobny, K., Symalacja *procesów chemo-mechanicznych w porowatych żelach i identyfikacja parametrów modelu*. Praca doktorska, IPPT PAN, Warszawa 2012.

Determination of pore size distribution in sintered glass bead samples based on mercury porosimetry and microtomographic image analysis

Marcin Kempiński, Marcin Burzyński, Mieczysław Cieszko, Zbigniew Szczepański
Institute of Mechanics and Applied Computer Science, Kazimierz Wielki University
Kopernika 1, 85-074 Bydgoszcz, Poland
kempinski@ukw.edu.pl; *marcin.burzynski@post.pl*

Keywords: pore size distribution, sintered glass beads, MIP, μCT

In the paper the capillary and random chain models of pore architecture, [1], are applied for determining the limit pore size distributions in sintered glass bead samples based on mercury intrusion curves, [2]. They estimate the range of pore sizes in the investigated material. It is proved that capillary model, commonly used in mercury porosimetry, and the chain model are two limit cases of net models of pore architecture for a given pore size distribution. For both limit pore architectures in the layer of porous material subjected to two-side intrusion of mercury, the expressions describing capillary potential curves were derived. The capillary and chain model with constant length has been used as a basis for the procedure of determining the limit pore size distributions in sintered glass bead samples. The limit distributions are compared with distributions determined from microscopic image analysis of samples obtained by the micro computed tomography (μCT) method. These distributions are considered as actual distributions of the pore space and are determined by prescription to each point (voxel) of the pore space of porous material, the diameter of the maximal sphere that contains this point and is completely inside the pore space, [3]. They

We consider the models of the pore space of porous materials in which the individual pores are cylindrical links of random length and diameter distributions. Two independent factors determinate the pore space structure of such media: the link size distributions and the way of their connections. The second factor is called the pore space architecture. The pore architecture causes that even for the same pore diameter distribution in the model material its pore space structure can be different. Regarding the pore architecture, in the paper we will distinguish three hinds of models of the pore space structures: capillary, chain and network. In the capillary model the links of equal diameter are joined in series and form the long capillaries of constant diameters crossing the whole material. In the chain model the links are joined at random in series and form the capillaries of step-wise changing cross-section. In the network model a random connected links from the space network.

Three special cases of the capillary potential curves of porous layer are presented in Figure 1. They concern the chain pore architecture of the layer with the same link diameter distribution and different distributions of link length: capillary model (CM), chain model with constant (PCM) and random (SCM) link length.

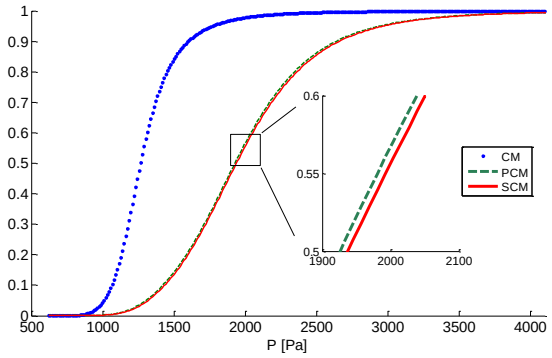

Figure 1: Capillary potential curves of porous layer for capillary model (CM), periodic (PCM) and stochastic (SCM) chain model of the pore space.

From Figure 1 results that link length distribution in the chain model does not influence significantly the capillary potential curves. Therefore description of the capillary potential curve for porous material of chain pore architecture can be effectively represented by model with constant link length.

It can be shown that capillary potential curves limit such curves determined for network models of the same pore size distribution. This means that both models can be used for estimation of the range of pore diameter distribution based on the mercury intrusion data.

The μCT is a very modern, non-destructive method used in the identification of the spatial structure of heterogeneous materials and small physical objects. In this method, as in the computed tomography applied in the medical diagnostics, X-rays are used reaching the image resolution of one micrometer. Microtomographic scans of samples of porous materials are the basis for spatial reconstruction of the microscopic pore space geometry or the skeleton architecture. The μCT method has been used to tests and verification of the proposed method of determining the limit pore size distributions of the mercury intrusion curve.

References:

[1] Cieszko M., Kempiński M., Determination of Limit Pore Size Distributions of Porous Materials from Mercury Intrusion Curves. Engng. Trans. 54, 2, pp. 143-158, 2006.
[2] Webb P.A., Orr C., Analitical Methods in Fine Particle Technology. Micrometitics Instrument Corporation. Norcross. GA USA, 1997.
[3] Hildebrand T., Ruegsegger P., A new Method for the Model-Independent Assessment of Thickness in Three-Dimensional Images, Journal of Microscopy, 185, 1, pp. 67-75, 1997.

Numerical simulation of the dynamic response due to discharge initiation of the grain silo

Rafał Kobyłka, Józef Horabik, Marek Molenda
Institute of Agrophysics of the Polish Academy of Sciences
Doświadczalna 4, 20-290 Lublin
rkobylka@ipan.lublin.pl

Keywords: numerical simulations, DEM, modelling, stress distribution, grain silo

Evolution of stress distribution inside the storage silo is an inherent effect in dynamic operations of handling of granular materials. Sudden increase in lateral pressure with ramp down of vertical pressure, which takes place at the opening of discharge gate, may create severe pulsations of bin structures and can lead to its damage. Due to discontinuity and heterogeneity of granular systems, mechanism of generation and propagation of stress waves is very complex and not completely understood, yet. With an increase in availability of affordable computing power, numerical methods became promising solution for examination of such and similar problems.

In the reported study, numerical simulations of the discharge initiation of the grain silo was performed. Discrete Element Method (DEM) modeling was carried on in a flat-bottomed cylindrical bin, having diameter of 0.12 m and height of 0.5 m. 118 000 spherical particles, with diameter of 3.79±0.05mm and material parameters of wheat, were used. Based on DEM modeling, the propagation of the stress wave and its influence on the loads on construction members of the silo were evaluated. DEM was proven to be promising tool allowing insight into mechanisms of stress transmission inside the granular solids and on the silo wall.

Modelling and Simulation of the Porous Media Flow in COMSOL Multiphysics®

Tomasz Krupicz
Comsol Multiphysics GmbH
tomasz.krupicz@comsol.de

Keywords: simulation software, multiphysic, porous media flow

Introduction

The COMSOL Multiphysics® simulation software is a numerical tool based on the finite element method where all underlying equations can be coupled with each other and solved simultaneously in mutual dependence on each other within one model.. With COMSOL the realistic interaction between electromagnetic, mechanical, thermal, chemical and fluid flow aspects can be combined in a user-friendly and intuitive software environment without the need for in-depth programming.

COMSOL's core package includes all finite element functionality for creating geometries, defining materials and basic physical properties, meshing, setting up studies and optimizing solver settings, solving the models and post-processing. Add-on modules allow using predefined physics definitions and multiphysics couplings.

Recently introduced the new Application Builder, which is available in the COMSOL Multiphysics® software, allows creating specialized applications from COMSOL models for use by others, from colleagues to customers, using the new COMSOL Server™ as platform for sharing apps. [1]

Simulation of the porous media flow

Knowledge of the physical properties of a media flowing through a porous material is necessary as they can be used to evaluate the behaviour, usefulness or application of a subsurface formation. Our world is a multiphysical world in which different physical and chemical aspects have an impact on each other and have to be considered simultaneously to describe particular phenomena accurately. COMSOL Multiphysics® offers a possibility to model additional important phenomena connected with porous media flow, like: thermal expansion or chemical reactions.

Determining material properties at the pore-level can significantly improve the predictions of the flow behaviour at the macroscopic level. In the pictures below (Fig.1.) the physical properties (porosity and permeability) of a the natural porous media are analysed for determining the pore size distribution [2]. The important features here are that in a short period of time any porous media pattern can be modelled obtaining an accurate numerical simulation of the properties like velocity or pressure distribution. In the same way the heat transfer phenomenon can be modelled obtaining a temperature distribution or heat losses in a different kinds of porous structures.

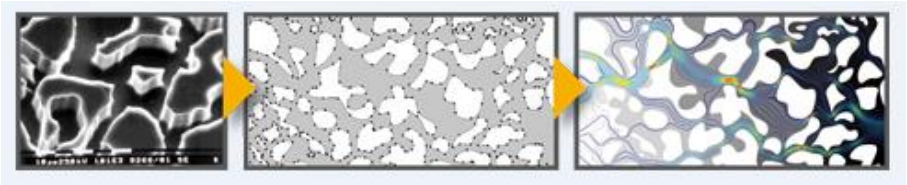

Fig.1. Produced by scanning electron microscope images, the geometry of microscopic pores can be imported to COMSOL where the velocity and pressure distributions are calculated.

Subsurface Flow Module

Being the most special for porous media flow simulations the Subsurface Flow Module can model subsurface flow in channels, saturated and variably saturated porous media, or fractures, and couple these to simulations of solute and heat transport, geochemical reactions, electromagnetic fields and poroelasticity. It can be used for modeling groundwater flow, the spread of waste and pollution through soil, the flow of oil and gas to wells, and land subsidence due to groundwater extraction.

When heat transfer occurs, it may be modelled through conduction, convection, and dispersion, and different conductivities that occur between the solid and fluid phases are also taken into account. In many cases, the solid phase can be made up of differing materials with different conductivities, and there can also be a number of differing fluids.[1]

Material transport can be coupled to subsurface flow and can occur through convection and diffusion. Properties, like diffusion, can be described by equations dependent on the variables, such as concentration, or be made anisotropic.[1]

The Fracture Flow interface also solves for pressure on internal (2D) boundaries within a 3D matrix, and is automatically coupled to the physics describing the porous media flow in the surrounding matrix. [1]

Moreover the functionality of COMSOL Multiphysics®, together with the Subsurface Flow Module allows building applications on the basis of the previously created model, which then can be opened via COMSOL Server™.[1]

References:

[1] https://www.comsol.com/products
[2] http://www.comsol.com/models

Model research of a two-bed single-stage silica gel-water adsorption chiller for low grade thermal energy

Jaroslaw Krzywanski[1], Malgorzata Szyc[2], Wojciech Nowak[3], Zygmunt Kolenda[3]
[1]Jan Dlugosz University in Czestochowa, 13/15 Armii Krajowej Av., Czestochowa, Poland
[2]Czestochowa University of Technology, 73 Dabrowskiego, Czestochowa, Poland
[3]AGH University of Science and Technology, 30 Mickiewicza Av., Krakow, Poland
jkrzywanski@tlen.pl

Keywords: low grade heat, adsorption chiller, silica gel, cooling capacity

In their vast majority, high valued energy sources, e.g. electricity and fossil fuel driven appliances are used for the heating and cooling purposes. However, there are a wide range of low grade sources of thermal energy, e.g. sewage water, underground resources, solar heat, low grade waste heat which also can be used to deliver useful heating or cooling [1]. Adsorption cycles have a distinct advantage over other systems in the ability to use low grade heat, especially heat of low near ambient temperature. Besides zeolite/water the porous solid silica gel-water is also considered as one of the most promising pairs of adsorbent-adsorbate, best suited for the solutions using low grade sources of thermal energy [2-5]. It is due to relatively easy regeneration process of the adsorbent. These two pairs adsorbent-adsorbate mostly have found their implementation in commercialised chillers offered by suppliers on market. There are a few applications with adsorption chillers in industrial scale in Europe. Adsorption chillers can use solar energy, district heating system and other waste heat sources. Complex review of existing installation can be found inter alia in [6].

The main feature of adsorption chillers is its lower sensitivity to hot water inlet temperature fluctuations. It makes that adsorption chillers are more suitable for low grade sources of thermal energy exploitation in comparison to their main competitors, i.e. absorption chillers. The improvement of total efficiency of adsorption process is however still challenging task.

The work presents a model of a single-stage adsorption chiller with silica gel acting as a solid porous sorbent and water working as refrigerant. The validation of the model was successfully performed against the experimental results from the existing adsorption chiller installed at National University of Singapore. Such approach was undertaken since the comparison between desired and calculated data is regarded as the most difficult type of model's validation procedure [7].

The performed model allows to predict the behaviour of the adsorption chiller.

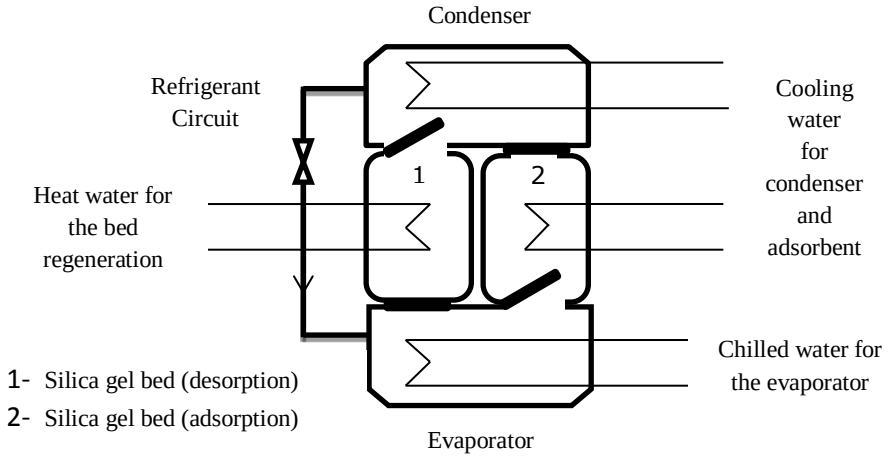

Fig.1. Schematic diagram of an adsorption chiller.

References:

[1] Ammar Y., Joyce S., Norman R., Wang Y., Roskilly AP.: *Low grade thermal energy sources and uses from the process industry in the UK*. Applied Energy, 2012;89:3–20.
[2] Demir H., Mobedi M., Ülkü S.: *A review on adsorption heat pump: problems and solutions.* Renew Sustain Energy Rev, 2008;12:2381–403.
[3] Szyc M., Nowak W.: *Operation of an adsorption chiller in different cycle time conditions.* Chemical and Process Engineering 201; 4;35:109–19.
[4] Szyc M., Nowak W.: *Analysis of cooling cycle in single-stage adsorption chiller*, Polish Journal of Environmental Studies 2014;23:1423–26.
[5] Chorowski M., Pyrka P.: *Modelling and experimental investigation of an adsorption chiller using low-temperature heat from cogeneration*. Energy 2015;92:221–29.
[6] Wu D.W., Wang R.Z.: *Combined cooling, heating and power: A review.* Prog. Energy Combust. Sci 2006;32:459–95.
[7] Krzywanski J., Nowak W., *Modeling of bed-to-wall heat transfer coefficient in a large-scale CFBC by fuzzy logic approach*, International Journal of Heat and Mass Transfer 2016;94:327–34.

Particle diameter distributions in granular beds - analysis and generation

Seweryn Lipiński
Department of Electric and Power Engineering, Electronics and Automation, Faculty of Technical Sciences,
University of Warmia and Mazury in Olsztyn
seweryn.lipinski@uwm.edu.pl

Keywords: granular bed, particle diameter distribution, virtual diameter distributions, tomographic imaging

One of the most important issues of research on granular beds is the problem of analysing the distribution of size of particles forming a granular bed – regardless of whether it is a bed of a natural origin or an artificially created one. This issue is very complex and highly dependent on the purpose of research, as well as on the bed type - its complexity in particular. Another important aspect is how to generate a virtual diameter distribution with specified parameters.

Both of these issues are to be described in the first part of the lecture.

In the context of the first topic, presentation describes the process of recognizing the type of distribution of the particle diameters. Distributions most commonly used in practice (i.e. normal, log-normal, Weibull, log-hyperbolic and skew log-Laplace), including indication of their specific applications, are also to be presented.

In the context of the second topic, presentation describes the method of generation of a virtual diameter distribution of a given type and with given statistics, divided into a certain number of fractions. Two exemplary distributions of a normal character, with the same statistics, but different number of fractions, are shown in in Fig. 1.

Both of the above-described aspects are complementary to each other, what allows realizing, for example, studies on the influence of the particle diameter distribution of the bed on its parameters such as permeability, porosity, tortuosity and others.

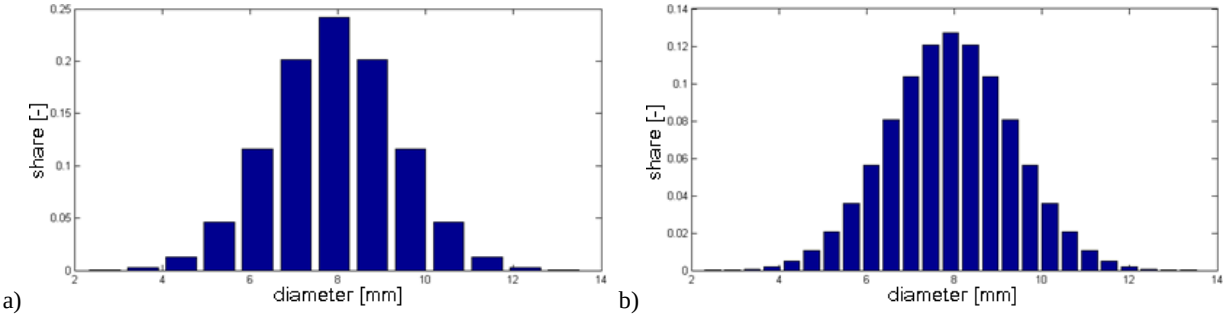

a) b)

Fig.1. Virtual diameter distributions of normal character: the distribution of average 8 [mm] diameter and 2 [mm] variance divided into 13 (a) and 25 (b) fractions.

The second part of the lecture focuses on the method of obtaining information on the internal structure of granular beds based on multislice computed tomography (CT) research. The subject of analysis are tomograms of a Plexiglas cylinder filled with glass marbles – shown in Fig 2a).

In order to obtain numerical information on the spatial location of the centre of each of the marbles forming the granular bed, methods of morphological image processing are applied. This approach was chosen because of ease of implementation and computational efficiency.

The output information is numeric data on the spatial location (x, y and z coordinates) of marbles forming the granular bed. This data can be used to create a virtual bed having exact equivalent in reality, like the one shown in Fig. 2b) – it is based on the data obtained from tomograms of cylinder shown in Fig. 2a).

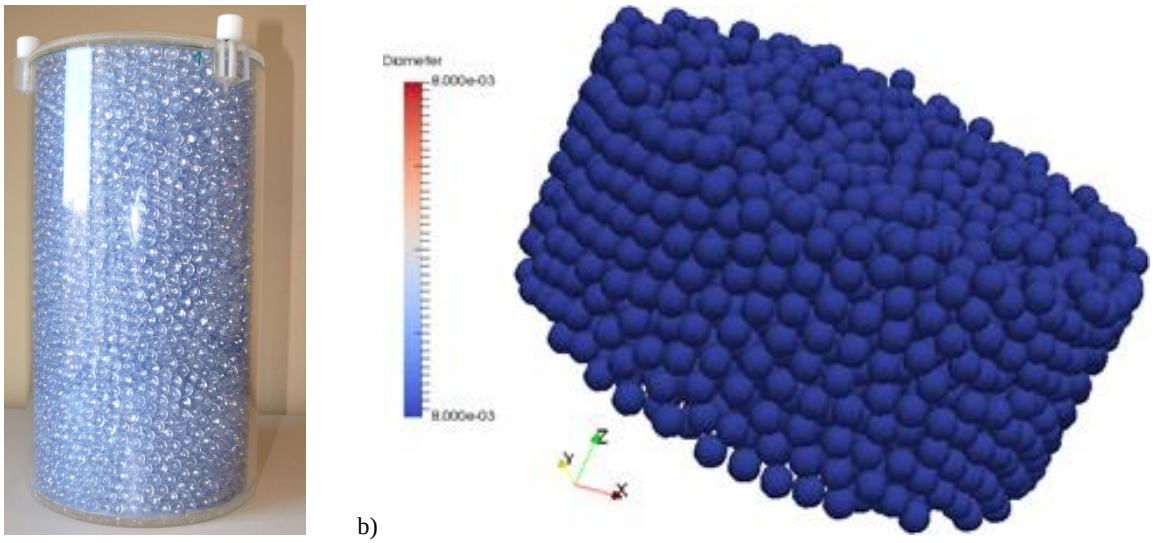

a) b)

Fig.2. Research material - glass marbles with 8 [mm] diameter placed in Plexiglas cylinders having a diameter of 150 [mm] (a) and virtual bed consisting of spheres having a diameter of 8 mm (b), created based on information obtained from the analysis of multislice CT research of granular bed shown in Fig 2a).

Determination of cores electrisation during the flow in the modified Wurster apparatus

Wojciech Ludwig[1], Tadeusz Mączka[2]
[1]Wroclaw University of Technology, Faculty of Chemistry, Department of Chemical Engineering
[2]Wroclaw Electrotechnical Institute, Short-run and Experimental Production Workshop
wojciech.ludwig@pwr.edu.pl

Keywords: electrisation, cores, Wurster, spout-fluid bed

Among many known equipment applied to coating particles and tablets spouted bed apparatus seems to be the optimal construction [1]. In the fifties of the XX century coating was realized in spouted bed apparatuses, in which spraying nozzle was placed in the upper part of the chamber with the bed. Although both the yield of such a process as the quality of produced coat were low. Since that apparatuses with a spraying device placed in the bottom part of the bed were introduced. In this system probability of collisions of particles with drops of coating solution and the yield of the process are higher, drying time is shorter, although high risk of agglomeration takes place, because of high concentration of wetted particles close the nozzle [2].

Some type of modification of the design described above is the Wurster apparatus [2], [3]. Wurster apparatus is a spouting device with a draft tube and an additional fluidizing air stream (spout-fluid bed). At the bottom of the chamber there is a mesh used to distribute hot air stream. A spraying nozzle is positioned in the center of the distributor, placed at the bottom of the bed. Coating solution is sprayed through the nozzle or several nozzles and deposited upon particles at the time, when they flow through the entrainment zone. Every particle obtains a small part of the coat during its flow through the spraying zone. Particles are dried inside draft tube, flow into fountain zone, and next in the annulus they settle down again to the entrainment zone. Repeated movement (regular circulation) of particles leads to creation of solid layer on their surface. Wurster apparatus is considered as the best device for periodical coating of grain materials [1], [4].

Wurster apparatus of unique construction was designed and built during former research. This apparatus is characterized by very long draft tube, equipped with nozzles in the central part of the device and deflector placed in the fountain zone [5]. It enables obtaining very high particles velocity and because of that high coating yield. Unfortunately, proposed design solution causes several negative phenomena connected with cores electrification. It occurs during particles friction with the walls of draft tube and apparatus as well as during rapid impact on deflector. It leads to agglomeration of the particles and accumulation of the bed on the wall surface of the equipment, which interfere with circulation and reduce effectiveness of coating process. The authors have carried out investigations on counteracting those negative phenomena. One of the preparatory stages is the work presented here.

The purpose of this paper was determination of the value of cores electrification during their flow in the modified Wurster apparatus, applied for dry encapsulation of pharmaceutical materials. Previous works of the authors dealt with vulnerability of the particles of different diameter, produced by Syntapharm (Cellets 1000, 700 and 100) on electrification in laboratory conditions. The values of resistivity, times of charge relaxation and electrification degrees, determined in line with polish standards PN-92/E-05201, PN-92/E-05203 confirmed supposition, that examined materials could cause fire or explosion, but they are suitable for dry electrostatic coating [6]. The presented work gives the results of examination on particles electrification in real conditions of their stable circulation in a column. The measurement system, that was applied allowed determination of electrification potential and discharge current. Those quantities, which are the measures of charge accumulation on cores were determined for several particles (Cellets 1000, 700 and 500) with the different humidity, for different mass of the bed and spouting gas velocities.

During experimental work it was stated, that electrical potential stabilizes very quickly in the apparatus (a few minutes) achieving high values in the range of 14-33 kV, which could lead to electric discharge between the walls of the equipment and the supporting structure, which imposes application of grounding of the metal parts of the column. Electrification potential grows with augmentation of the bed mass and its humidity, and it decreases with the drop of circulating particles diameter. Minor influence of the fountain gas on examined quantity was observed.

Discharge current changes with time, oscillates about the average value and it achieves the values in the range of 0.1-3.7 μA. Its average value grows with the growth of humidity, bed mass and fountain gas velocity. Quantity, that was examined achieved the bigger values for the case of particles with lower diameter.

Final conclusions on electrification of cores, that have been examined could be drawn only on the base of the value of electric charge collected on the bed. The authors predict modification of the lower part of the apparatus, to enable the measurement of electric charge with the use of Faraday cage method.

Acknowledgments
The studies were funded by the Polish National Science Centre within the framework of the research grant UMO-2013/09/B/ST8/00157.

References:

[1] Teunou E., Poncelet D.: *Batch and continuous bed coating- review and state of the art*, Journal of Food Engineering 53: 325-340, 2002
[2] Wurster D. E.: *Means of applying coatings to tablets or like*, Journal of the American Pharmaceutical Association 48(8): 451, 1950
[3] Wurster D. E., Lindlof J. A.: *Particle coating apparatus*, US patent 3241529, 1966
[4] Karlsson S., Bjoern I. N., Folestad S., Rasmuson A.: *Measurements of the particle movement in the fountain region of a Wurster type bed*, Powder Technology 165: 22-29, 2006
[5] Szafran R.G., Ludwig W., Kmieć A.: *New spout-fluid bed apparatus for electrostatic coating of fine particles and encapsulation*, Powder Technology 225: 52-57, 2012
[6] Mączka T.: *Study on the electrostatic properties of cores*, Report no. 504-002104-026-ZT/TM-25/2015, Wroclaw Electrotechnical Institute, 2015 (in Polish)

Macroscopic description and numerical analysis of concrete imbibition

Janusz Łukowski, Mieczysław Cieszko
Institute of Mechanics and Applied Computer Science
Kazimierz Wielki University, Bydgoszcz
januszl@ukw.edu.p1, cieszko@ukw.edu.pl

Keywords: concrete imbibition, macroscopic description, capillary transport, numerical analysis

A new macroscopic description is proposed for the imbibition process of fluid occurring in concrete considered as a porous material of homogeneous and isotropic pore space structure. Theoretical considerations are based on the continuum model of the capillary transport of liquid and gas in unsaturated porous materials, proposed by one of authors of the present paper [1]. The key assumptions of this model are: division of liquid in the pore space into two macroscopic constituents called mobile liquid and capillary liquid; description of menisci motion by an additional macroscopic velocity field; parametrization of saturation changes by a macroscopic pressure-like quantity that for quasi static and stationary processes is equal to the capillary pressure. The capillary liquid forms a film on its contact surface with the skeleton. This liquid is immobile and contains the whole interfacial (capillary) energy of liquid in the pore space. The remaining part of the liquid surrounded by the layer of capillary liquid and menisci forms the mobile liquid. Both liquids exchange mass, linear momentum and energy in the vicinity of menisci surfaces and this occurs only during menisci motion in the pore space. The additional velocity field describing menisci motion reflects the complexity of kinematics in unsaturated porous materials and enables the modeling of mechanisms of menisci motion in the pore space. For all constituents of the porous medium, balance equations of mass, linear momentum and energy are formulated and constitutive relations for mechanical processes are derived. Based on equations of this theory, evolution equations for the imbibition processes in porous materials were derived.

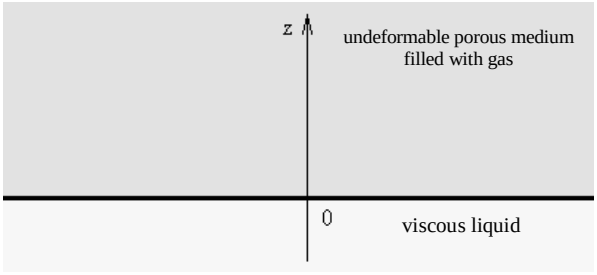

Fig.1. Scheme of the analyzed system.

A one dimensional system is considered, composed of two half spaces (Fig.1). The half space $z > 0$ is occupied by undeformable porous material filled with gas (air), whereas the half space $z < 0$ is occupied by incompressible wetting fluid. We analyze a nonstationary process of liquid imbibition by the porous material caused by the capillary forces and impeded by the gravity and viscous interaction of liquid with the skeleton. It is assumed that: gas is inert and its pressure is constant; the inertial forces in the mobile liquid are omitted and at the beginning of the process liquid is present at the contact surface $z > 0$.

The system of equations describing nonstationary imbibition process is composed of: balance equations for mass and forces in the mobile liquid, evolution equation for saturation, and constitutive equations for the stress tensor and viscous interaction force in the mobile liquid, for velocity of diffusive transport of menisci, and for relation of saturations with the mobile and capillary liquids. For the limit case of static distribution of mobile liquid attained at the end of the imbibition process this system of equations reduces to the form

$$\frac{\partial s_m}{\partial p}\left(1+\frac{ds_c}{ds_m}\right)-C_m(s_m,p)\left(\frac{\partial s_m}{dz}-\rho_m g\frac{\partial s_m}{\partial p}\right)^2=C_s(s_m,p)\,, \tag{1}$$

$$\frac{dp}{dz}=-\rho_m g \tag{2}$$

where by s_m, s_c, ρ_m, g, p saturation with the mobile and capillary liquid, mass density, gravity acceleration and pressure are denoted, respectively. Quantities $C_m(s_m,p)$, $C_s(s_m,p)$ are coefficients characterizing the internal pore space structure of the porous material. Equation (1) is strongly nonlinear and is solved using numerical methods.

References:

[1] Cieszko M.: *Macroscopic Description of Capillary Transport of Liquid and Gas in Unsaturated Porous Materials*, Meccanica 22: 1-22, 2016.

Immersed boundary method

Maciej Marek
Institute of Thermal Machinery, Faculty of Mechanical Engineering and Computer Science, Częstochowa University of Technology, al. Armii Krajowej 21, 42-200 Częstochowa
marekm@imc.pcz.czest.pl

Keywords: immersed boundary method, direct forcing, finite volume method, projection method, random packed bed

The objective of the lecture is to provide a short introduction to main ideas of the immersed boundary method (IBM) [1] and its application to direct numerical modelling of flows through random packed beds.

First, finite volume methods on structured computational grids (and simple domain geometries) will be shortly discussed together with basics of the projection method employed for the solution of Navier-Stokes equations for incompressible flow. Then, the immersed boundary method will be presented as a way of studying flow around complex solids on structured grids [2]. Different variants of IBM will be reviewed but the lecture will focus on direct forcing method in which only a simple modification of projection scheme is required to impose the correct flow velocity on solid boundaries. Advantages and disadvantages of various approaches will be discussed.

IBM is a very convenient method for flow analysis at the micro-scale of random packed beds as it is not required to generate complex body-fitted computational grids. Construction of such a body-fitted grid is a highly non-trivial task even for simple packings, like spheres, as the porous channels between contacting particles can become extremely narrow at some points. Many authors, in order to obtain a grid of sufficient quality, modify the structure of a bed by increasing the distance between the particles or introduce artificial bridges at the contact points (see [3] for a review of such techniques).

Application of IBM to simulation of flow in packed beds will be shown for two kinds of packing: Raschig rings (hollow cylinders) and spheres. This type of micro-scale simulation gives an opportunity to study the details of the flow: velocity distribution in the pore space (Fig.1a), pressure drop and the dependence of flow characteristics on the microscopic structure of the bed (ordering of particles, their shape, dimensions etc.). Of course, such detailed analysis is limited to only a small fragment of the packed bed. Additionally, full information about flow velocity allow for examining of the geometrical structure of the bed itself (e.g. tortuosity [4]).

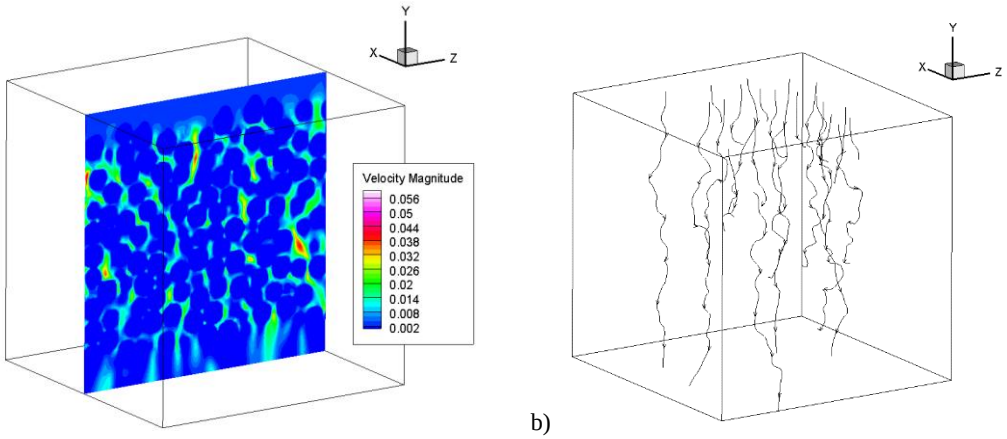

a) b)

Fig.1. Simulation of flow through a random packed bed of spheres: velocity magnitude in the mid-plane (a) and sample trajectories of massless particles advected passively with the flow.

Using the results of flow simulation tortuosity T of a bed can be calculated in two ways: either by explicit calculation of length of paths travelled by particles passively advected in the flow velocity field (Fig. 1b), or with the help of formula proposed by Duda et al. [4]:

$$T = \frac{\int_V u(\mathbf{r})dV}{\int_V u_y(\mathbf{r})dV} \tag{1}$$

where numerator corresponds to the mean value of velocity magnitude in the pore space and the denominator to the mean value of the streamwise component. The advantage of the second approach is that the tortuosity can be estimated directly from the velocity field. The results obtained with theses two methods will be compared.

References:

[1] Mittal R., Iaccarino G.*: Immersed Boundary Methods*, Annu. Rev. Fluid Mech. 37: 239-261, 2005
[2] Marek M.: *CFD modelling of a gas flow through a fixed bed of Raschig rings*, Journal of Physics: Conference Series 530: 012016, 2014
[3] Finn J., Apte S. V.*: Relative performance of body fitted and fictitious domain simulations of flow through fixed packed beds of spheres*, International Journal of Multiphase Flow 56: 54-71, 2013
[4] Duda A., Koza Z., Matyka M.: *Hydraulic tortuosity in arbitrary porous media flow*, Physical Review E 84: 036319, 2011

The Lattice Boltzmann Method

Maciej Matyka, Jarosław Gołembiewski
Faculty of Physics and Astronomy, University of Wrocław, 50-204 Wrocław, Poland
maciej.matyka@uwr.edu.pl

Keywords: computational fluid dynamics, kinetic theory, porous media, simulation

Simulation of the fluid flow in complex geometries is tedious task that consume relatively large computational resources, i.e. for grid generation. Possible solution to grid generation problem is to use mesoscopic methods, e.g. the Lattice Boltzmann Model based on kinetic theory of gases. It proved its capabilities to perform fast and reliable simulation in porous media. In the talk I will introduce the Lattice Boltzmann method (LBM). I will describe how does it differ from standard computational fluid dynamics tools. A review on its recent development will be given. I will present computational code of basic LBM solver implemented in C/C++ with remarks on its further development for more complex flows. Some results of the basic version of the code will be presented (see e.g. Fig. 1). We will discuss projects in which it was used in our group in the context of porous media and computer graphics & animation. Its excellent properties to run on Graphics Processing Units (GPU) will be addressed.

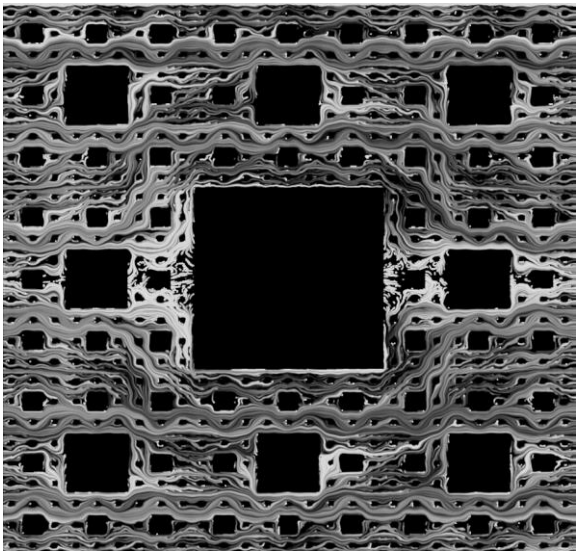

Fig.1. Fluid flow through 4-generation Sierpiński fractal. Simulation done with the Lattice Boltzmann Method. Visualization done by smearing path lines of massless particles advected in the flow.

Application of the Trefftz method for determination of the permeability of the porous medium

Magdalena Mierzwiczak[1], Jakub Krzysztof Grabski[1], Jan Adam Kołodziej[1]
[1]Institute of Applied Mechanics, Poznan University of Technology, ul. Jana Pawła II 24, 60-965 Poznań
magdalena.mierzwiczak@put.poznan.pl

Keywords: Trefftz method, special purpose Trefftz functions, method of fundamental solutions, permeability

Permeability is one of basic parameters of the porous medium which characterizes ability of fluid to penetrate the porous region. Thus determination of the permeability is very important issue which allows analyse flow through the porous media. The Darcy equation is commonly used for description of flow through porous medium. It has the following form

$$\mathbf{q} = \frac{\mathbf{K}}{\mu}\nabla p, \tag{1}$$

where $\mathbf{q}$ is the filtration velocity, $\mathbf{K}$ is the permeability tensor of the porous medium, μ is the dynamic viscosity of the fluid and p is the pressure.

In 1926 Erich Trefftz proposed the new method for solving problems described by partial differential equations [1]. The approximate solution in the method is a linear combination of trial functions which fulfil exactly the governing equation of the considered problem. However real development of this method came only with development of computer techniques. One of the version of the Trefftz method is boundary collocation technique. In the method the governing equation is fulfilled exactly by the trial functions (which are often called Trefftz functions) while the boundary conditions are satisfied in an approximate way. Different applications of the method can be found in [2].

Sometimes it is also possible to fulfil some of the boundary conditions by the Trefftz functions. Such version of the Trefftz method is called the Trefftz method with special purpose Trefftz functions in the literature [3]. The method was successfully applied in many problems in applied mechanics, e.g. conductive heat flow [4], fluid flow in conduits with polygonal cross-section [5] or elastic torsion of bars [6].

Another version of the Trefftz method is the method of fundamental solutions (MFS). The MFS was proposed in 1964 by Kupradze and Aleksidze [7]. The numerical implementation of the MFS was given by Mathon and Johnston [8].In the MFS the approximate solution is a linear combination of fundamental solutions which are functions of distance between the points and the source point. The fundamental solutions fulfil exactly the governing equation and the unknown coefficients of the approximate solution are calculated using the boundary collocation technique [2]. The source points are located outside the considered region which has similar shape to the boundary of the considered region. Some interesting review of applications of the MFS can be found in [9-11].

In order to determine the permeability of flow in the present paper firstly a microstructural flow in a regular array of cylindrical fibres is considered. Based on the velocity field the filtration velocity is calculated and then using the Darcy equation the permeability of porous medium can be determined. The obtained results are compared for different versions of the Trefftz method.

References:

[1] Trefftz E.:*Ein Gegenstück zum Ritzschen Verfahren*, Proceedings of the 2nd International Congress of Applied Mechanics (Zurich), Orell Fussli Verlag:131-137, 1926
[2] Kołodziej J.A., Zieliński A.P.: *Boundary collocation techniques and their application in engineering*, WIT Press, 2009
[3] Kołodziej J.A., Uściłowska A.:*Trefftz-type procedure for Laplace equation on domain with circular holes, circular inclusions, corners, slits and symmetry*, CAMES: Computer Assisted Methods in Engineering and Science 4: 507-519, 1997
[4] Kołodziej J.A., Stręk T.:*Analytical approximations of the shape factors for conductive heat flow in circular and regular polygonal cross-sections*, International Journal of Heat and Mass Transfer 44: 999-1012, 2001
[5] Kołodziej J.A., Uściłowska, A., Ciałkowski, M.: *Semi-analytical approximations of the laminar friction coefficients for flow in conduits with polygonal cross-section*, Acta Mech. 158: 127-144, 2002
[6] Kołodziej J.A., Fraska A.: *Elastic torsion of bars possessing regular polygon in cross-section using BCM*, Computers and Structures 84: 78-91, 2005
[7] Kupradze V.D., Aleksidze M.Q.: *The method of functional equations for the approximate solution for certain boundary value problems*, USRR Computational Mathematics and Mathematical Physics 4: 82-126, 1964
[8] Mathon R., Johnston R.L.: *The approximate solution of elliptic boundary value problems by fundamental solutions*, SIAM Journal of Numerical Analysis 14: 638-650, 1977
[9] Fairweather G., Karageorghis A.: The method of fundamental solutions for elliptic boundary value problems, Advances in Computational Mathematics 9: 69-95, 1998
[10] Fairweather G., Karageorghis A., Martin, P.A.: The method of fundamental solutions for scattering and radiation problems, Enginering Analysis with Boundary Elements 27: 759-769, 2003
[11] Karageorghis A., Lesnic D., Marin L.: A survey of applications of the MFS to inverse problems, Inverse Problems in Science and Engineering 19: 309-336, 2011

Preparation of three-dimensionally ordered macroporous Y-doped strontium titanate

Adrian Mizera, Łukasz Łańcucki, Ewa Drożdż
AGH University of Science and Technology
amizera@student.agh.edu.pl

Keywords: polystyrene, strontium titanate, 3DOM

The perovskite (ABO_3) stable structure enables substitution of aliovalent cations in A as well as in B position. Due to its potential mixed ionic-electronic conductivity (MIEC) these materials can be applied in solid-state ionic devices as solid oxide fuel cells (SOFC), chemical sensors or batteries. One of the most interesting potential application of such materials is using them as an anode backbone (as an alternative to nickel-cermet material) in SOFC fuel cells. The basic requirements for anode materials are high porosity (above 40vol.%) and high conductivity.

Strontium titanate (STO) is one of the perovskite type structure ceramic material. Pure $SrTiO_3$ is a dielectric material but its conductivity can be easily modified by incorporation of donor and acceptor type dopants into perovskite structure. Doping $SrTiO_3$ with donors results in converting the original material into n-type semiconductor and significant increase of electron conductivity of materials. Presented results concern the STO materials doping with yttrium in strontium position. Dopant cation have a higher charge than the host -strontium. Therefore, structure needs to release free electron in conductive band to maintain the electroneutrality.

A required porosity level can be obtained by proper synthesis method. As 3DOM (three-dimensionally ordered mesoporous) surface precursors may be used e.g. monodispersed polystyrene granules, silica, poly(methyl acrylate). In the presented research, the microstructure of regular pores and high specific surface area were achieved with using of polystyrene template. The synthesis was performed using citrate wet method. Solution containing titanium, strontium and yttrium ions was applied onto polystyrene monodispersed granules, dried and calcined in air atmosphere. The samples of $Sr_{1-x}Y_xTiO_3$ where x is in the range 0.0 - 8.0 mol.% were prepared.

As a result of applied synthesis method the homogenous three-dimensionally ordered macroporous Y-doped strontium titanate materials was obtained (Fig. 1).

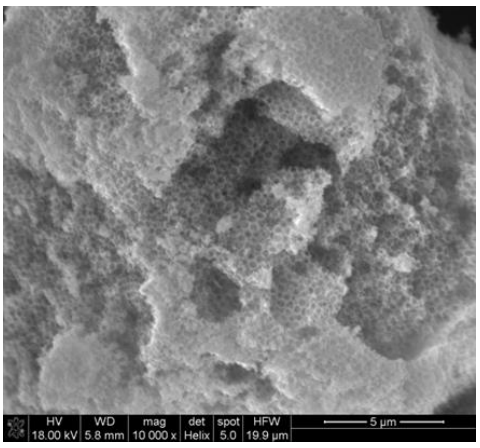

Fig.1. SEM picture of obtained Y-doped $SrTiO_3$ material.

The microstructure properties were studied using Scanning Electron Microscopy (SEM). The structure was studied using X-Ray Diffraction.

Acknowledgment
This work was financially supported by the National Science Centre of the Republic of Poland, Grant No 2014/14/EST5/00763.

References

[1] Hoa M. L., Lu M., Zhang Y.: *Preparation of porous materials with ordered hole structure*, Advances in Colloid and Interface Science 121: 9-23, 2006

[2] George C. N., Thomas J.K., Jose R., et al.: *Synthesis and characterization of nanocrystalline strontium titanate through a modified combustion method and its sintering and dielectric properties*, Journal of Alloys and Compounds 486: 711-715, 2009

Laboratory tests of the heat propagation and storage in a stone heat exchanger simulator

Krzysztof Nalepa
University of Warmia and Mazury in Olsztyn
krzysztof.nalepa@uwm.edu.pl

Keywords: ground heat exchanger, heat storage, passive cooling

This paper contains research results conducted on the model reproducing the true object of membrane-less heat exchanger, which is placed in the ground (under the ground surface) [1]. Such exchangers can be used as elements of passive cooling and heating of the ventilation air. [2] The research stand was built as the cuboidal case with internal dimensions of active chamber 440x440x1000mm. The chamber was filled with the gravel of 16-32 mm granulation. 36 temperature sensors were arranged inside the chamber in the manner facilitating information obtaining on the spatial temperature distribution in the porous bed. The air with monitored temperature was forced using electric ventilator (pump) with the efficiency regulation possibility. Air feeding and outflow was realized by settling chambers.

Sensors arrangement inside the simulator is presented in figure 1a. To present temperature and heat distribution over time, the plane of central vertical section was chosen.

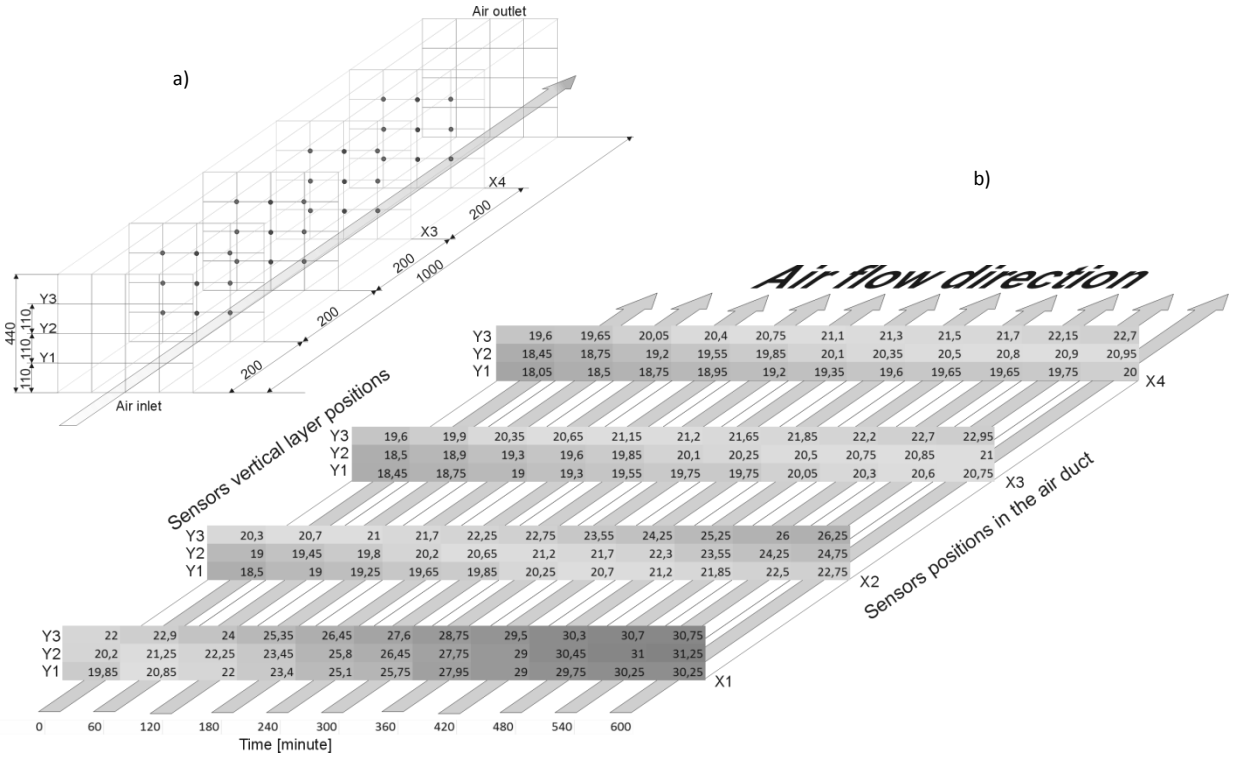

Fig.1. Temperature sensors position (a) and temperature distribution (b) in the selected section during simulator heating.

Temperature changes in the particular section points of the ground exchanger model illustrate heat transfer by filling elements of simulator chamber. The fastest temperature increase was noticed in the points closest to the warm air inlet. The slowest temperature increase is observed in the closing zone of simulator, which results from heat transmission in the first zone of simulator.

The ground heat exchanger simulator was built to acquire data for computational simulation model enabling an explanation of the phenomena occurring in the porous membrane-less heat exchangers absorbing and giving up heat to the ground. Preliminary tests results shows device usability for reproduction the ground heat exchangers work and underground heat storages in the laboratory conditions.

References:

[1] Nalepa K., Neugebauer M., Sołowiej P.: *Koncepcja i budowa gruntowego wymiennika ciepła, jako elementu systemu wentylacyjnego budynku mieszkalnego,* Inżynieria Rolnicza R. 12, nr 2(100): 203-208, 2008

[2] Spryszyński Z., *The technical and economic aspects of using a new method of heat/cool energy extraction from the ground*, Journal of Heat Recovery Systems, Volume 4, Issue 5, 313-316, 1984

Study of numerically generated Raschig rings orientation in a cylindrical container

Paweł Niegodajew, Maciej Marek
Czestochowa University of Technology, Institute of Thermal Machinery
al. Armii Krajowej 21, 42-200 Czestochowa, Poland
niegodajew@imc.pcz.czest.pl

At present, application of numerical method in generation of random packing geometries has appeared to be the alternative approach for complex and expensive experimental methods. Digital reconstruction of packed bed allows for detailed insight into the packing globally and locally. This work is devoted to the numerical generation of random packings of Raschig rings applied mostly in separation processes (see Fig. 1a). The detailed description of the algorithm used can be found in [1].The present study is focused on the analysis of particles orientation with respect to the container axis (see Fig. 1b). The results of Caulkin et al. 2009 [2] were used in the present work to verify the correctness of the numerically generated structure (see Fig. 1c). The investigation was performed globally and locally in various regions of the container: near wall, core and the bottom zone. The analysis concerns both varying particle height to particle diameter and column diameter to particle diameter ratios. The influence of the varying particle height to particle diameter ratio on global bed void fraction was also examined.

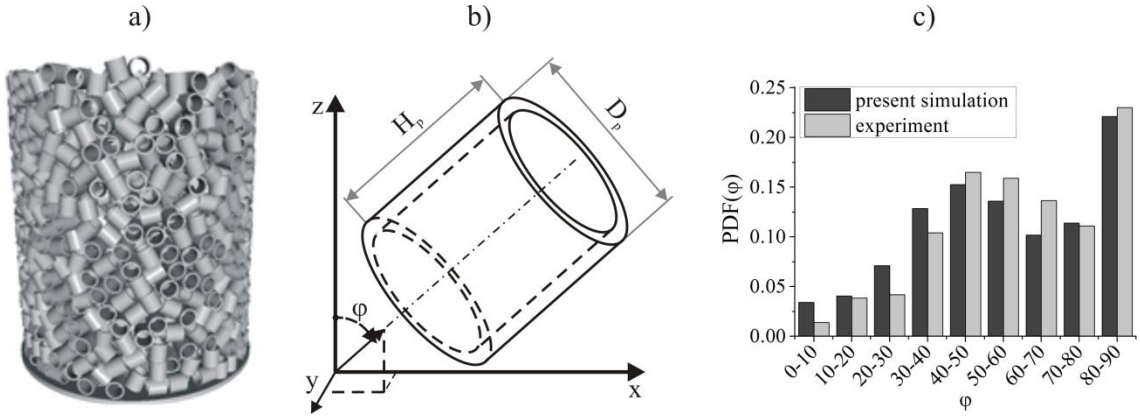

Fig.1. Numerically generated packed bed (a), definition of particle orientation angle (b) and model verification with the use of experimental data adopted from [2].

References:

[1] M. Marek, Numerical generation of a fixed bed structure, Chem. Process Eng. 34 (2013) 347–359.
[2] R. Caulkin, X. Jia, C. Xu, M. Fairweather, R. a. Williams, H. Stitt, et al., Simulations of Structures in Packed Columns and Validation by X-ray Tomography, Ind. Eng. Chem. Res. 48 (2009) 202–213.

Acknowledgements:
This study was performed within the framework of the contract: DEC-2014/15/B/ST8/04762 founded by National Science Centre.

Verification of cavitation models in ANSYS Fluent

Agnieszka Niedźwiedzka, Wojciech Sobieski
University of Warmia and Mazury in Poland, Faculty of Technical Sciences, 10-957 Olsztyn, Poland
agnieszka.niedzwiedzka@uwm.edu.pl

Keywords: Fluent, cavitation model, UDF

The first step before starting of any research work is making sure about the chosen method. In analytical calculations it seems to be simple. First of all, the derivation of formulas and correctness of the sources, which are used to draw data, should be checked. In the case of numerical simulations, the control of the used methods and tools is definitely more difficult. Typically, soft wares do not provide possibilities of access to the data entry method. Ansys Fluent gives users information about applied methods and tools, but it is impossible to check, that the proposed solution way is a properly application of the presented theories. Fortunately, Ansys Fluent gives users a possibility to interfere in the process of solution setups and methods in form of user defined functions (UDF). In cavitation modelling, through UDFs can be described the mass transfer rate between liquid and vapor phases. It allows to compare solutions achieved in two ways: using cavitation models direct from the interface or implemented through an UDF. The aim of the work is to compare the results of simulation of cavitating flow based on the tutorial example [1], made using models from the interface and their implemented equivalents. The motivation is luck of a such work in the literature.

In ANSYS Fluent is possible to apply from the interface three the most popular cavitation models: Schnerr and Sauer model [2], Singhal et al. model [3] and Zwart et al. model [4]. The source terms of the above mentioned models (for condensation – increase of liquid mass ($\dot{m}^{+}$), when the local fluid pressure increases above the saturated liquid pressure and evaporation – decrease of liquid mass ($\dot{m}^{-}$), when the local fluid pressure drops below the saturated liquid pressure) are collected in the Table 1.

Table 1. Source terms of the models.

	Schnerr and Sauer model	Singhal et al. model	Zwart et al. model
$\dot{m}^{+}$	$\frac{\rho_v \rho_l}{\rho_m} \alpha_v (1-\alpha_v) \frac{3}{R} \sqrt{\frac{2}{3} \frac{(p-p_{sat})}{\rho_l}}$	$C_p \frac{\sqrt{k}}{\sigma} \rho_l \rho_l \sqrt{\frac{2}{3} \frac{(p-p_{sat})}{\rho_l}} f_v$	$C_p \frac{3\alpha_v \rho_v}{R} \sqrt{\frac{2}{3} \frac{(p-p_{sat})}{\rho_l}}$
$\dot{m}^{-}$	$-\frac{\rho_v \rho_l}{\rho_m} \alpha_v (1-\alpha_v) \frac{3}{R} \sqrt{\frac{2}{3} \frac{(p_{sat}-p)}{\rho_l}}$	$-C_d \frac{\sqrt{k}}{\sigma} \rho_l \rho_v \sqrt{\frac{2}{3} \frac{(p_{sat}-p)}{\rho_l}} (1-f_v-f_g)$	$-C_d \frac{3\rho_v (1-\alpha_v)\alpha_{nuc}}{R} \sqrt{\frac{2}{3} \frac{(p_{sat}-p)}{\rho_l}}$

References:

[1] Ansys Fluent 12.0 Tutorial guide, 2009.
[2] Schnerr G. H., Sauer J.: *Physical and numerical modeling of unsteady cavitation dynamics.* In: Proceedings of the Fourth International Conference on Multiphase Flow (ICMF'01), New Orleans, USA, 2001.
[3] Singhal A. K., Athavale M. M., Li H., Jiang Y.: *Mathematical basis and validation of the full cavitation model.* Journal of Fluids Engineering 124, 617-624, 2002.
[4] Zwart P. J., Gerber G., Belamri T.: *A two-phase flow model for prediction cavitation dynamics*. In: Proceedings of the Fifth *International Conference on Multiphase Flow (ICMF 2004)*, Yokohama, Japan, 2004.

A finite deformations poroelastic model of lymphedematous tissue in indentation test

Joanna Nowak, Mariusz Kaczmarek
Institute of Mechanics and Applied Computer Science, Kazimierz Wielki University,
Kopernika 1, 85-074 Bydgoszcz, Poland
joanna_n@ukw.edu.pl

Keywords: indentation test, finite deformations, lymphedema, mathematical model, numerical predictions

Indentation test is an objective diagnostic method used to assess the tissues stiffness, constituting an alternative to a standard "palpation test". Frequently the test has a form of the shallow examination, that is: after setting constant force (possibly small one to limit strains), penetration depth is measured [1]. This work refers to results of simulations taking advantage of the so-called deep tonometry. The flat-ended indenter penetrates tissue to the depth of 10 mm, with approximately constant velocity 1 mm/s. The measured quantity is the accompanied force, which along with the applied deformation are used to assess stiffness of the tissue. Figure 1 shows schematic representation of the proposed idea of the test, where **h** indicates the position of surface of tissue with respect to the head of indenter, and $\mathbf{U_{disp}}$ is the indenter's displacement. The contact surface of the indenter is 1 cm^2. The friction between indenter and tissue is neglected.

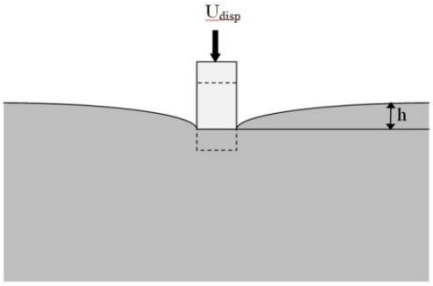

Fig.1. Schematic representation of the indentation test.

The lymphedematous tissue is modelled as homogeneous and isotropic porous medium filled with interstitial liquid. The solid skeleton is described with help of the effective stress law and neo-hookean material. The interaction force between phases is proportional to the relative velocity of liquid and permeability is assumed to be constant. Viscous stress in liquid phase is neglected. The Lagrangian formulation of the model proposed by Borja [2] is adopted. Then, the mechanical equilibrium equation takes the form

$$\nabla_X \cdot \mathbf{P} = \mathbf{0} \tag{1}$$

where $\mathbf{P}$ denotes the total stress tensor, which is decomposed into effective stress and pore pressure $\mathbf{P} = \tilde{\mathbf{P}} - B\theta\mathbf{F}^{-t}$. The Kirchhoff pressure in liquid θ is related to Cauchy pore pressure p by $\theta = J^t p$; $\tilde{\mathbf{P}}$ is the first Piola-Kirchhoff effective stress tensor. $J = \det(\mathbf{F})$ where $\mathbf{F}$ is the deformation gradient, B represents a material coefficient. For the neo-hookean hyperelastic material the effective stress tensor $\tilde{\mathbf{P}}$ is related to elastic energy function W

$$\mathrm{W} = \frac{\mu}{2}[tr(\mathbf{C}) - 3] - \mu \ln(J) + \frac{\lambda}{2}(\ln J)^2 \tag{2}$$

where $\mathbf{C}$ is the right Cauchy-Green deformation tensor. The equation expressing mass balance of lymph fluid and solid skeleton takes the form

$$\left(B - \frac{\phi p}{K_f}\right)\frac{dJ}{dt} + \frac{\phi}{K_f}\frac{d\theta}{dt} = -\frac{1}{\rho_f}\nabla_X \cdot \mathbf{Q} \tag{3}$$

where ϕ denotes porosity and $\mathbf{Q}$ is macroscopic liquid flux with respect to matrix in Lagrangian form, which is related to spatial discharge velocity $\mathbf{q}$

$$\mathbf{Q} = J\mathbf{F}^{-1}\mathbf{q} \tag{4}$$

Numerical simulations are performed using Comsol Multiphysics environment. The displacement of the indenter is applied incrementally. The fully coupled solver is based on Newton-Raphson method for solving non-linear finite elements equations at each time step. For such formulated model the sensitivity analysis is performed taking into account the influence of stiffness and permeability on mechanical response of lymphedematous tissue examined in the deep tonometry test. The results obtained show significant role of stiffness and permeability. Results for the maximum force in the test allow for evaluation of tissue's stiffness and characteristics of relaxation of the tissue correspond to permeability. The knowledge on indentation test of lymphedema tissue can be useful to optimise therapeutic method.

References:

[1] Zheng, Y., Mak, A.F.T., Lue, B., Objective assessment of limb tissue elasticity: development of a manual indentation procedure, *J. Rehabil. Res. Dev.*, Vol.36, 1999.

[2] Li, Ch., Borja, R.I., Regueiro, R.A., Dynamics of porous media at finite strain, *Comput. Methods Appl. Mech. Engrg.*, Vol. 193, 2004.

The Cauchy problem for the time-fractional advection diffusion equation in a layer

Yuriy Povstenko[1], Joanna Klekot[2]
[1]Institute of Mathematics and Computer Science, Jan Długosz University in Częstochowa, Poland
[2]Institute of Mathematics, Częstochowa University of Technology, Poland
j.povstenko@ajd.czest.pl

Keywords: porous medium, non-Fickian diffusion, fractional calculus, Mittag-Leffler function

The standard advection diffusion equation

$$\frac{\partial c}{\partial t} = a\Delta c - \mathbf{v}\cdot \mathrm{grad} c \tag{1}$$

results from the balance equation for mass and the constitutive equation

$$\mathbf{j} = a\ \mathrm{grad} c + \mathbf{v}c \tag{2}$$

and has several physical interpretations in terms of Brownian motion, diffusion or heat conduction with additional velocity field, transport processes in porous media, groundwater hydrology, diffusion of charge in the electric field on comb structures, etc. [1], [2], [3]. In the last few decades, equations with derivatives of fractional order have attracted considerable interest of researchers due to many applications in physics, geophysics, geology, rheology, engineering and bioengineering. Time-derivative of fractional order describes memory effects, operators of fractional differentiation with respect to space variables describe the long-range interaction.

The time-nonlocal generalizations of the constitutive equation for the matter flux (2) were studied in [4], [5]. In the case of "long-tail" power kernel

$$\mathbf{j} = D_{RL}^{1-\alpha}[a\ \mathrm{grad} c + \mathbf{v}c] \tag{3}$$

where $D_{RL}^{\alpha}c(t)$ is the Riemann-Liouville fractional derivative of the order α. In combination with the balance equation for mass, Eq. (3) leads to the time-fractional advection diffusion equation

$$\frac{\partial^{\alpha} c}{\partial t^{\alpha}} = a\Delta c - \mathbf{v}\cdot \mathrm{grad} c \tag{4}$$

with the Caputo fractional derivative. In the literature there are only several papers in which the analytical solutions of Eq. (4) were obtained. A comprehensive survey of different approaches to solving the fractional advection diffusion equation as well as of the numerical methods used for its solving can be found in [6]. In the present paper, we study Eq. (4) in a layer $0 < x < L$, $-\infty < y < \infty$. The Cauchy problem with zero boundary conditions is considered:

$$\frac{\partial^{\alpha} c}{\partial t^{\alpha}} = a\left(\frac{\partial^2 c}{\partial x^2} + \frac{\partial^2 c}{\partial y^2}\right) - v\frac{\partial c}{\partial x} - v\frac{\partial c}{\partial y} \tag{5}$$

$$t = 0: \quad c = f(x,y) \tag{6}$$

$$x = 0: \quad c = 0 \tag{7}$$

$$x = L: \quad c = 0 \tag{8}$$

The new sought-for function $u(x,y,t)$

$$c(x,y,t) = \exp\left[\frac{v(x+y)}{2a}\right] u(x,y,t) \tag{9}$$

allows us to eliminate the gradient term from (5). The fundamental solution to the Cauchy problem is obtained using the Laplace transform with respect to time t, the exponential Fourier transform with respect to the spatial coordinate y and the finite sin-Fourier transform with respect to the spatial coordinate x.

The logarithmic singularity term is separated from the solution. Expressions amenable for numerical treatment are derived. The numerical results are illustrated graphically. To evaluate the Mittag-Leffler function appearing in the solution, the algorithm suggested in [7] has been used.

References:

[1] Kaviany M.: *Principles of Heat Transfer in Porous Media*, Springer, 1995
[2] Nield D.A., Bejan A.: *Convection in Porous Media*, Springer, 2006
[3] Scheidegger A.E.: *Physics of Flow through Porous Media*, University of Toronto Press, 1974
[4] Povstenko Y.: *Theory of diffusive stresses based on the fractional advection-diffusion equation*, pp. 227-242, In: Fractional Calculus: Applications, NOVA Science Publishers, 2015
[5] Povstenko Y.: Fractional Thermoelasticity, Springer, 2015
[6] Povstenko Y.: *Fundamental solutions to time-fractional advection diffusion equation in a case of two space variables*, Mathematical Problems in Engineering 2014: 705364-1-7, 2014
[7] Gorenflo R., Loutchko J., Luchko Yu.: *Computation of the Mittag-Leffler function and its derivatives*, Fractional Calculus and Applied Analysis 5(4): 491-518, 2002

Three dimentional analyses of seepage resistance of a steel sheet pile wall

Eugeniusz Sawicki
Wrocław University of Technology, Faculty of Civil Engineering
eugeniusz.sawicki@pwr.wroc.pl

Keywords: leakage, joint resistance, imperviousness of SSP wall, SSP wall, seepage resistance

The aim of this article is to present the 3D numerical calculations results of the seepage resistance of steel sheet pile (SSP) wall with sealed and unsealed (filled by soil) joints. Unlike to the approach presented in [1] and [2] (concept of joint resistance) and unlike to [3] in present work the leakage through SSP wall was determined for one joint of full length (Fig. 1). In the analyzed example the SSP wall passed through one kind of soil but some conditions (permeability of joint and of surrounding soil) changed depending on the adopted assumptions.

To find the distribution of the total head in the calculation area Laplace equation was used. To determine the velocity field Darcy's law was adopted. The validity of Darcy's law in the task of this kind can be questionable and this issue was discussed in the paper.

In the first step the discharge flowing through the single joint of SSP wall based on 3D numerical simulations was determined. In the next step the joint resistance was estimated and the discharge was found analytically.

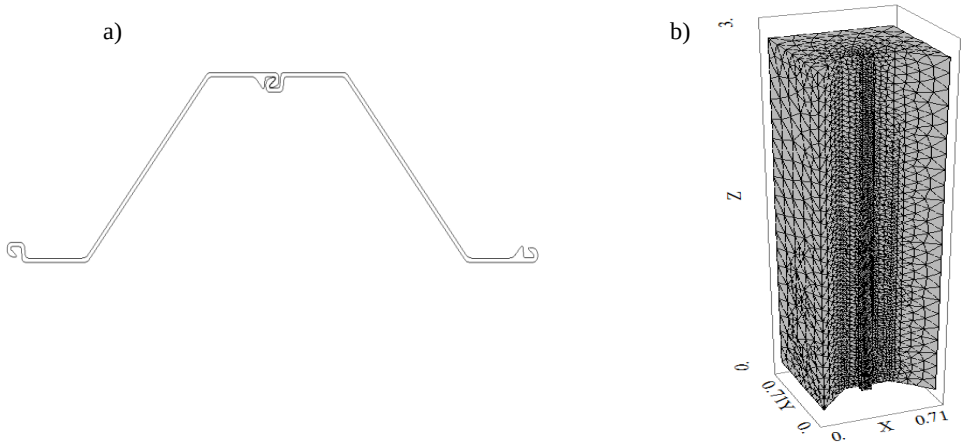

Figure 1: a) profile example of SSP wall, b) Finite elements mesh for one joint and surrounding soils.

The results obtained using these two methods were compared. And the conclusions are as follows: it seems possible to estimate the „joint permeability" coefficient using numerical methods, in some conditions the analytical results are far away from numerical ones due to the nonlinear pressure distribution along the joint, it is necessary to collect in-situ data to confirm the usefulness and reliability of obtained solutions and proposed methods of determination of SSP wall seepage resistance.

References:

[1] *Steel Sheet Piling. The Impervious Steel Sheet Pile Wall. Part 1: Design. Part 2: Practical Aspects*, http://www.arcelormittal.com/palancole/uploads/files/AMCRPS_Impervious_EN.pdf
[2] Widong M., *Design, Execution and Monitoring of Impervious Steel Sheet Pile Walls Embedded in Impermeable Layers*, http://folk.ntnu.no/emdal/ngf/informasjon/downloads/permanent_spunt_okt_2004/MarcWidong-Imperviouswall.pdf
[3] Polska Norma, PN-EN 12063, *Wykonawstwo specjalnych robót geotechnicznych - Ścianki szczelne*, (2001)

Investigation of emulsions imbibition process in hydrophilic/oleophilic granular porous media

Olga S. Shtyka, Jerzy P. Sęk
Faculty of Process and Environmental Engineering, Lodz University of Technology, Poland
olga.shtyka@edu.p.lodz.pl

Keywords: emulsion, imbibition process, granular medium

The transport of fluid through porous media is regarded as a complicated process. This phenomenon can occur under the influence of the capillary suction-pressure and is known as a spontaneous imbibition or wicking [1], [2]. The capillary pressure appears as a consequence of the surface energies interchanging during the porous medium wetting with a permeant. The opposite forces to the driving one are viscous dragging and gravity [1], [2], [3]. It remains to be of practical importance as a fundamental phenomenon due to its wide application in numerous industries processes and its frequent occurrence in the nature [3], [4].

Over the last decades, there has been a continuous interest in single phase liquids wicking, mostly organic substances, through ordered and disordered porous structures. In literature there are also discussions concerning the mechanisms of the imbibition and the influence of the contact angle, surface tension, viscosity, mean pore radius and channels tortuosity on it [1], [2], [3], [5]. However, the process of two-phase liquids penetration in porous structures driven by capillary pressure has not yet been fully investigated and understood. There is an obvious lack of experimental data and modelling approaches.

The present work focuses on the investigation of the kinetics of granular porous material imbibition with two-phase liquids such as emulsions. There is an assumption that the imbibition of porous structures with a permeant consisting of two phases, differs significantly from the process with a single-phase liquid. It relates firstly to different viscosity and level of pores surface wettability with each component of an emulsion.

The research was conducted to evaluate the changes of an imbibed emulsion mass and the height of its front with time of imbibition process. The discussed aspect was also the dependence of such variations of the permeant properties and its composition as well as structures of used porous media. The kinetics of the process and the role of the previously mentioned factors were investigated by means of the classical imbibition test described elsewhere [6].

The object of the current investigation was a granular medium represented by spherical grains with hydrophilic/oleophilic properties. There were three different porous media which differed from each other by the average diameter of particles that was equal to 100, 200 and 500 μm. The bulk density was found in a range of 1400–1600 kg/m^3. The mean porosity of media also varied and laid in a range of 0.3–0.4. The height of the granular bed was the same in all investigated cases and equalled 0.15 m.

The wicking liquids were represented by stabilized oil-in-water emulsions with different dispersed phase concentrations – 10%, 30% and 50%. The emulsions were prepared by stirring of the refined vegetable oil (EOL Polska Sp.z.o.o., Poland) or kerosene Shellsol D–60 (Chmenia–Łódź S.A., Poland) with water and a non-ionic surfactant. Oil with a viscosity of 52.31±0.42 mPa·s was used as a model liquid of high-viscous substances, while the kerosene (μ=1.23±0.20 mPa·s) represented oils with low viscosity. The investigated emulsions differed from each other by viscosity, which was found to be in a range of 2–70 mPa·s. Ethoxylated fatty acid (PCC Exol SA, Poland) as a non-ionic surfactant was used in a fraction of 2 vol% to stabilize the prepared emulsions.

The obtained experimental results allowed to describe the kinetics of the spontaneous imbibition process occurring in a granular porous media in a form of the variation of an imbibed emulsion mass m_{im} and changes of the height of its front h_{im} as a function of time t_{im}. The maximal imbibed mass m_{max} and the maximal achieved height h_{max} and their dependence on the media and bed properties were other important investigated aspects. It was found that the kinetics of a two-phase liquid imbibition in a granular porous medium mostly depended on pores size between grains, droplets size of the dispersed phase and also on the viscosity of emulsions as well as their initial concentration.

The mathematical equation describing the imbibed emulsion mass changes and the height of its penetration versus time was proposed using the obtained experimental data. The high correlation values and the low normalized root mean square error confirmed appropriation of the used equation and the obtained results.

References:

[1] Masoodi R., Pillai K. M.: Darcy's law-Based Model for Wicking in Paper-like Swelling Porous Media, AIChe J. 56(9): 2257–2267, 2010

[2] Zhmud B. V., Tiberg F., Hallstensson K.: Dynamics of Capillary Rise, Journal of Colloid and Interface Science 228: 263–269, 2000

[3] Masoodi R., Pillai K. M., Varanasi P. P.: Darcy's law based models for liquid absorption in polymer wicks, AIChe J., 53(11): 2769-2782, 2007

[4] Cai J., Yu B., Zou M., Luo L.: Fractal Characterization of Spontaneous Co-current Imbibition in Porous Media, Energy Fuels 24: 1860–1867, 2010

[5] Xue H. T, Fang Z. N., Yang Y., Huang J. P., Zhou L. W.: Contact Angle Determined by Spontaneous Dynamic Capillary Rises with Hydrostatic Effects: Experiment and Theory, Chemical Physics Letters 432(1–3): 326–330, 2006

[6] Sęk J. Shtyka O. S., Szymczak K.: Modelling of the Spontaneous Polypropylene Sorbents Imbibition with Emulsions, Journal of Environmental Engineering and Landscape Management, 23(2): 83–93, 2015

The synthesis of mesoporous materials with diatomite

Małgorzata Skibińska
Department of Crystallography, Faculty of Chemistry,
Maria Curie-Sklodowska University, Maria Curie-Sklodowska Sq. 3, 20-031 Lublin, Poland
malgorzata_skibinska90@wp.pl

Keywords: mesoporous materials, diatomite, silica

The aim of this work was the synthesis of hierarchical material containing diatomite and SBA-15. Diatomite is a loose, porous, lightweight rock. It was created as a result of accumulation and compaction of diatoms- unicellular eukaryotic algae [1]. Diatomaceous earth is made in 60-95% of amorphous silica. Diatomite is formed with hydrated SiO_2 and classified as opal-A. Minerals products were divided into three groups, opal-A, -C, -CT, depending on the degree of crystallinity and crystalline structure. Opal-A is predominantly amorphous. Opal-CT is a semi-crystalline. It consists of crystalline regions, cristobalite and tridymite and the opal-C creates a well-organized form silicate mainly in the form of cristobalite. Silica present in the diatomite comprises from 3-8% of structural water. Depending on the place of exploration of diatomite may differ slightly morphology, appearance, chemical composition [2]. Features that make that it is so widely used is low density, low thermal conductivity, high melting point (from 1400 to 1750 °C depending on the presence of impurities), soluble only in highly alkaline solutions, chemical inertness. It is used as a food additive or an anti-caking agent. Diatomite is used not only in food but also in pharmaceutical industry, plastics, agriculture, or in the dry cleaners. The most significant application of diatomite was the production of dynamite by Alfred Nobel. This mineral is readily available and inexpensive, so is widely used [3]. SBA-15 is a mesoporous silica. It is characterized by parallel ordered structure. It consists of a plurality of interconnected channels, cylindrical pores and thick walls. The pores form a hexagonal structure [4]. A characteristic structure present in SBA-15 is the crown, formed by the micropores which connecting with mesopores [5]. It is obtained by applying the triblock copolymer PEO20-PPO70-PEO20 called P123. For the synthesis of SBA-15 used is a sol-gel method. SBA-15 is one of the most popular mesoporous silica materials. This is due to its unique properties, large mesoporous, thick walls, the presence of micropores, high thermal stability and catalytic activity. That the material had even better adsorption capabilities like. It may be modified in several ways [6].

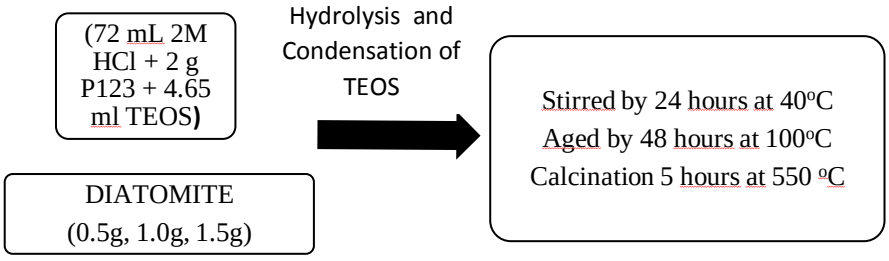

Fig. 1. The synthesis of hybrid materials with diatomite.

The use of diatomite addition to the classic synthesis of SBA-15 allows for materials with new properties. These materials are mesoporous, with different specific surface area and pore volume of micropores depending on the amount of diatomite to be added. Synthesized materials have an ordered structure but it is a different structure than the classical structure of SBA-15.

References:

[1] M. Sprynskyy, Heterogeniczność strukturalna oraz właściwości adsorpcyjne adsorbentów naturalnych, Wydawnictwo Naukowe Uniwersytetu Mikołaja Kopernika, 2012
[2] A. Chaisena, K. Rangsriwatananon, *Effects of thermal and acid treatments on some physico-chemical properties of lampang diatomite*, Suranaree J. Sci. Technol. 11: 289, 2004
[3] H. E. G. M. M. Bakr, *Diatomite: Its Characterization, Modifications and Applications,* Asian Journal of Materials Science 2(3): 121, 2010
[4] A. P. Giaquinto, Synthesis, Modification, and Characterization of Spherical SBA-15 Ordered Mesoporous Silica and Evaluation in High Performance Liquid Chromatography, Seton Hall University, 2012
[5] J. Thielemann, Synthesis,Characterization and in situ Catalysis of Silica SBA-15 Supported Molybdenum Oxide Model Catalysts, Technische Universitat Darmstadt, 2010
[6] N. Rahmat, A. Zuhairi Abdullah, A. Rahman Mohamed, *A Review: Mesoporous Santa Barbara Amorphous-15, Types, Synthesis and Its Applications towards Biorefinery Production,* Am. J. Applied Sci. 7(12): 1579, 2010

Application of CFD method for the air distribution and thermal control calculation in ventilated public space

Aldona Skotnicka-Siepsiak
The Institute of General Construction and Building Physics; The University of Warmia and Mazury
aldona.skotnicka-siepsiak@uwm.edu.pl

Keywords: thermal comfort, air division, air conditioning

Correct air distribution in room is necessary for thermal comfort. Room air distribution characterizes how the air is introduced to, flows through, and in which way air is removed from spaces. In spite of correct estimation of air quantity, temperature and humidity, fan and ducts, when the room air distribution is incorrect there won't be thermal comfort in space. Location and interaction between the air outlets and inputs have fundamental meaning for air distribution in space. Many other factors have also impact on thermal comfort in room, for example physical activity, temperature of the air and walls, humidity and velocity of the air, cleanness of air, the noise and many others. For keeping thermal comfort in the room we must know and control at least temperature, humidity, velocity of the air and temperature of the walls [1].

Each room or ventilated space requires an individual calculation of factors, which have impact on thermal comfort and analysis for the way of air distribution on it. By using Computational Fluid Dynamics (CFD) we are able to compare an optional ways of air distribution on the stage of conception. Thanks to that we can decide about the best method of air distribution, without risk that accomplished conception will fail.

The example of objects, where the CFD simulation were done are a didactic rooms. In the one case, for the lecture hall, the floor space of the hall is 239.9 m2 and it capable of holding 224 people. For the air heating system used in the space, the distributions of velocity, temperature, as well as the PMV and PDD indices have been subjected to an analysis by using Software FloVENT from Mentor graphics. In the second case the class room is much smaller (60 m^2) and its prepared for 46 students, also by using FloVENT, the validation of ventilation system was made as well as checking of the optimal variant for modernization of the ventilation system.

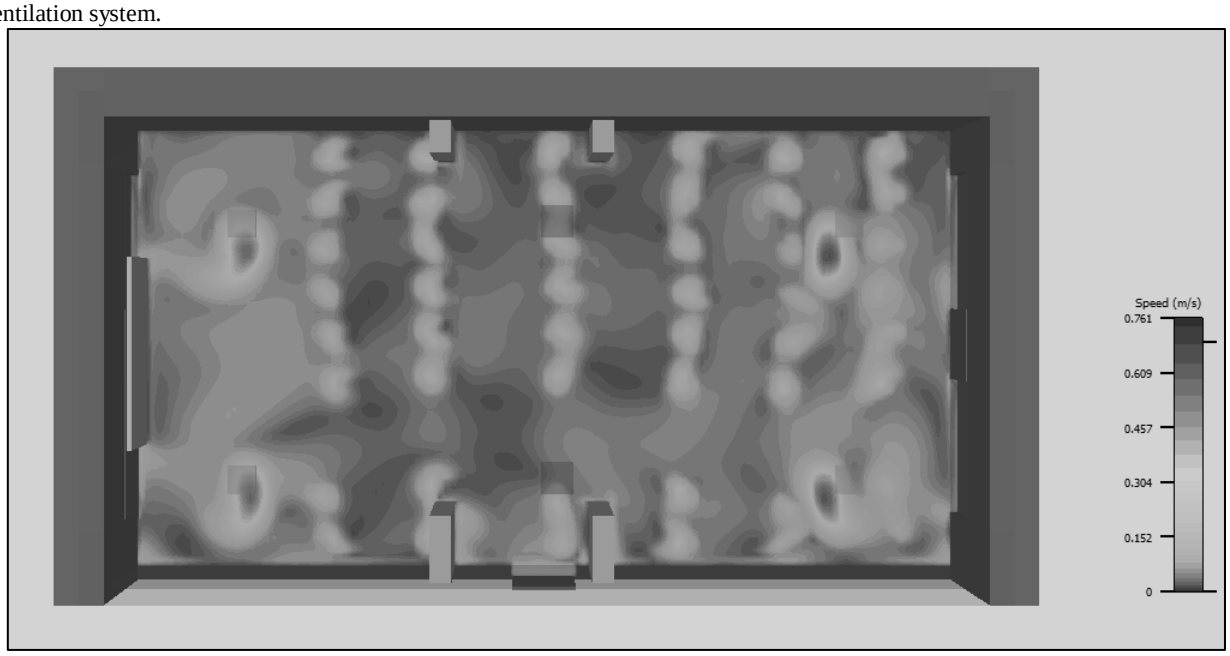

Fig. 1: Speed of distributed air in class room with mechanical ventilation.

Figure 1 representing example results for speed of the air in a class room. In analysed case, the biggest value of the speed were notice near the nozzle. Also the impact of the convection effect is shown as a higher air speed above the human had.

Thanks to CFD models, we are able to choose the best way of room air distribution. Nowadays, when ventilation is much common, the engineers need an objective tool for estimation of its consequences. We cannot forget that CFD models have limitations, even though, results of simulations give the objective information about parameters in space. What is more, the way in which results are illustrated gives chance for using them during discussion with investor or other people, who are not engineers.

References:

[1] Recknagel, Springer, Hönmann, Schramek, *Ogrzewanie i klimatyzacja*. EWFE-Wydanie 1; Gdańsk 1994

The PathFinder Project

Wojciech Sobieski
University of Warmia and Mazury, Olsztyn, Poland
wojciech.sobieski@uwm.edu.pl

Keywords: granular beds, tortuosity, porosity, numerical modelling, Path Tracking Method

The PathFinder Project it is an informal research project launched in the year 2013 by the author [1]. The main aim was to create a research group dealing with investigations of porous media, with a special focus on granular beds. It was assumed that by linking different research approaches, applied or developed by individual members of the group, a new quality of investigations may be obtained. It is important that the members of this project represent different research centres so that the know-how and technical base may be shared, which would significantly expand the research possibilities in this field.

The origins of the activities that led to the creation of the project date back to 2009 [2]. At that time the PathFinder numerical code, destined for granular beds and serving to analysing of their spatial structure [3], was developed by the author. Since this time several new directions of investigations have begun and currently the project covers the following points (Fig. 1):

- measurements and analysis of physical properties of particles as well as of granular beds;
- measurements and analysis of the particle size distributions;
- measurements and analysis of the particle shapes;
- measurements and analysis of the fluid flow through porous beds;
- determination of the spatial structure of granular beds with the use of CT-IA methods;
- determination of the spatial structure of granular beds with the use of the Discrete Element Method;
- calculating different parameters characterising the spatial structure of granular beds based on virtual beds or numerical representation of real beds;
- modelling the fluid flow through porous beds with the use of Finite Volume Method, Finite Element Method, Lattice Boltzmann Method or Immersed Boundary Method;
- development of different additional software useful in performed investigations.

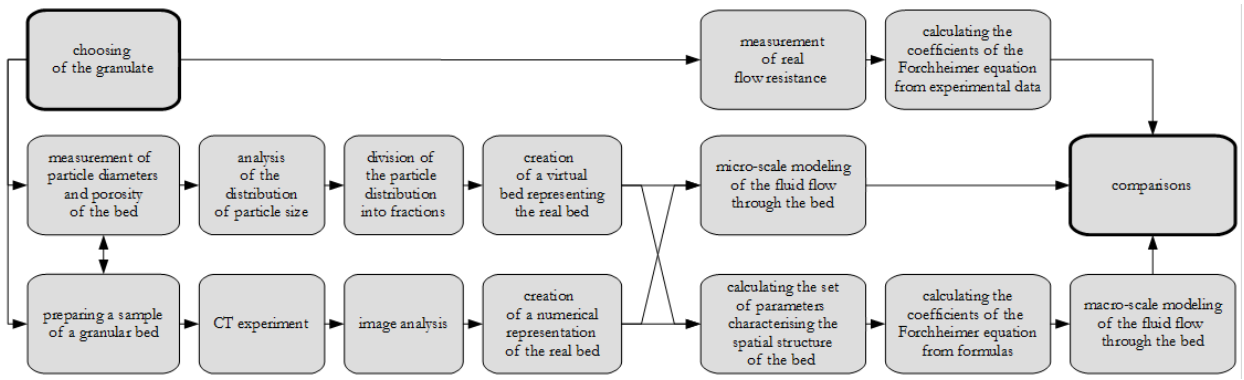

Fig.1. Connection diagram between main tasks of the PathFinder Project.

In the PathFinder Project, the connection between investigations in the micro- and macro-scales is important. Currently the main direction selected by the author is related to macro-scale modelling, but with the use of the knowledge acquired in micro-scale. The key role is played here by a set of parameters characterising the spatial structure of a granular bed (calculated by the PathFinder code if the data on the locations and sizes of all particles is available). This set is defined as follows:

$$\Phi = \{d(\mu,\sigma^2), \phi(V_p,V), \varepsilon(V_s,V), \tau^g(L_p,L_0), S_0(S_s,V_s,V), \dots\} \quad (1)$$

where: d – representative particle diameter [m], μ – average value [m], σ^2 – variance [m^2], ϕ – porosity [m^3/m^3], V_p – volume of the pore part of the porous medium [m^3], V – total volume of the bed [m^3], ε – packing coefficient [m^3/m^3], V_s – volume of the solid part of the porous medium (volume of all particles) [m^3], τ^g – geometric tortuosity [m/m], L_p – length of the flow path [m], L_0 – depth of the porous bed [m], S_0 – specific surface of the porous body [m^2], S_s – inner surface of the porous body [m^2].

If the set (1) is known (obtained from the micro-scale), than different macro-scale laws may be applied, e.g. the very popular Forchheimer law

$$\frac{dp}{dx} = A(\Phi)\cdot(\mu\cdot\vec{v}_f) + B(\Phi)\cdot(\rho\cdot\vec{v}_f^2) \quad (2)$$

where: p – pressure [Pa], x – coordinate along which the pressure drop occurs [m], $A(\Phi)$ [1/m^2] and $B(\Phi)$ [1/m] – two generalized parameters, dependent on the set Φ characterizing the spatial structure of the porous medium, μ – dynamic viscosity of the fluid [kg/m·s)], ρ – density of the fluid [kg/m^3)], $\vec{v}_f$ – filtration velocity [m/s].

References:

[1] PathFinder Project [on-line]. URL: http://www.uwm.edu.pl/pathfinder/index.php (Available at February 1, 2016). University of Warmia and Mazury in Olsztyn (Poland).
[2] Sobieski W.: *Calculating tortuosity in a porous bed consisting of spherical particles with known sizes and distribution in space*. Research report 1/2009, Winnipeg (Canada), 2009 (in Polish).
[3] Sobieski W., Lipiński S.: *PathFinder User's Guide* [on-line]. URL: http://www.uwm.edu.pl/pathfinder/index.php (Available at February 1, 2016). University of Warmia and Mazury in Olsztyn (Poland), 2013.

Stochastic model of solid particle projective image

Aleksander Sulkowski
Wrocław University of Technology, Faculty of Mechanical and Power Engineering,
Department of Cryogenic, Aeronautic and Process Engineering
aleksander.sulkowski@pwr.edu.pl

Keywords: solid particle, projective image, probability space, random variable, distribution function

Particle size and shape are two essential parameters affecting structure of granular material and determining its properties and technological behaviour [1]. Thus geometrical description of solid particle becomes one of the most important problems in powder technology [2].

In the paper solid particle denotes some material object represented by its geometrical model C, which is assumed to be a subset of three dimensional real space satisfying the following conditions: C is compact (closed and bounded) and connected set [3], being the closure of its connected interior Int(C) [3]. Thus it is required that the following condition is satisfied

$$C = \overline{(\mathrm{Int}(C))}. \tag{1}$$

It is assumed that geometrical description of real particle can be based on an information provided by its two dimensional projective image visualized on certain projection plane E, as shown in the Fig.1.

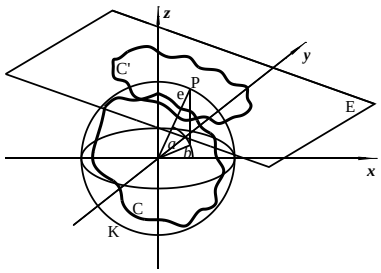

Fig.1.Orthogonal projection of solid particle on a screen plane in three dimensional coordinates system.

Thus numerical value of any particle size or shape parameter Φ_C [1], found for the considered image, depends on the position of particle C towards the projection plane during the measurement procedure and for irregularly shaped particles can vary in a wide range. Since the position of particle investigated is randomly changed, stochastic changes of particle image are observed. Consequently it was assumed that Φ_C is the random variable assigning positive real number to each particle projective image corresponding to the current particle position in relation to the projection plane E. Thus Φ_C is the random variable defined on a probability space Ω, being the collection of all possible particle positions towards the plane E. It was shown that each particle position mentioned can be uniquely determined by the pair of observation angles – rotation angle α and tilt angle β which undergo the following constraints: $\alpha \in [0, 2\pi]$ and $\beta \in [0, \pi/2]$. Thus the probability space Ω can be represented by the Cartesian product of both said closed intervals. Namely

$$\Omega = [0, 2\pi] \times [0, \pi/2] = \{(\alpha, \beta): 0 \le \alpha \le 2\pi,\ 0 \le \beta \le \pi/2\} \tag{2}$$

Thus each elementary event "ω" in Ω is represented by the pair of angles (α, β) mentioned, ($\omega = (\alpha, \beta)$). By σ-algebra of events F we understand collection of all Borel subsets [4] of two dimensional real space $\mathbf{R}^2$, contained in the set Ω, given by Eq.(2). Probability measure P(A) of any measurable subset (event) A of the space Ω is defined by the formula

$$P(A) = \lambda(A)/\lambda(\Omega), \tag{3}$$

where $\lambda(\bullet)$ denotes Lebesgue measure [4] in two dimensional real space $\mathbf{R}^2$. Thus complete probability system (Ω, F, P) is constructed. Consequently, any size or shape parameter Φ_C [1], corresponding to a given particle projective image, can be considered as the random variable defined on the space Ω and obviously takes the form of two variable function $\Phi_C(\alpha, \beta)$, measurable with respect to σ-algebra F. Distribution function of the random variable $\Phi_C(\alpha, \beta)$ is then given by the formula

$$F_\Phi(t) = P(\Phi_C(\alpha, \beta) < t) = \lambda((\alpha, \beta): \Phi_C(\alpha, \beta) < t)/\lambda(\Omega) \quad . \tag{4}$$

In case $F_\Phi(t)$ is a differentiable function, the density $f_\Phi(t)$ of the random variable $\Phi_C(\alpha, \beta)$ can be found as

$$f_\Phi(t) = dF_\Phi(t)/dt\,. \tag{5}$$

Particular form of distribution and density functions mentioned can be found under condition, analytical form of random variable $\Phi_C(\alpha, \beta)$ is known. It was suggested to derive exact formulas defining functions $F_\Phi(t)$ and $f_\Phi(t)$ in case random variable $\Phi_C(\alpha, \beta)$ denotes random projective Heywood diameter [1] of selected, geometrically regular, particle models.

References:

[1] Wanibe Y., Itoh T.: *New Quantitative Approach to Powder Technology*, John Wiley & Sons Ltd., N.Y., 1998
[2] Sztaba K.S.: *Relacje pomiędzy wielkościami ziarn mineralnych określanymi z przyjęciem różnych założeń definicyjnych*, Inż. Ap. Chem., 45, nr 4, 2006
[3] Rudin W.: *Functional Analysis*, Mc. Graw-Hill Book Company, N.Y., 1973
[4] Fremlin D.H.: *Measure theory vol. 1,2*, Torres Fremlin, Colchester, 2000

Random Heywood diameter of selected geometrical particle models

Aleksander Sulkowski
Wrocław University of Technology, Faculty of Mechanical and Power Engineering,
Department of Cryogenic, Aeronautic and Process Engineering
aleksander.sulkowski@pwr.edu.pl

Keywords: solid particle, projective image, Heywood diameter, distribution function, density function

The bulk properties of particulate solid materials are, to a large extent, dependent on their constituent particles size [1]. Several definitions of particle size are based on two dimensional characteristics of particle orthogonal projections [2].

As an example of particle projective dimension, consider Heywood diameter H_C defined to be the diameter of a circle whose area is the same as that of particle projective image S_C [3]. Thus H_C is given by the formula: $H_C = 2\sqrt{S_C/\pi}$. Obviously, for real particle C the value of the diameter H_C strictly depends on its position towards the screen plane. Every projection direction is uniquely determined by a pair of angles – rotation angle α and tilt angle β, undergoing the following constraints: $\alpha \in [0, 2\pi]$ and $\beta \in [0, \pi/2]$ [4]. Thus the space of all possible projection directions Ω takes the form: $\Omega = [0, 2\pi] \times [0, \pi/2] = \{(\alpha, \beta): 0 \le \alpha \le 2\pi,\ 0 \le \beta \le \pi/2\}$. Since the position of observed particle is changed randomly, its Heywood diameter should be considered as two variable random function $H_C(\alpha, \beta)$, expressed by the formula

$$H_C(\alpha, \beta) = 2\sqrt{S_C(\alpha, \beta)/\pi}\,, \tag{1}$$

where $S_C(\alpha, \beta)$ denotes the area of particle image projected in the direction defined by the pair of angles (α, β). For real particles, the form of the function $H_C(\alpha, \beta)$ can be found experimentally. In case of geometrical particle model, it is possible to derive analytical form of above dependence. Consider cuboidal object with dimensions: a, b, h, as shown in the Fig.1

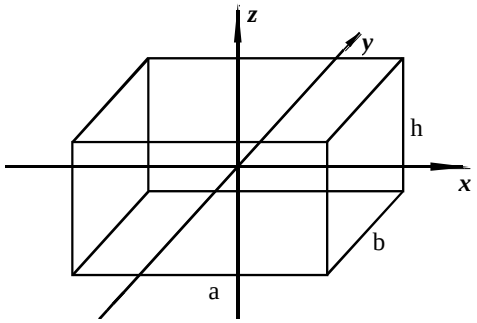

Fig.1. Cuboidal particle in a three dimensional coordinates system.

Random projective Heywood diameter $H_C(\alpha, \beta)$ of above object is given by the formula (2). Its graph is presented in the Fig.2.

$$H_C(\alpha, \beta) = 2\sqrt{\left(ah|\cos\alpha\cos\beta| + bh|\sin\alpha\cos\beta| + ab|\sin\beta|\right)/\pi}\,. \tag{2}$$

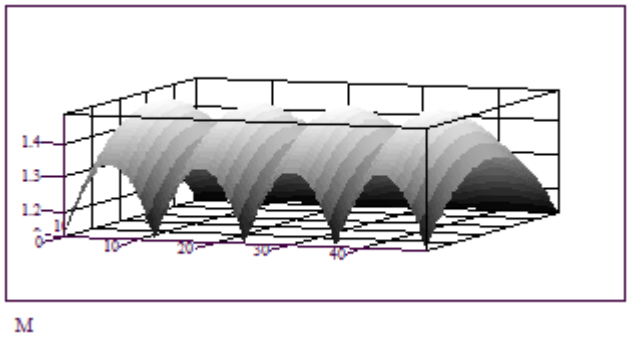

Fig.2. Random Heywood diameter of cuboidal particle.

In the paper analytical form of the distribution function $F_C(t) = P\left(H_C(\alpha, \beta) < t\right)$ of above random Heywood diameter $H_C(\alpha, \beta)$ was found. Similar constructions were derived for cylindrical, conical and ellipsoidal solid particle models.

References:

[1] Ohser J., Mucklich F., *Statistical Analysis of Microstructures in Materials Science* , John Wiley & Sons Ltd., N.Y., 2000
[2] Sztaba K.S.: *Relacje pomiędzy wielkościami ziarn mineralnych określanymi z przyjęciem różnych założeń definicyjnych*, Inż. Ap. Chem., 45, nr 4, 2006
[3] Wanibe Y., Itoh T.: *New Quantitative Approach to Powder Technology*, John Wiley & Sons Ltd., N.Y., 1998
[4] Rudin W.: *Functional Analysis*, Mc. Graw-Hill Book Company, N.Y., 1973

Application of micro computed thomography and mercury porosimetry to determination of internal structure of aerated concretes

Zbigniew Szczepański, Mieczysław Cieszko, Marcin Kempiński, Marcin Burzyński, Paweł Gadzała
Institute of Mechanics and Applied Computer Science,
Kazimierz Wielki University Kopernika 1, 85-074, Bydgoszcz, Poland
zszczep@ukw.edu.pl

Keywords: porosity, pore size distribution, aerated concrete, micro-computed tomography, mercury porosimetry

Two complementary methods: the micro-computed tomography (μCT) [1] and the mercury intrusion porosimetry (MIP) [2] are used in the paper to determine the internal pore space structure of autoclaved aerated concretes (AAC). It concerns the parameters of super-micron pore and sub-micron pore porosities and their pore size distributions.

Identification of microscopic pore geometry and macroscopic parameters of the pore space structure of AAC is a very important issue in the study of their physical properties. The internal pore structure defines mechanical properties of AAC and plays important role in many physical and chemical processes occurring in such materials, e.g. in moisture and heat transport, wave propagation and chemical reactions.

The AAC belong to the group of porous materials with double porosities. It means that their pore space is formed by pores of two classes of sizes: super-micron pores and sub-micron pores. The characteristic sizes of super-micron pores ranges from several microns to millimeter and sizes of sub-micron pores are from several nanometers to micron. The volumes of both types of pores occupied in AAC are comparable. This makes investigations of such materials very difficult. The volume fraction of a given pore type in the pore space of AAC samples has a strong influence on their properties. A large fraction of sub-micron pores decreases the mechanical strength of the material, whereas large fraction of super-micron pores has a positive influence on the insulating properties of the material. Study includes investigation of the super-micron pore space structure and investigation of the sub-micron pore space structure.

Due to limited resolution of the μCT scans they have been applied to investigate the super-micron pore space structure and due to bottle ink effect the MIP data was used to investigate the sub-micron pore space structure. A new method is used in the paper for determination of AAC sample super-micron pore porosity based on model of the histogram of 3D μCT scans and optimization procedure, [3]. This allowed precise definition of the threshold value of relative density preserving porosity during reconstruction of the binary image of the super-micron pore space. Next, the method of inscription of the largest spheres into the super-micron pore space is used to calculate the pore size distribution in this space. To determine the pore size distribution in the sub-micron space contained in porous skeleton of AAC samples the MIP data has been applied. It is possible because two parts of the mercury intrusion curve related to intrusion into super-micron pore and sub-micron pore spaces are distinctly separated. The analysis of this curve was performed basing on the capillary and chain models of the pore space and optimization method, [4]. This allows determining the limit pore size distributions in the skeleton pore space.

Both complementary methods have been applied to investigation of the pore space structure of four classes of AAC samples produced by SOLBET Capital Group. Part of the obtained results are presented in Fig.1.

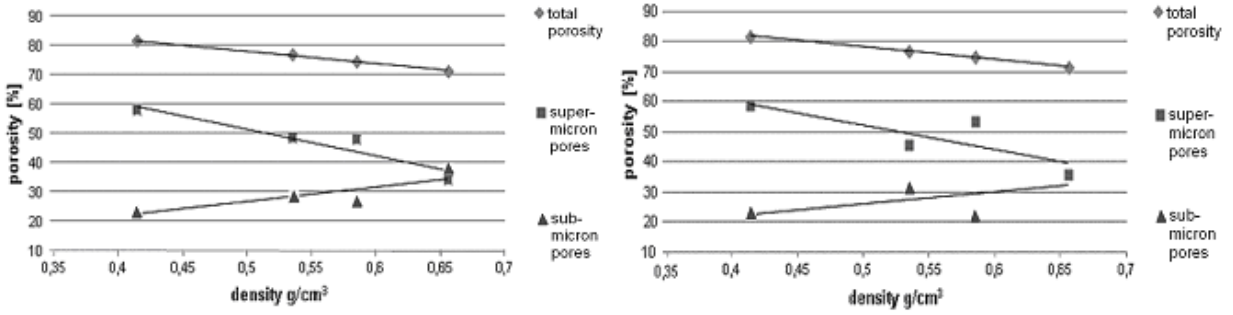

Fig.1. Dependence of total, super-micron pore and sub-micron pore porosities on density of AAC samples determined by the MIP method and by 3D µCT image analyses.

References:

[1] Stock S. R., *Micro computed tomography: methodology and applications*. CRC Press, Boca Raton 2008.
[2] Webb P. A., Orr C.,*Analitical methods in fine particle technology*, Micrometics Instrument Corporation, Norcross. GA USA 1997.
[3] Cieszko M., Szczepański Z., Gadzała P., *Determination of bone porosity based on histograms of 3D lCT images*, 50, 2, 948-959, 2015.
[4] Cieszko M., Kempiński M., *Determination of Limit Pore Size Distributions of Porous Materials from Mercury Intrusion Curves*. *Engng. Trans*. 54, 2, 143-158, 2006.

Diffraction techniques for analysis of block-copolymer based nano-porous materials.

Piotr P. Szewczykowski
Univeristy of Science and Technology in Bydgoszcz,
piotr.szewczykowski@utp.edu.pl

Keywords: block-copolymers, nano-porous, scattering techniques

Block copolymers have the ability to self-assemble into different structures in the nanoscale.[1] Different morphologies of the material can be obtained by modifying the volume fraction of one block to the other and operating below the order-disorder temperature (T_{ODT}). Lamellar (LAM), hexagonal (HEX) gyroid (GYR) or body centered cubic (BCC) morphology can be observed in case of diblock copolymers. There is much wider range of complicated structures for three block copolymers (not considered here). [2]

In order to obtain a nano-porous material the minority block needs to be removed by etching. Crosslinking is necessary for block-copolymers with elastomeric majority block (matrix). Pores will collapse if samples are not sufficiently crosslinked (high Laplace pressure). [3]

Some of the morphologies can be aligned in one direction by applying mechanical shear force, solvent evaporation, electric or magnetic field before the crosslinking and etching operation. Obtaining this kind of materials gives a variety of different applications in lithography, membrane technology or catalysis.

Many different techniques are being used to identify and analyse structure, pore size or internal surface area of nano-porous materials. Scanning and transmission electron microscopy are commonly used for direct identification of the morphology, however very often a complicated sample preparation is needed. Therefore diffraction techniques are being used at the first stage of material identification. By using Small Angle X-ray Scattering (SAXS) we can identify the hexagonal morphology as well as confirm the orientation of hexagonally packed cylinders (Fig. 1).

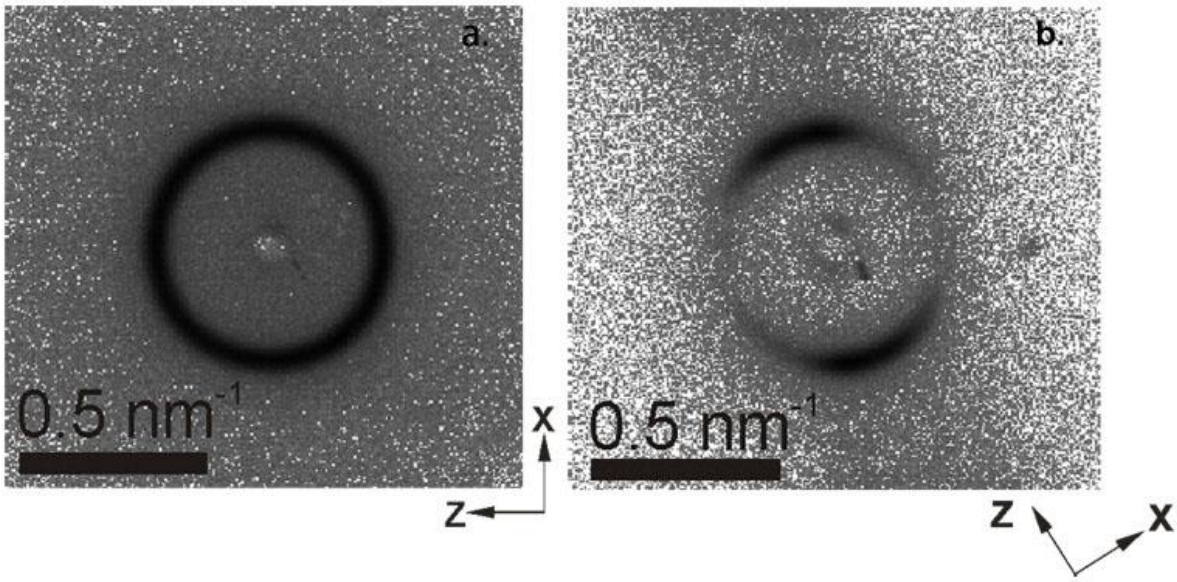

Fig.1. Two dimensional (2D) SAXS profiles for HEX unoriented (a) and oriented (b) sample by shear stress.

Interesting experiments can be provided with Small Angle Neutron Scattering and deuterated solvents. For example opening of the collapsed pores in case of not sufficiently crosslinked samples can be observed. [4]

Some of the experiments presented within this work were provided during author's PhD studies at the Technical University of Denmark.

References:

[1] Mai Y., Eisenberg A.: *Self-assembly of block copolymers*, Chem. Soc. Rev. 41: 5969-5985, 2012
[2] Thomas E.L., Lescanec R.L.: *Phase Morphologies in Block Copolymer Systems*, Philosophical Transactions: Physical Sciences and Engineering 338(1686): 149-166, 1994
[3] Muralidharan V.; Hui C.Y.: *Stability of nanoporous materials,* Macromolecular Rapid Communications 25 (16): 1487-1490, 2004
[4] Szewczykowski P.P., Andersen K., Schulte L., Mortensen K., Vigild M.E., Ndoni S.: *Elastomers with Reversible Nanoporosity*, Macromolecules, 44(15): 5636-5641, 2009

Agglomeration of particles in the freeze/thaw process

Janusz Szpaczyński
Department of Cryogenic, Aeronautical and Process Engineering, Faculty of Mechanical and Power Engineering, Wrocław University of Technology, 50-370 Wrocław, Poland
janusz.szpaczynski@pwr.edu.pl

Keywords: dewatering, sludge, freeze/thaw, agglomeration

Growing ice crystals attach to its structure molecules of pure water and most of impurities in the form of solid or dissolved compounds are rejected by the growing "face" of ice crystals.

The paper presents the concept of agglomeration of small size particles by freezing. Experimental studies have demonstrated that the freezing of suspension contributing to the agglomeration and separation of colloidal particles. Results have shown that the agglomeration of colloidal particles changes the characteristic of sludge and improves its filterability. After freezing and thawing solids can be easy separated by filtration or sedimentation.

The purified liquid has a high clarity, because most of the colloidal particles are agglomerated in a natural way, without the use of flocculants.

The results of filtration tests for single and multiple freezing were presented. It was found that higher degree of agglomeration of colloidal particles in wastewater frozen several times were present. Furthermore, the results shown that the freeze/thaw process gives better results than use of flocculants. The structure of sludge after the freeze/thaw process and dewatering was photographed and analyzed.

It was concluded that the freeze/thaw process gives great opportunities to improve efficiency of filtration and dewatering.

Numerical model of the fracture process of asphalt mixture using the semi-circular bending test

Cezary Szydłowski, Józef Judycki, Piotr Jaskuła, Jarosław Górski
Faculty of Civil and Environmental Engineering, Gdańsk University of Technology
cezary.szydlowski@pg.gda.pl

Keywords: asphalt mixture, semi-circular bending test, fracture, finite element modelling

Asphalt mixtures are made from mineral aggregate and binder. Compacted mixtures contains air voids. The amount of voids depends on the type of asphalt mix and varies from 1 to 25 % by means of volume. If the void content exceeds the range of 3% to 5% the asphalt mix can be classified as a porous medium. Asphalt pavements of highways are prone to deterioration under traffic load and environmental conditions. Cracking, fatigue cracking and low-temperature cracking are the major failure modes. Presently, the Polish and foreign regulations do not specify a direct criterion to classify a designed asphalt mix due to its cracking resistance. Fracture properties of asphalt pavement can be defined on the basis of fracture mechanics and strictly related to the laboratory test results. One of the most suitable and frequently used method is the bending test of semi-circular specimens (SCB).

Determination of fracture mechanics parameters of mineral-asphalt mix on the basis of bending test of the pre-cut semi-cylindrical specimens is a relatively simple task. The major concern is to unify parameters of the experiments: temperature, loading velocity and strain measurement mode. Figure 1 presents specimens and selected results of mineral-asphalt mix tests, conducted by the Road Construction Division at the Faculty of Civil and Environmental Engineering, Gdańsk University of Technology [1].The nine tested asphalt mixes were selected with respect to aggregate type and void content. Consequently, the fracture toughness K_{IC} was estimated, using the following equation

$$K_I = \sigma_0 Y_I \sqrt{\pi a} \tag{1}$$

where a is the cut depth, σ_0 test extreme stress, Y_I normalized stress intensity factor due to type I fracture.

Extreme bending stress in the specimen are computed using Eq. (2), where F is the maximum test force, r - specimen radius, B - specimen thickness:

$$\sigma_0 = F/2rB \tag{2}$$

The normalized stress intensity factor is given by the following equation

$$Y_I = 4.782 - 1.219(a/r) + 0.063\exp(7.(\tag{3}$$

Next the J-integral is specified by Eq. (4), where U is the strain energy to failure of the specimen, B is the thickness of specimen, dU/da is the variation of strain energy with the variation of notch depth:

$$J_C = -\left(\frac{1}{B}\right)\frac{dU}{da} \tag{4}$$

The authors' investigations [1] made it possible to conclude that the fracture resistance assessment of asphalt mixes based on K_{IC} alone is insufficient. It is therefore recommended to direct the tests on the fracture energy J_C, using specimens of variable pre-cutting notch depth and applying a crack-mouth-opening displacement (CMOD) detector. Such a research has been already scheduled.

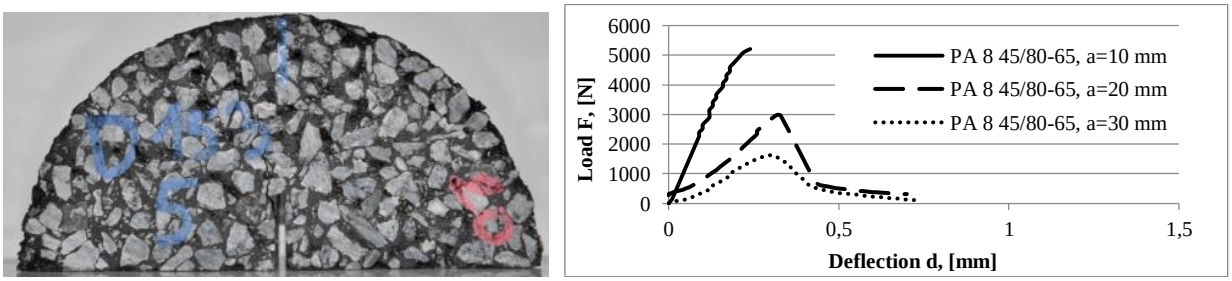

A B

Fig.1. A) The SCB specimen for the fracture resistance experiment B) bending load vs. deflection graph, different values of cutting depth considered [1].

The in-depth understanding of the specimen failure mechanism requires the constitutive relations defined. It is a considerable task, mostly due to material inhomogeneity. Attempts are made to this problem, using both available software and the author-made models. Material model calibration may be conducted on the basis of well performed experiments only.

The works presents an attempt to model the fracture of specimens, in more general terms, asphalt pavements by means of available engineering software. Computational analysis of a two-dimensional plane strain model was made, assuming homogeneous material of appropriately averaged material parameters based on reference values. The second stage of computations is made for a three-dimensional model. The next stage is to find out a precise description of a nonhomogeneous material, regarding bitumen, aggregate and voids. Calibration of the latter model is bound to bring about a high amount of work. A nonlinear fracture description should be applied.

The last stage of the work is to consider random variation of governing parameters and location of aggregate particles in specimens. Statistical dispersion of experimental data should be linked with the uncertainty of aggregate location and the values of material parameters.

References:

[1] Szydłowski C., Judycki J.: Laboratory investigation of asphalt mixtures fracture toughness using semi-circular beams (SCB). Highway engineering 10: 348-353, 2015, in Polish

Modelling flows through porous media. A short overview of the mathematical models and computational approaches

Anna Trykozko
ICM - Interdisciplinary Centre for Mathematical and Computational Modelling, University of Warsaw,
Pawińskiego 5a, 02-106 Warszawa
a.trykozko@icm.edu.pl

Keywords: porous media, flow equation, upscaling, numerical methods

1. One of the characteristic attributes of porous media is their multiscale nature and, as its consequence, a range of mathematical models referring to specific scales of resolution. The finest scale, also referred to as the pore-, or microscale, corresponds to the resolution where it is possible to distinguish a solid skeleton Ω_S and a pore space Ω_F available for fluid in a sample of a volume Ω of a porous medium, $\Omega = \Omega_S \cup \Omega_F$, Fig. 1a. When considered at microscale, flow is observed only in the pore space Ω_F, with pressure p and velocity $\mathbf{v}$ related to each other by Navier-Stokes equations.

Pore-scale representation of porous medium is not appropriate to describe the flow and transport in domains of sizes relevant for aquifer-related applications. In order to set-up models for larger areas, a macroscale approach becomes appropriate [1], where a system composed of a solid phase Ω_S and voids Ω_F is replaced by a conceptual continuum covering the whole Ω, Fig. 1b. An effective macroscale representation of geometric features of a microscale structure is expressed in terms of a permeability $\mathbf{k}$ [m^2], characterizing the porous medium at each point of Ω. The momentum equation in a flow model at the macroscopic scale is most often expressed by a linear Darcy's law, linking velocity (a flow rate) with a pressure drop. The range of applicability of Darcy's law is limited to a certain range of low flow velocities. As flow velocities increase, a growing contribution of inertia forces results in an inadequacy of Darcy's law and, thus, in a need to introduce extended nonlinear models.

In my talk a brief overview of the above mentioned models will be given along with some qualifications of computational methods applicable at different scales and for different models.

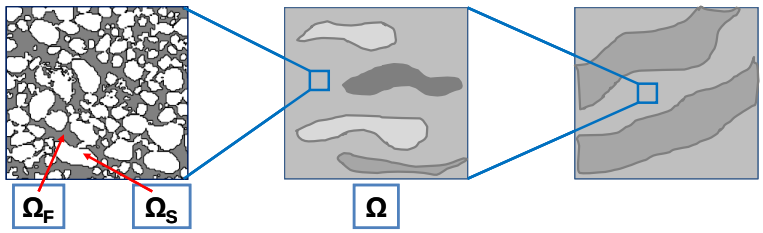

Fig. 1. a) Microscale. Domain available for flow Ω_F - grey, solid skeleton Ω_S - white. b) Macroscale. Depending on a resolution, a medium is considered, heterogeneities appearing at different space scales may be distinguished. In both cases, the medium is treated as a continuum.

2. A range of diverse models will be used to address problems related to scaling. Scales and scaling issues are inherently linked to the problems of modelling flows through porous media. An appropriate definition of parameters and the models in a space scale adequate to processes under consideration, as well as specifying the interscale relationships, is critical for a success in modelling. Relationships between different space scales of a process description are determined by *scaling*. In the context of porous media, the scaling links two scales: the one of higher resolution, referred to as a fine scale, and a coarse scale of lower resolution. A transfer from the fine to coarse scale is performed by upscaling. A need for upscaling results from limitations of the model sizes, perception capabilities as well as the availability of physical measurements and experimental validation [2]. In the case of numerical computations, model's size is related to the number of computational cells and its limitations are imposed by available computing resources as well as realistic simulations times. Another reason for upscaling reflects a discrepancy between sizes of the modelled domains and a resolution of available data.

A general framework of the upscaling procedure consists of the following elements:

- Data defining a fine scale problem: (i) macroscale flow equation or Navier Stokes equations, (ii) geometry of a flow domain Ω or Ω_F, (iii) fluid parameters, (iv) boundary conditions.
- Numerical model, consisting of (i) computational mesh and (ii) numerical code.
- Simulation results which are solutions of the flow equation at a fine scale.
- Derivation of parameters of the coarse scale, and, accordingly, other relationships based on averaged variables of the fine scale model.

3. A computational example of the upscaling procedure applied to linking micro- and macro scales following the methodology of [3] will be presented as concluding the talk.

References:

[1] Bear J., Cheng A.: *Modeling groundwater flow and contaminant transport*, Springer, 2010.
[2] Małecki J.J., Nawalany M, Witczak S., Gruszczyński T.: Wyznaczanie parametrów migracji zanieczyszczeń w ośrodku porowatym dla potrzeb badań hydrogeologicznych i ochrony środowiska. Poradnik metodyczny. Uniwersytet Warszawski Wydział Geologii. 2006.
[3] Peszynska M., Trykozko A.: *Pore-to-core simulations of flow with large velocities using continuum models and imaging data*, Computational Geosciences 17, 623-645, 2013.

Discrete Element Method

Joanna Wiącek
Institute of Agrophysics of the Polish Academy of Sciences
Doświadczalna 4, 20-290 Lublin
jwiacek@ipan.lublin.pl

Keywords: Discrete Element Method, DEM, granular matter

Discrete Element Method (DEM) is one of the numerical methods, based on a microstructural approach, in which the dynamics of each particle are computed with particle interactions modelled at various levels of complexity. Cundall and Strack [1] have proposed the method in 1979 to simulate interactions occurring between rigid rock blocks. The DEM has largely been employed as an academic research tool since its introduction over twenty years ago but ongoing increases in computing power and improved methodology have increased its application also to industrial problems. The method initiated the development of computational techniques based on the micromechanical approach. DEM is a numerical technique for computing the motion of a large number of particles interacting with each other through collisions. The technique allows for establishment of positions and velocities of particles in system through time integration of the ordinary differential equations (*ODE*) formed for each individual particle on the basis of Newton's second law of motion. The application of a time integration scheme allows for solution of the *ODE* system providing information about velocities and positions of particles. There are many time integration schemes for DEM simulations, some of which are borrowed from molecular dynamics. The numerical scheme is stable only for very small elementary time step Δt, which results in a significant limitation of discrete element method. The resultant force and moment are assumed to act on a particle during the elementary time step. It is also assumed that accelerations are constant during the interval Δt. The iteration cycle, presented in Fig. 1, is repeated for each particle in granular packing during DEM simulation.

The deformations of rigid particles in DEM are usually treated as virtual deformations, which means that particles are allowed to overlap locally at contact points rather than deform due to contact force. The deformations of particles are very small in comparison to the deformation of a particulate assembly and forces resulting from a contact between two particles are related to their overlap by contact force model. Static balance is achieved by a system through dispersion of energy which is a consequence of friction and damping. The tangential contact force is related to normal force by the Coulomb's friction law.

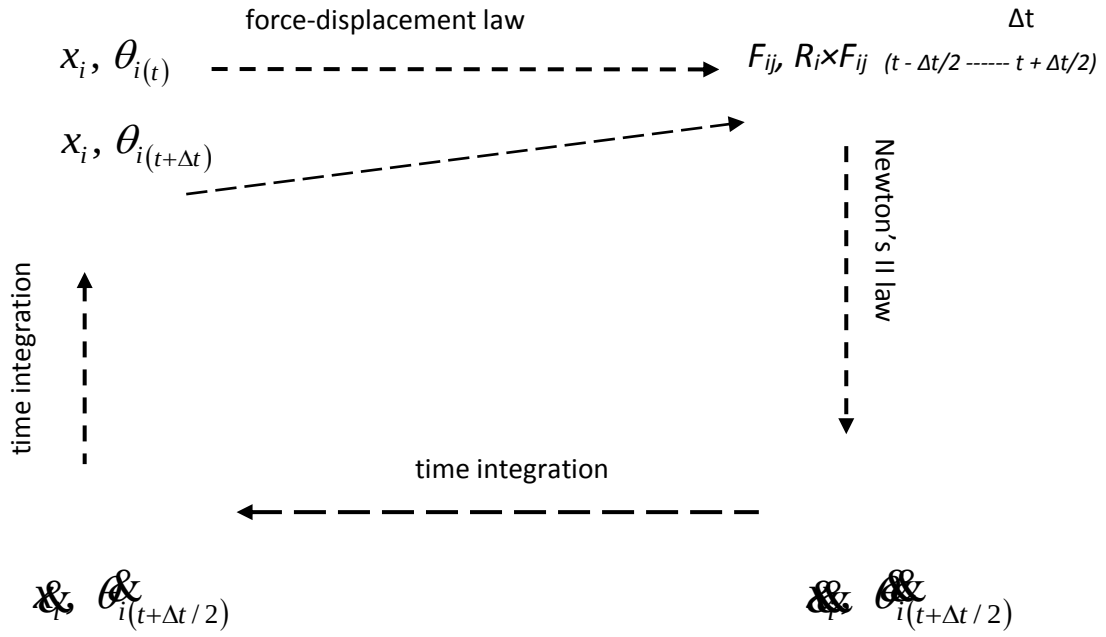

Fig.1. Scheme of calculation cycle in DEM.

The application of the Discrete Element Method to model particulate assemblies allows us to look inside the material and understand fundamental particle interactions which determine the complex, macro-scale response. The DEM provides detailed information on structural and micromechanical properties of granular materials which leads to more accurate interpretation or design of effects encountered in industry.

References:

[1] Cundall P.A., Strack O.D.: A discrete element model for granular assemblies. Géotechnique 29: 47-65, 1979

Heat treatment processes as examples of heat transfer in porous media

Rafał Wyczółkowski
Department of Industrial Furnaces and Environmental Protection,
Czestochowa University of Technology, Al. Armii Krajowej 19, 42-200 Częstochowa
rwyczolkowski@wip.pcz.pl

Keywords: heat treatment, steel porous charge, heat transfer, porous media

The transport of heat inside different porous media has attracted the attention of scientist and engineers due to its many technical and practical applications. Areas and applications where the study of heat transfer becomes mandatory are: extraction of geothermal energy, soar pounds, food preservation, building environment, microstructure electronics, global warming, power pants, gas-cooled nuclear reactors, catalytic reactors and high performance cryogenic insulations [1]-[4]. However in industrial practice exist another one area where take place heat transfer processes in porous media, which is not mentioned in the literature. It relates to the heat treatment of metal porous charge [5]. These types of charge are two-phase structures consisting of a metal (steel, aluminium, copper) skeleton of the solid phase and the voids which are filled with gas. The gas phase of the porous charge is the atmosphere of the furnace in which the heat treatment is performed. It is mostly air or flue gas. When the process relates to the steel it may be carried out in protective atmosphere. In such case this medium may be nitrogen, hydrogen, carbon dioxide or some other gas not entering into chemical reaction with the treated material.

There are three groups of porous charge: coils, bundles and beds. In the coils are heated the sheets and wires, and in the bundles are heated all types of long elements, i.e. bars, tubes, sections and shapes. While in beds are heated small elements which are introduced to the furnace in a large amount in special containers or baskets. The examples of mentioned porous charge types are shown in Fig. 1.

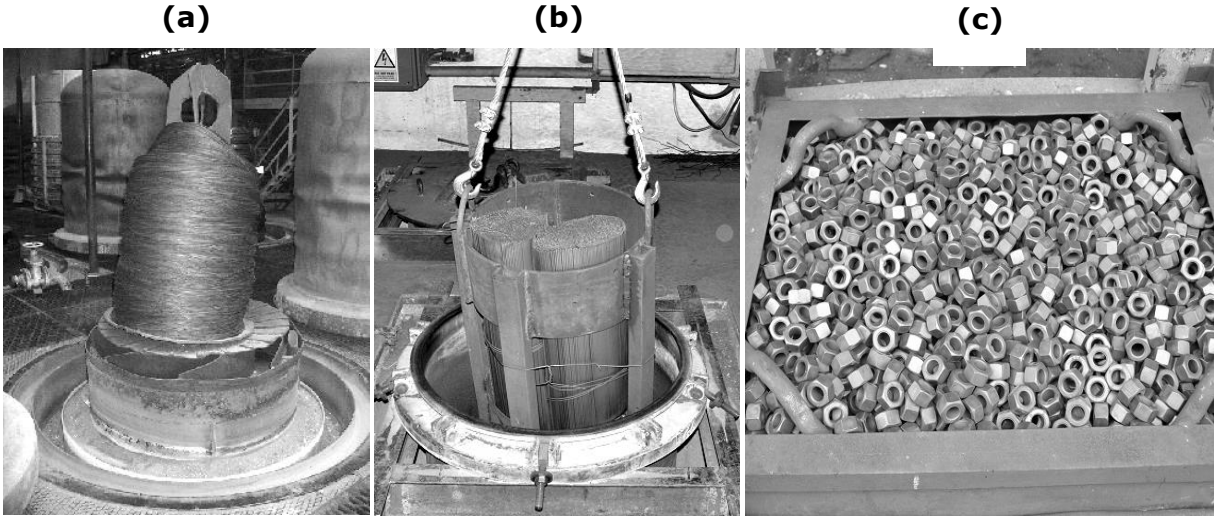

Fig.1. Examples of steel porous charge: a) coil of wire, b) bar bundle, c) bed of nuts.

Besides the porosity another special feature of this type of charge is lack of continuity of solid phase. This makes that porous charge has quite different physical properties than steel monolithic elements. In addition during porous charge heating in its area occur complex heat transfer. Thermal energy in this system is transferred through the following mechanisms [6]:

- conduction in the solid phase;
- conduction in the gas;
- free convection of gas;
- thermal radiation between surfaces of the individual elements of the charge sections;
- contact conduction at the locations of contact between adjacent elements.

The proposed article will contain:

- detailed characterization of porous charge;
- its basic physical properties;
- analysis of the heat transfer mechanisms that take place during the heating process;
- discuss of the problems related to the control of the heating process parameters.

References:

[1] Ochsner N., Murch G.E., de Lemos M.J.S.: *Cellular and Porous Materials, Thermal Properties Simulation and Prediction*, WILEY-VCH Verlag GmbH & Co. KGaA, Weinheim 2008
[2] Koster A., Matzner H.D., Nichols D.R.: *PBMR design for the future*, Nuclear Engineering and Design 222: 231-245, 2003
[3] Fogler H.S.: *Elements of Chemical Reaction Engineering*, 3rd edition, Prentice-Hall, 1999
[4] Tien C.L., Cunnington G.R.: *Cryogenic insulation heat transfer*, Advances in Heat Transfer 9: 349-417, 1973
[5] Wyczółkowski R.: *Klasyfikacja i charakterystyka wsadów porowatych spotykanych w praktyce przemysłowej obróbki cieplnej*, Hutnik Wiadomości Hutnicze, 79: 877-879, 2012
[6] Wyczółkowski R.: *Identyfikacja mechanizmów transportu ciepła w obszarze stalowego wsadu porowatego w postaci wiązek elementów długich*, Hutnik Wiadomości Hutnicze, 80: 380-383, 2013

Use of the visualization techniques to the research of heat transfer in porous charge

Rafał Wyczółkowski
Department of Industrial Furnaces and Environmental Protection,
Czestochowa University of Technology, Al. Armii Krajowej 19, 42-200 Częstochowa
rwyczolkowski@wip.pcz.pl

Keywords: porous charge, effective thermal conductivity, thermography, Schlieren method

Steel remains the primary construction material which is evidenced by the increasing level of world steel production. The primary challenge for manufacturers is to produce steel products of the best quality at the lowest cost. Operations which basically determine the quality of final products is heat treatment. For these reason, manufacturers of steel need to optimize heat treatment processes. This is done mostly by calculations using appropriate numerical models [1], [2]. One of the input data for such models are the thermophysical properties of the heated elements. When the heated charge has a porous structure (like bundles of long elements which examples are shown on Fig. 1), the basic thermal property is the effective thermal conductivity k_{ef} [3]. This parameter is commonly used in the theory of porous media [4], [5]. But in contrast to the thermal conductivity of solid materials k_s, the value of coefficient k_{ef} is not a material quantity. It only quantitatively defines the ability of the porous medium to heat transfer. The k_{ef} coefficient is a function of complex heat transfer mechanisms related to conduction, convection and radiation, which occur within the porous medium. Thus the knowledge about this heat transport modes is necessary to establishing the value of k_{ef} coefficient.

Fig.1. Examples of steel long elements bundles: bundle of bar, bundle of tubes, bundle of section.

The knowledge about the phenomenon of heat transfer in porous charge can be obtained based on two experimental visualization techniques which are: thermography and a Schlieren method. Thermography gives the possibility to obtain a complete picture of the temperature field in the area under consideration [6]. The data collected in this can be used to determination of the effective thermal conductivity of the examined medium by the resistor approach. This approach assumes that each of the heat transfer mechanisms in the tested sample of porous charge is characterized by a heat resistance. A suitable combination of these resistances gives, in turn, the total thermal resistance R_{tot} of the tested medium. Having this parameter, it is an easy task to calculate the effective conductivity of the sample. Resistances for different mechanisms of heat exchange can be determined using the analysis of the temperature field in the recorded infrared images.

The Schlieren method is a technique relying on the angular deflection of light rays passing through a transparent fluid region that is characterized by the inhomogeneity of the index of refraction, n [7]. The gradients of the n index are caused by the inhomogeneity of the temperature, density or concentrations of various components. Devices using the above-mentioned phenomenon for the visualization of the inhomogeneity of a medium are referred to as Schlieren apparatuses. The study of natural convection makes use of the effect of fluid density inhomogeneity caused by a varying temperature field on the propagation of light. This technique allows to analyse the convection that occurs in the inner areas of the bundles of tubes or rectangular profiles (charge of mixed porosity) [8].

The article presents results of experimental tests performed with these two techniques with respect to the different types of steel porous charge. Obtained results gives valuable information about qualitative and quantitative nature of the analysed phenomenon.

References:

[1] Sahay S.S., Krishnan K.: *Model based optimization of continuous annealing operation for bundle of packed rods*, Ironmaking and Steelmaking, 34: 89-94, 2007
[2] Sahay S.S., Mitra K.: *Cost model-based optimization of carburizing operation*, Surface Engineering, 20: 379-384, 2004
[3] Wyczółkowski R., Benduch A.: *Effective thermal conductivity as a basic thermal property of steel porous charge*, Aktualne Zagadnienia Energetyki tom III, Oficyna Wydawnicza Politechniki Wrocławskiej, 391-406, Wrocław, 2014
[4] Kaviany M.: *Principles of heat transfer in porous media*, Springer-Verlag, New York, 1991
[5] Van Antwerpen W., du Toit C.G., Rousseau P.G.: *A review of correlations to model the packing structure and effective thermal conductivity in packed beds of mono-sized spherical particles*, Nuclear Engineering and Design, 240: 1803-1818, 2010
[6] Wyczółkowski R., Benduch A.: *The use of thermovision at heat flow analysis in bundles of steel bars*, The International Forum of Students and Young Researchers, Topical Issues of Rational Use of Natural Resources, Sankt Petersburg, Russia: 12-14, 2014.
[7] Panigrahri P.K., Muralidhar K.: *Imaging Heat and Mass Transfer Processes Visualization and Analysis*, Springer Science, New York, 2013
[8] Wyczółkowski R., Kolmasiak C., Urbaniak D., Wyleciał T.: *Use of the Schlieren method to the convection analysis in the steel charge of mixed porosity*, Archives of Metallurgy and Materials, 60 (4): 2949-2954, 2015

Relationship between particle shape characteristics and water permeability of fine grained soils

Zofia Zięba
Wroclaw University of Environmental and Life Sciences, Institute of Building Engineering
zofia.zieba@up.wroc.pl

Keywords: particle shape characteristics, soil microstructure, effective porosity, permeability coefficient

In order to properly describe ground water movement, it is necessary to precisely recognize the determinants of water flow. One of them is the soil microstructure. However, it is usually omitted in engineering practice.

The aim of this paper is to prove the relationship between the particle shape characteristics of fine grained soils and their water permeability.

In order to analyse this phenomenon, laboratory tests of the permeability coefficient k_{10} of four soils were conducted. The analysed soils were characterised by the same grain size distribution and extremely different particle structure, which varied from ideally spherical, smooth grains to particles of a highly irregular shape and high surface roughness (Fig.1).

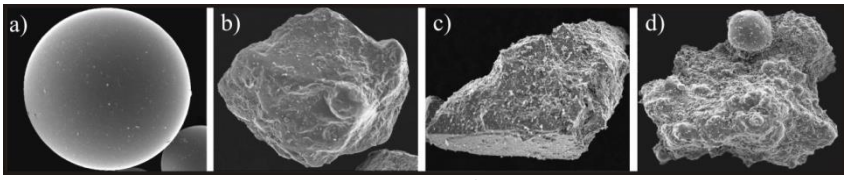

Fig.1. Scanning electron microscope (SEM) images of selected soils: a) glass microbeads GM; b) sandy silt from Krakowiany SSK; c) sandy silt from Graniczna SSG; d) fly ash FA.

The soil shape characteristics were described by the total shape index ζ_{0C}. This parameter defines the variability of three particle shape properties, such as sphericity, angularity and roughness of grains [1]. According to literature, this is the only available method that expresses several shape characteristics with use of a single parameter.

The obtained ζ_{0C} values were the highest for perfectly round and smooth glass microbeads particles and decreased with the increase in the complexity of the geometry and configuration of grain surface (Table 1).

The permeability coefficient tests showed that the flow capability decreased with the increase in the irregularity of soil particles. This is a reverse relation than the general porosity *n* values showed, which were the highest for soils of the most complex grain structure (Table 1).

In order to link the obtained permeability coefficient with the soil microstructure, the empirical analysis of effective porosity was conducted based on two analytical models [2], [3]. The selected models were modified by introducing the total shape index ζ_{0C}. This enabled the creation of a new definition of effective porosity n_e, as the product of general porosity *n* and the ζ_{0C} index. It was proven that the shape and the degree of particles surface complexity determine the capability to retain bound waters, which significantly narrows the cross-section of unobstructed pores [4].

Based on obtained correlation, the method of determining the permeability coefficient k_{SEM} by analysing SEM images [5] was modified. The application of the ζ_{0C} index to determine the effective pores allowed to define the permeability coefficient $k_{(M)SEM}$ based on SEM photographs with reference to soil microstructure influence.

Moreover, it was proven that empirical formulas, which are recommended by Eurocode 7 as one of the methods to calculate the permeability coefficient are not a reliable way to determine this parameter due to omitting the soil microstructure [6].

All analyses were verified by the results of laboratory tests. The partial results are presented in table 1.

Table 1. Results of the analyses for density index $I_D = 0.6$.

Type of soil	Porosity n	Total shape index ζ_{0C}	Efective porosity ne	Permeability coefficient					
				k_{SEM}	$k_{(M)SEM}$	Krüger formula	Slichter formula	USBR formula	Laboratory tests
[-]	[-]	[-]	[-]	[m·s^{-1}]	[m·s^{-1}]	[m·s^{-1}]	[m·s^{-1}]	[m·s^{-1}]	[m·s^{-1}]
GM	0.32	1.00	0.32	$1.33 \cdot 10^{-5}$	$1.33 \cdot 10^{-5}$	$5.97 \cdot 10^{-7}$	$7.93 \cdot 10^{-7}$	$3.24 \cdot 10^{-4}$	$1.18 \cdot 10^{-5}$
SSK	0.40	0.67	0.27	$1.56 \cdot 10^{-5}$	$6.99 \cdot 10^{-6}$	$3.46 \cdot 10^{-7}$	$1.69 \cdot 10^{-6}$	$3.24 \cdot 10^{-4}$	$6.45 \cdot 10^{-6}$
SSG	0.44	0.58	0.26	$1.25 \cdot 10^{-5}$	$4.24 \cdot 10^{-6}$	$2.97 \cdot 10^{-7}$	$2.34 \cdot 10^{-6}$	$3.24 \cdot 10^{-4}$	$4.53 \cdot 10^{-6}$
FA	0.45	0.48	0.22	$1.28 \cdot 10^{-5}$	$2.95 \cdot 10^{-6}$	$3.38 \cdot 10^{-8}$	$2.03 \cdot 10^{-6}$	$3.24 \cdot 10^{-4}$	$2.53 \cdot 10^{-6}$

References:

[1] Parylak, K.: *Characteristic of particles shape of fine-grained cohesionless soils and its significance in strength assessment*, Zeszyty Naukowe Politechniki Śląskiej, No. 90, Gliwice, 2000.

[2] Wolski, W.: *Filters, General Report*, Proceedings of The IX European Conference on Soil Mechanics and Foundation Engineering, Vol. 3, Dublin,1351-1366,1987.

[3] Inraratna, B., Vafai, F.: *Analytical model for particle migration within base soil- filter system*, Journal of Geotechnical and Geoenvironmental Engineering, Vol. 123, No. 2, 100-109, 1997.

[4] Zięba Z., *Influence of microstructure on hydraulic properties of fine grained soils*, Journal of Hydrology and Hydromechanics, Under Review.

[5] Kozłowski, T. Kurpias-Warianek, K. Walaszczyk, Ł.: *Application of SEM to Analysis of Permeability Coefficient of Cohesive Soils*, Archives of Hydro-Engineering and Environmental Mechanics, Vol. 58, No. 1-4, 47-64, 2011.

[6] Parylak K., Zięba Z., Bułdys A., Witek K., *The verification of determining a permeability coefficient of non-cohesive soil based on empirical formulas including its microstructure,* Acta Scientarum Polonorum Architectura, 12(2)2013, 43-51.

A role of the effective stress in modelling of CO_2 sequestration

Paweł Ziółkowski, Janusz Badur
Energy Conversion Department, Institute of Fluid Flow Machinery PAS-ci, Gdańsk
pziolkowski@imp.gda.pl

Keywords: effective stress, CO_2 sequestration, poro-mechanics, poro-thermo-chemo-mechanical interactions

The effective stress is the first and probably most important factor that influences the effectiveness of CO_2 sequestration. The effective stresses not only govern the mechanical state of coal matrix by limiting its strength and fracture but influences on CO_2 slippage and sorption/desorption capacity. Therefore, a correct definition of effective stress tensor plays a basic role in mathematical modeling of CO_2 sequestration. The increase of gas sequestration pressure up to 10 MPa results an decrease of effective stresses, which, in turn, increases the coal matrix sorption capacity as well as the permeability and non-Darcian slippage rate [1].

First, the most important effect is positive influences of the effective stress on the capacity of a coal seam to CO_2 sorption. Sorption is the physical process related with the release the amount of sorption heat and the coal volumetric swelling due to CO_2 change of molecular configuration. It is known as the Czapliński-Hołda effect [2], when CO_2 absorbed at a coal surface changes dynamically as the pore pressure changes. A Langmuir type isothermal equation is usually used to describe gas sorption in coal matrix [3]. However, since the volumetric swelling strain, induced by CO_2 sorption, is more than 1.7 times higher than from CH_4 , due to different sorption capacity, it is observed an evolution of new fractured porosity in comparison to a natural, CH_4-saturated coal bed [4].

In the paper we concentrate on two elements. Firstly, standing on a ground of thermodynamical derivation of the Terzaghi effective stress principle [5] we define an effective stress tensor with complete effects of thermo-chemo-porosity interactions. Secondly, since the pore size for coal matrix ranges in 1 nm and 100 nm [2,3], that causes non-Darcy flows in CO_2 sequestration processes as well as in laboratory permeability tests [4], we have decide, for description of gas flowing through a porous medium with nano-scale pore size, to take into account the Duhem, Navier and du Buat contributions of velocity slip at the gas-solid interface.

Performed by authors numerical simulations have shown a pressure range where slip effects becomes significant which result in the Klinkenberg effect for a marco-scale porous medium flow [1]. The Klinkenberg relation treats the effective permeability as a function of local gas pressure, as follows: $k = k_0(1 + b_K/p)$ where k_0 is the absolute permeability and b_K is the Klinkenberg slip constant. Additionally, in the paper some mathematical relation between Duhem, Navier and du Buat viscosity coefficients and the Klinkenberg slip constant has been indicated and evaluated.

References:

[1] Klinkenberg L.J.: *The permeability of porous media to liquids and gases*, Drilling and production practice, 1941.
[2] Czapliński, A., Hołda, S.: *Changes in mechanical properties of coal due to sorption of carbon dioxide vapour*, Fuel, 61:1281–1282, 1982.
[3] Masoudian, M., Airey, D., El-Zein, A.: *A chemo-poro-mechanical model for sequestration of carbon dioxide in coalbeds*, Geotechnique 63: 235–243, 2013.
[4] Espinoza D.N., Vandamme M., Pereira J.M., Dangla P., Vidal-Gilbert S.: *Measurement and modeling of adsorptive–poromechanical properties of bituminous coal cores exposed to CO2: Adsorption, swelling strains, swelling stresses and impact on fracture permeability*, Int. Journal of Coal Geology 134–135:80–95, 2014.
[5] Badur J., Ziółkowski P., Kowalczyk T.: *A thermo-dynamical justification of the effective stress principle,* submitted, Arch. Hydro-Eng. Environ. Mech., 2016.

NOTES